EVAPORATION FROM AEOLIAN SOILS WITH SHALLOW WATER TABLES

By

ACHAMYELEH GIRMA MENGISTU

A dissertation submitted in fulfilment of the requirements in Master's Degree qualification in Inter-disciplinary Soil Science in the Department of Soil, Crop and Climate Sciences, Faculty of Natural and Agricultural Sciences, at the University of the Free State, Bloemfontein, South Africa.

February, 2016

Supervisor: Prof. L.D. van Rensburg

Co-supervisor: Dr. S. Mavimbela

DECLARATION

I, Achamyeleh G. Mengistu, declare that the master's degree research dissertation or interrelated publishable manuscripts/published articles or course work Master's degree mini-dissertation that I herewith submit for the Master's Degree qualification in Inter-disciplinary Soil Science at the University of the Free State is my independent work, and that I have not previously submitted it for a qualification at another institution of higher education.

I, Achamyeleh G. Mengistu, hereby declare that I am aware that the copy right is vested in the University of the Free State.

I, Achamyeleh G. Mengistu, hereby declare that all royalties as regards intellectual property that was developed during the course of and/in connection with the study at the University of the Free State, will accrue to the university.

....

Signature Date

ACKNOLEDGEMENT

I am very grateful to GOD the ALMIGHTY for without his graces and blessings this study would not have been successful.

I would like to express my special appreciation and thanks to my supervisor Prof. Leon Daniel van Rensburg, you have been a tremendous mentor for me. I would like to thank you for encouraging me and for allowing me to grow as a research scientist. Your advice on both research as well as on my career have been priceless. I would also like to thank my co-supervisor, Dr. Sabelo Mavimbela, for your insightful and brilliant comments and also words of encouragement. Your guidance helped me in all the time of the research and writing of this thesis.

I would also like to express my special thanks to the following institutions:

Polytechnic of Namibia: For granting me a bursary for my study through the Intra-ACP Scholarship which was funded by the European Commission.

University of the Free State, Department of Soil, Crop and Climate Sciences: For its financial assistance and providing me all research facilities.

South African Weather Service: For providing me daily meteorological data of the study area.

Finally my gratitude goes to those who helped me during the study, Dr. Eyob Tesfamaryam, staff member of the University of Pretoria, thank you very much for lending me a laboratory equipment (the KD2 Pro Thermal Analyser). Students, colleagues or staff members from the University of the Free State especially Prof. Robert Schall (special assistance in data analysis in SAS ver 9.4). Dr. Weldemichael A. Tesfuhuney (unreserved assistance in data analysis), Dr. B. T. Kuenen, Mr. Cinsani Tfwala, Mr. Derick Wessels, Mr. George Madito and Mr. Elias Jokwane thank you very much for your help during field and laboratory experiments.

DEDICATION

I dedicate this dissertation to my parents Girma Mengistu and Tiru Yassabe and my late sister Erebeb Girma.

TABLE OF CONTENTS

LIST OF TABLES

LIST OF FIGURES

ABBREVIATIONS

$\sum E_s$-cumulative evaporation from bare soils

AED-atmospheric evaporation demand

ANOVA-analysis of variance

b_0, b_1, and b_2-empirical constants dependent on soil textural compositions

C_f-shape factor in determining K_s

Cl-A_p-Clovelly soil with the top horizon

CLASS-the Canadian Land Surface Scheme

Cl-B-Clovelly soil with the B horizon

C_n-volumetric heat capacities of the solid phase

C_p-volumetric heat capacities of moist soil

C_v volumetric heat capacities of the gaseous phase

C-volumetric heat capacity

C_w-volumetric heat capacities of the liquid phase

C_y-clay content

D_f-hydraulic diffusivity

D_r-water loss as drainage

D-thermal diffusivity

DUL-drained upper limit of soils

E_s-soil water evaporation from bare soils

g-gravitational potential

G-soil heat flux

HELP-the Hydrologic Evaluation of Landfill Performance

h_{max}-critical water table depth

H_s-sensible heat

H-total hydraulic head

Hu-A_p-Hutton soil with the top horizon

Hu-B-Hutton soil with the B horizon

IOA-index of agreement

I_s-water applied as sub-surface irrigation

K_n-weighting factor of components of the soil

kPa-kilopascal (unit for matric suction)

K_s-saturated hydraulic conductivity

K_t-thermal conductivity

K_v-vapour hydraulic conductivity

l- Empirical pore-connectivity parameter

LL-lower limit of soil

L_o-the latent heat of vaporization of water

m- van Genuchten's empirical parameter

MD-measurement depth

No EF-no formation of evaporation front

No WT-no water table

n-van Genuchten parameter which is a measure of pore size distribution

PE-potential evaporation

p-pressure potential

PTFs-pedotransfer functions

P-water gained as precipitation

q_h-the total heat flux density

Q_l-steady state flow rate

q_L-liquid water flux

Q-sources and sinks of energy

q_v-water vapour flux

RMSE-root mean squared of error

$RMSE_u$-unsystematic root mean squared of error

R_n-net solar radiation

R_o-water loss due to runoff

r-radius

R-ratio of E_s to PE

S_e-normalized water content/effective saturation

SHAW-simultaneous heat and water

S_h-the storage of heat in the soil

S_i-silt content

S-sink term for root water uptake

SWAMP-soil water management program

SWB-soil water balance model

SWRC-soil water retention curve

T_r-water loss due to transpiration

T-soil temperature

t-time

W_{gains}-total gains of water in a soil profile

W_{losses}-total losses of water in a soil profile

WT-water table depth

x-distance in the x-axis

X_n-volume fraction of the component of the soil

y-distance in the y-axis

z-distance in the z-axis

α-van Genuchten parameter which is the inverse of the air entry suction

β-the contact angle between water and soil particles

γ-surface tension between the water and air

ΔW-change in water content in a soil profile

θ_l-volumetric water in liquid phase

θ_n-volumetric fraction of solid phase

θ_r-residual water content

θ_s-saturated volumetric water content

θ_v- volumetric water in vapour phase

θ-volumetric water content

ρ_w-density of water

ψ-matric suction

ψ_a-air entry value

λ_n-thermal conductivity of the fractional constituent

λ-pore size distribution index

ρ-the density of a porous media

ABSTRACT

Soil water evaporation under water table conditions was identified as a very important water loss in the soil water balance in aeolian soils. Globally it is estimated that 7.2×10^{13} m^3 of water lost through evapo-transpiration per year. In South Africa, an average of 65% of the precipitation will be lost through evapotranspiration. The main aim of this study was to determine the effect of water table depth on daily evaporation (E_s) for two aeolian soils that cover large areas in Africa below the equator. The study was divided in to three content chapters: The first chapter concentrated on characterization of the basic soil physical properties, the second content chapter investigated the effect of soil water content and temperature on the thermal properties, while the last content chapter described the effect of soil type and water table depth on the daily rates of evaporation as well as the temperature distribution in the profiles.

In the first content chapter, soil physical properties were determined with application of laboratory, field or indirect estimation methods and summarized as follows. (i) Particle size analysis was determined in laboratory by the pipette method. The two soils had similar textural class (loamy-sand) in the A_p horizon, but Clovelly categorized as sandy and Hutton as sandy-loam in the B-horizon. (ii) Bulk density was determined by the core sampling method and varied between 1.3 to 1.7 g cm^{-3} with Clovelly the lowest. (iii) Soil water retention curves (SWRCs) were determined in laboratory by the Hanging Water Column and the Pressure Plate Apparatus (assisted by the RETC computer program and the van Genuchten model). The water content at lower suctions was higher in Clovelly than Hutton and the opposite was true for higher suctions to the dry end. Hence, Clovelly had a well-developed S-shape SWRC than Hutton. (iv) Saturated hydraulic conductivity (K_s) was determined *in situ* by the constant head permeameter and was higher in the Clovelly soil. (v) Unsaturated hydraulic conductivity (K_L) and hydraulic diffusivity (D_f) were estimated from the SWRCs by the Mualem-van Genuchten conductivity model. The Clovelly soil horizons had higher K_L and D_f. (vi) The pore volume-pore size response curve was inferred from the SWRC by applying the capillary theory. The classification of the soil pore by their function proposed in the literature was also modified based on the concepts of field water capacity of soils.

In the second content chapter, the influence of soil water content and temperature on thermal properties (K_t, C and D) was analysed in laboratory using the KD_2 Pro Thermal Analyser. Five water and temperature levels were investigated in a two factor factorial experiment. The results

showed an interaction effect between water and temperature on all thermal properties. From the analysis, three important water content and temperature combinations were identified, i.e. wetting of a dry soil with a rising temperature (up to 60^{o}C), the effect of freezing (0^{o}C) and thawing (10^{o}C) with increasing water content, and the excessive wetting of soils beyond 0.16 mm^3 mm^{-3} with increasing temperature. The relationship between thermal properties with the combined effect of soil water content and temperature was non-linear. A mathematical model was also developed with an average R^2 of 0.8 that enables to estimate the three thermal properties by using the soil water content and temperature data. The validation procedure showed that the model can predict thermal properties within the temperature range of 0-60^{o}C.

In the last content chapter, soil water evaporation and temperature distribution on the different water table depths was characterised. Time series soil water and temperature data was collected by using DFM probes. The soil water evaporation was determined by the water balance technique. Whereas the effect of water table depth on the diurnal temperature distribution was analysed by using the daily experimental mean, water table mean and the daytime amplitude temperatures as indicators of temperature variation. The study showed that the daily rate of evaporation (E_s) and the cumulative evaporation ($\sum E_s$) was highly influenced by potential evaporation and the soil's hydraulic properties. In shallow water table depths of 0-500 mm, E_s was shown to be dependent on the potential evaporation. However, as the water table depth increased beyond 500 mm, the soil hydraulic properties were the determinant factors. The results showed that as the water table depth increased, daily and cumulative evaporation also increased linearly. The relative loss of water by E_s was compared among the water table depths and the average contributions from two measurement cycles varied from a minimum of 5.55% from the No WT treatment to a maximum of 100% from the 0 mm depth. The influence of soil type was also significant with higher E_s in Hutton soil.The distribution of temperature was affected by the water table depth. As the water table depth increased, the temperature of the profiles increased and vice versa. But there was no significant difference in temperature distribution between the two soils.

A significant amount of water is lost through E_s from shallow water tables especially from 0-500 mm depth. This unproductive water loss can be converted into transpiration if water table depth under irrigated crop fields are maintained within 500 to 1000 mm depth. In addition, integration of conservation tillage practices such as mulches and zero tillage could reduce evaporation. A further study on the contributions of shallow water table depths on evaporation under different conservation tillage are recommended.

CHAPTER 1
MOTIVATION AND OBJECTIVES

1.1 Motivation

Soils that developed from aeolian sand deposits are regarded as the backbone of crop production in South Africa (Harmse and Hattingh, 2012). These soils are also seen as the future food basket in the continent, as it covers an estimated 909 million ha (Thomas *et al.*, 2005) and 303 million ha bellow the equator (Schlegel *et al.,* 1989; Thomas and Shaw, 1990; Thomas *et al.,* 2005; Harmse and Hattingh, 2012). The reason for this expectation is that where thick layers of aeolian sands are deposited on highly permeable fractured rock it normally results in a Class 1 irrigable soil due to its excellent internal and external drainage and moderate to high water holding capacity (Le Roux *et al.*, 2013). Conversely, where these sands are deposited on poorly permeable or impermeable material (clay or dense lime layers), the soils are viewed as non-irrigable as it requires artificial drainage. However, sandy to sandy loam soils with restricted drainage in semi-arid areas are prime soils for dry land farming as it tends to form water tables under water-conservation tillage practices (Ehlers *et al.*, 2007). Bennie *et al.* (1995) estimated that the water-table soils under dry land amounts to about 1.5 million ha in South Africa, while much of the total irrigated soils of 1.3 million ha comprise of aeolian sandy deposits. The estimated coverage of aeolian sand deposits in Africa, south of the equator and Northern Free State, South Africa are shown in Figure 1.1 and 1.2, respectively.

On the other hand, South Africa's water demand has been increasing since the last two decades and is more likely to face shortages given the recent decline of rainfall potential in the region (Blignaut *et al.*, 2009; Archer *et al.*, 2010). For example Bennie and Hensley (2001) reported that in the semi-arid areas of South Africa where most of dry land crop production occurs, the aridity indices vary in between 0.2 to 0.5 showing that the amount of precipitation fails to meet the evaporative demands. Therefore the prospect of increasing available surface water resources is low whereas groundwater is increasingly becoming an important water resource (Pietersen *et al.*, 2011). In this regard, efficient water use and control of unproductive water losses such as runoff (R_o) and evaporation (E_s) is essential for effective water resource management.

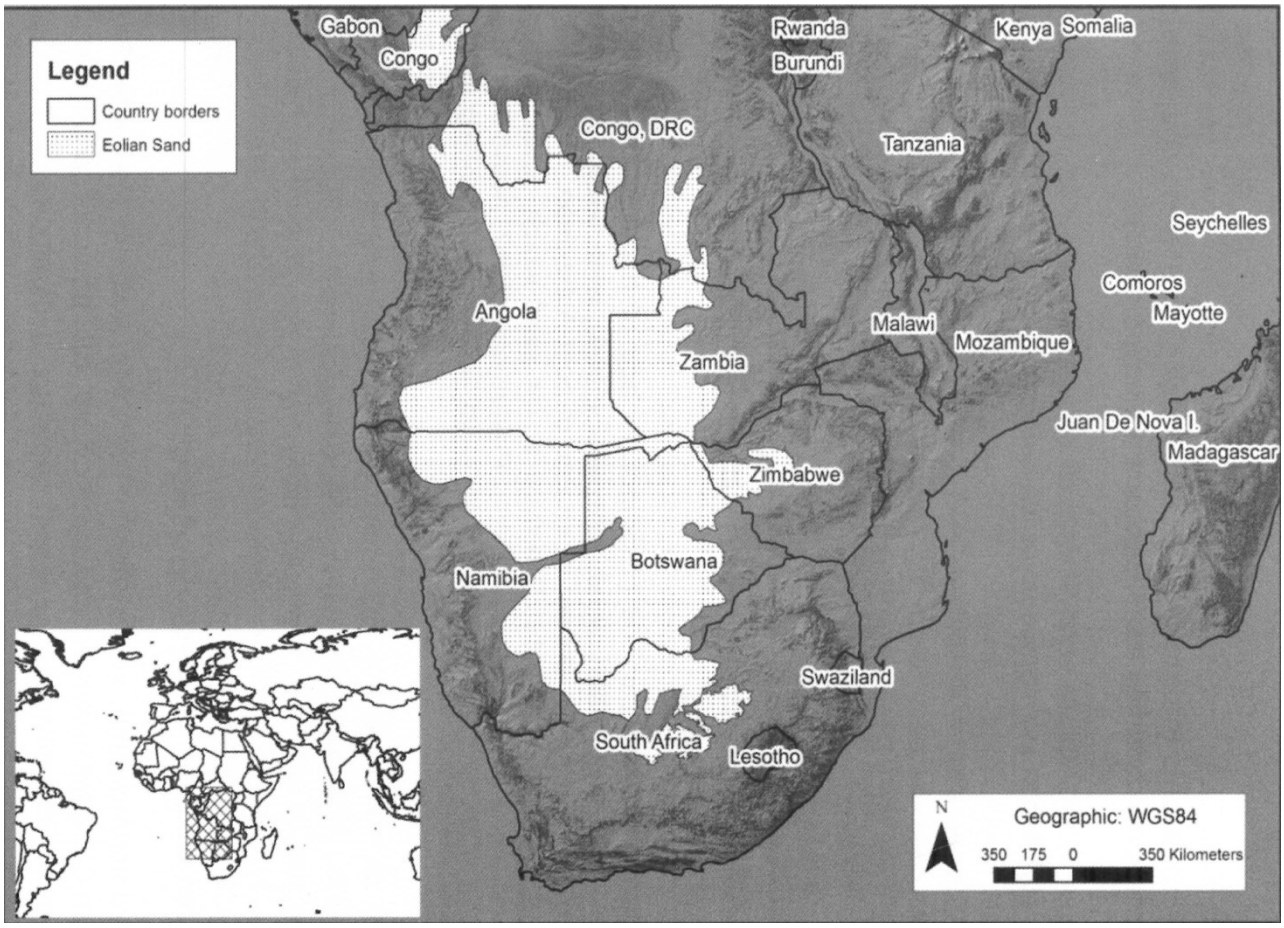

Figure 1.1 Distribution of aeolian sand deposits in Africa, south of the equator (Harmse and Hattingh, 2012).

In many dry regions, the water stored near the soil surface is more vulnerable to E_s owing to the high radiation and prolonged sunshine hours. In these areas the drying front has been observed to advance up to depths of 1m (Hensley, 2000; Hillel, 2004). As a result evaporation accounts for the highest losses of surface and shallow ground water. Reports show that the total annual losses of water through evapotranspiration was estimated to be 67% of annual rainwater (Jovanovic *et al.*, 2015). Out of the total evapotranspiration about 53% is in the form of transpiration (T_r) and E_s accounting for 39%. The rest (8%) occurs from rainfall intercepted on vegetation canopies. Bennie and Hensley (2001) also reported that during fallow periods E_s can amount to 60 to 70% of annual rainfall in the driest summer cropping areas. Soil water evaporation from bare surfaces could also be exacerbated in shallow profiles or by the activities of shallow water tables (Ripple *et al.*, 1972; Chari *et al.*, 2012). Water table is often classified to be shallow if found within the vicinity of 1.8 m depth from the soil surface (Ehlers *et al.*, 2007).

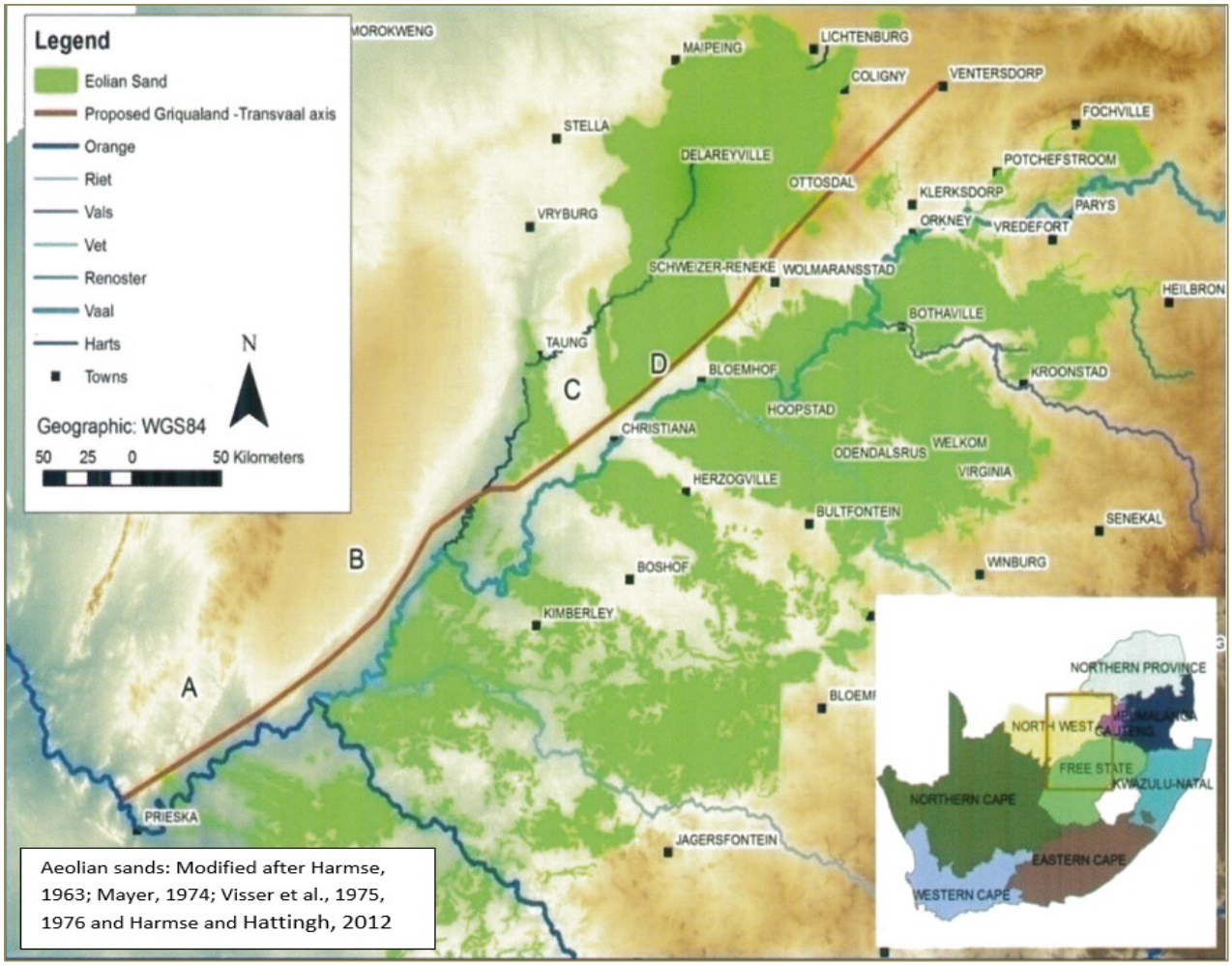

Figure 1.2 Distribution of aeolian sand deposits in Northern Free State Province, South Africa (Harmse and Hattingh, 2012).

Incidence of shallow water table in the Free State Province is also high on irrigated fields, especially along the Orange River Basin. Long-term irrigation practices often results to the formation of perched or shallow water tables that could lead to several inefficiencies of the soil water balance. Poor drainage, low rainfall utilization and appreciable E_s are some of the inefficiencies (Bennie and Hensley, 2001; Ehlers *et al.*, 2003). The long term application of irrigation water without considering the contribution from the shallow water table even leads to over-irrigation and then causes rising of the water table with its soluble salts. This will cause a permanent loss of land due to salinization. For example a study conducted by Ojo (2013) on salinity on Vaal Harts Irrigation Scheme (in the Free State Province, South Africa) found that a total 3964 ha of land was salt affected. Five years later this area has expanded to 553391 ha, and he estimated that by 2020 as much as 46% of the total irrigated area will have visible surface signs of salinity.

Despite the effort of previous studies to address E_s, it could be acknowledged that it is still a big challenge especially where deep soil water storage is practiced. The contribution of shallow water tables to soil water evaporation from bare surfaces is not yet fully understood and quantified. Shallow water table contribution to evapotranspiration on dry land crop production has been fairly addressed in various studies (Bennie, 1994; Cholpankulov *et al.*, 2008; Ehlers *et al.*, 2003; Fan and Miguez-Macho, 2010; Luo and Sophocleous, 2010). Although the findings of these works have been profound, they fell short in quantifying the capillary contribution of shallow water tables to soil water evaporation in which to a greater extent is the predominant phenomenon in most dry areas.

1.2 Scope and objectives

The main aim of this study was to determine the effect of water table depth on E_s for two aeolian soils that cover large areas below the equator in the African continent. This study excludes evapotranspiration as there is sufficient information regarding on the effect of water table depth on ET as indicated in the literature review. Hence, the objectives of the main chapters of this thesis are explained as follows:

(i) To review literature regarding theories, concepts and applications that govern water and energy flows during evaporation in soils with shallow water table (Chapter 2).

(ii) To characterize aeolian soil's hydraulic properties and how they were affected by pore volume-size distribution (Chapter 3).

(iii) To determine the effect of soil water and temperature on aeolian soils thermal properties (Chapter 4).

(iv) To describe the effect of shallow water table and aeolian soils on soil water evaporation and soil profiles temperature distribution (Chapter 5).

CHAPTER 2

LITERATURE REVIEW

2.1 Introduction

Soil water evaporation is a dominant component of the soil water balance especially in arid and semi-arid climatic zones where precipitation is very limited. Under these circumstances crop production in South Africa usually take place under irrigation or dry land conditions with sufficient soil profile water storage capacity. The soil water balance function could be summarised as follows;

$$\Delta W = W_{gains} - W_{losses}, \tag{2.1}$$

Where ΔW refers to the change in the soil water content in the profile, W_{gains} refers to the total soil water gained to the profile, W_{Losses} refers to the total of soil water lost from the profile. This function could be expanded to become;

$$\Delta W = \left(P + I_s\right) - \left(R_o + D_r + E_s + T_r\right) \tag{2.2}$$

Where P refers to precipitation, I_s is for the irrigation, R_o is water loss due to runoff, D_r is for deep drainage, E_s refers to soil water evaporation and T_r is water loss through transpiration.

Recent reviews on the soil water balance (Bennie and Hensely, 2001; van Rensburg, 2010) emphasized the importance of understanding the role of each component in the water balance. Accordingly $ET_r = (E_s + T_r)$ and its relationships to certain field crops are well researched and the principles are captured with their integration in models such as SWAMP and SWB. However, an aspect of ET_r, which is not yet well researched and modelled, is the contribution of water tables to the soil water evaporation under fallow or bare soil conditions.

This chapter reviews the theoretical concepts and applications of soil-water evaporation from shallow water tables under bare or fallow conditions. The functional role of soil water and heat flow properties, diurnal soil temperature fluctuation and water table contribution to the soil surface evaporation are also reviewed.

2.2 Soil water flow

2.2.1 Theory

Water tends to flow from higher to lower water potential and this potential is referred as total potential energy (Marshall *et al.*, 1996; Hillel, 2004; Miyazaki, 2006). The total potential is primarily the sum of matric potential (ψ), gravitational potential (g) and pressure potential (p)

(Hillel, 2004; Miyazaki, 2006). Darcy (1856) was the first to propose the law of fluid flow in porous media with the assumption that the media must be uniform, saturated, permit steady flow and can be described as:

$$q_L = K_s \frac{dH}{dx}, \tag{2.3}$$

where q_L is the water flux, K_s is the saturated hydraulic conductivity, H is a hydraulic head and x is the distance in the direction of flow. In this case dH/dx together refers the hydraulic gradient. Later Darcy's equation was substituted by the governing flow equation also known as the Richard's equation (Richards, 1931). The Richard's equation was better in describing water flow in saturated and unsaturated flow, multi-dimensional flow, and steady unsteady flows. Based on this equation the simplified downward flow of water in soils is expressed by:

$$\frac{\partial \theta}{\partial t} = -\nabla k_L \nabla \psi + \frac{\partial k_L}{\partial z} \tag{2.4}$$

In three dimensional flows Equation (2.2) becomes:

$$\frac{\partial \theta}{\partial t} = -\frac{\partial}{\partial x}\left(k_L \frac{\partial \psi}{\partial x}\right) - \frac{\partial}{\partial y}\left(k_L \frac{\partial \psi}{\partial y}\right) - \frac{\partial}{\partial z}(k_L \frac{\partial \psi}{\partial z}) + \frac{\partial k_L}{\partial z}, \tag{2.5}$$

where K_L is the unsaturated hydraulic conductivity, ψ is matric suction, x, y and z are distances in the x, y and z directions, respectively.

Whereas the opposite flow, the one directional upward movement of water from a water table to the surface in simplified form is:

$$\frac{\partial \theta}{\partial t} = -\nabla . k_L \nabla \psi - \frac{\partial k_L}{\partial z}, \tag{2.6}$$

In three dimensional water flow by capillarity from water table:

$$\frac{\partial \theta}{\partial t} = -\frac{\partial}{\partial x}\left(k_L \frac{\partial \psi}{\partial x}\right) - \frac{\partial}{\partial y}\left(k_L \frac{\partial \psi}{\partial y}\right) - \frac{\partial}{\partial z}(k_L \frac{\partial \psi}{\partial z}) - \frac{\partial k_L}{\partial z} \tag{2.7}$$

Equations (2.3) to (2.7) are all based on Darcy and Richard's water flow equation and applicable when isothermal conditions are assumed. But the thermally induced water flow could significantly affect the net transfer of soil water by changing the hydraulic gradients and hydraulic conductivity (Cary, 1966). Some possible ways and reasons were suggested by Cary (1966) why water flows in the liquid phase under the influence of thermal gradient: (i) as the temperature drops, the surface tension of water against air increases and then water flow due

to surface tension gradient, (ii) as the temperature drops the matric suction also increases and water tends to move and (iii) due to difference in specific heat content, water could flow from the cool to warmer zone. Cary (1965) argued that water transfer in soil could be a result of a net motion of water molecules generated by random kinetic energy changes associated with the hydrogen bond distribution which develops under thermal gradients. Philip and de Vries (1957) also stated that the change in hydraulic properties on thermal gradients is due to the dependence of the surface tension on temperature at the air-water interface. Generally, soil water dynamics and surface energy fluxes will not be described accurately without considering the effect of temperature on soil water as vapour diffusion in soils is driven primarily by temperature gradients (Saito *et al.*, 2006). Liquid flow is probably the dominant mechanism of water movement in wet and nearly isothermal soil conditions. Coupled flow (liquid and vapour) often take place at intermediate volumetric soil water contents and where temperature gradients are appreciable. Hillel (1977) also explained that vapour diffusion is more likely to be the dominant mechanism of water transport in lower soil water content ranges.

2.2.2 Liquid water and vapour flow

As Saito *et al.* (2006) explained the general equation for estimating one dimensional flow of liquid and water vapour in unsaturated soil to be represented by the following mass conservation equation:

$$\frac{\partial \theta}{\partial t} = -\frac{\partial q_l}{\partial z} - \frac{\partial q_v}{\partial z} - S\,, \tag{2.8}$$

where θ is the total volumetric water content ($m^3\ m^{-3}$), which is the sum of the liquid water and vapour (θ_l and θ_v) components, q_l and q_v are the isothermal flux densities of liquid water and water vapour ($m\ s^{-1}$), respectively, t is time (s), z is the spatial coordinate positive upward (m), and S is a sink term usually accounting for root water uptake (s^{-1}).

The flux density of liquid water is described using a modified Darcy's law as given by (Philip and de Vries, 1957):

$$q_l = K_L.\left(\frac{\partial \psi}{\partial z} + 1\right), \tag{2.9}$$

where ψ is the matric suction (m) and K_L ($m\ s^{-1}$) is the isothermal hydraulic conductivity for liquid phase. The isothermal flux density for water vapour can also be calculated as follows (Philip and de Vries, 1957):

$$qv = K_v \frac{\partial \psi}{\partial z}, \tag{2.10}$$

where K_v (m s^{-1}) is the isothermal vapour hydraulic conductivities. By combining Equations (2.8), (2.9) and (2.10), the governing equation for the transport of liquid water and vapour in the vadose zone, first proposed by (Philip and de Vries, 1957), is obtained:

$$\frac{\partial \theta}{\partial t} = \frac{\partial}{\partial z}\left(K_L . \frac{\partial \psi}{\partial z} + K_L + K_v . \left(\frac{\partial \psi}{\partial z} \right) \right) \tag{2.11}$$

2.2.3 Soil hydraulic properties

These are properties that reflect the ability of the soil to transmit or retain water and its dissolved constituents (van Genuchten and Pachepsky, 2011). These properties are primary parameters of the Richard's equation. The soil water retention curve (SWRC), hydraulic conductivity under saturated (K_s) and unsaturated (K_L) and hydraulic diffusivity are the key hydraulic properties in the estimation of flow and transport processes in the vadose zone (Dane and Hopmans, 2002; Kosugi *et al.*, 2002).

2.2.3.1 Soil water retention curve

Soil water retention curve (SWRC) characterizes the relationship between soil volumetric water content (θ, m^3m^{-3}) and matric suction or tension, (ψ, kPa) (Reynolds and Topp, 2008). Soil water retention curve, which is also referred as the soil water characteristic curve, describes the tension at which water is held in the pore space at any given soil water content. Soil pores are classified into macro, meso and micro-pores and each pore class exhibit different capillary matric tension. Water fills the different pore sizes at different soil water contents and at near saturation all the pores conduct water. However, the macro-pores are the first to empty and last to be filled with water. The opposite occurs with micro-pores.

The θ-ψ relationship enhances the understanding of water flow during infiltration and redistribution or capillarity and evaporation (Bachmann and van der Ploeg, 2002). Issues of soil water storage, soil profile water availability to crop plants and permanent wilting point could be better understood when the θ-ψ relationship is known (Reynolds and Topp, 2008).

The matric suction at given water content is most importantly dependent on factors like temperature and interfacial tension and pore-space topology which is the way constituent pore spaces are inter-related or arranged (Bachmann and van der Ploeg, 2002). Tuller and Or (2004) showed SWRC is an important property dependent on size and connectivity of pore spaces hence highly influenced by texture and structure. More specifically Hillel (2004) explained that

at lower suction (<100 kPa) the amount of water retained depends on capillarity and the pore size distribution. This shows that water retention is strongly affected by soil structure at lower suctions. Similarly at higher suctions the retention of water is due adsorption, so it is influenced more by texture and specific surfaces.

Soil texture and structure affects hydraulic properties primarily in affecting the porosity of soils. Soil porosity can be of either textural (formed in between soil particles) or structural (formed between soil structures or aggregates) as it is well explained by Lal and Shukla (2004). The size and number of pores is not enough to describe the influence of pores, their pore size distribution is also important (Lal and Shukla, 2004). Luxmoore (1981) categorized hydraulically important soil pores in three categories as micro, meso and macro pores as shown in Table 2.1.

Table 2.1 Soil porosity classes and their functions as suggested by Luxmoore (1981)

Soil porosity class	Suction ranges (kPa)	Pore diameter (μm)	Dominant phenomena
Micro	>30	<10	Evapotranspiration; matric pressure gradient for water redistribution
Meso	0.3 to 30	10 to 1000	Drainage; hysteresis; gravitational driving force for water dynamics
Macro	< 0.3	>1000	Channel flow through profile from surface ponding and/or perched water table

The pore radius (r) is calculated from the capillary theory that relates matric suction (ψ) with the pore radius (r) as it is explained by Loll and Moldrup (2000) and Chimungu (2009):

$$r = \frac{2\gamma \cos\beta}{g\psi\rho_w} = \frac{3\times10^{-5}}{2\times\psi}, \tag{2.12}$$

where r is the pore radius (m), γ is the surface tension between the water and air (0.728 Nm^{-1} at 20ºC), β is the contact angle (assumed to be zero and Cos (0) is equal to 1), ρ_w is the density of water (0.998 Mg m^{-3}), g is the acceleration due to gravity (9.81 N Kg^{-1}) and ψ is the soil matric suction (m).

Regarding the pore classification, Greenland (1977) and Lal and Shukla (2004) also classified the pores based on their function as given in Table 2.2.

Table 2.2 Pore classification in relation to pore function (Greenland, 1977; Lal and Shukla, 2004)

Pore class	Pore diameter (mμ)	Dominant functions
Transmission pores	> 50	Air movement and drainage of excess water
Storage pores	0.5 - 50	Retention of water against gravity and release
Residual and bonding pores	0.005 - 0.5	Retention and diffusion of ions in solutions
Bonding pores	<0.005	Support major forces between soil particles

The volume of soil pore determines the maximum amount of water that specific soil can hold, but the presence of higher porosity will not always be enough to maximize water retention. The balanced arrangement of pores or pore size distribution plays an important role (Bio Inteligence Service, 2014). Structure is also another physical property that influences the soil water retention curve particularly around saturation (Hillel, 2004; Bio Inteligence Service, 2014). On the other hand, the presence of organic matter increases the water holding capacity of the soil, although the amount of organic matter and aggregate formation have little effect in lower water contents since water availability at lower water contents like permanent wilting point depends mainly on texture (Saxton and Rawls, 2006).

The SWRC could be determined from desorption or imbibition curves. The desorption curve involves the decrease of θ from saturation as ψ decreases from zero, whereas the imbibition curve describes the increase in θ from dryness as ψ increases from a large negative value (Rossi and Nimmo, 1994; Hillel, 2004; Reynolds and Topp, 2008). Therefore the relation between θ and ψ depends whether the soil is wetting or drying. The dependence of the SWRC on wetting or drying process is called hysteresis (Hillel, 2004; Perfect, 2005). Hysteresis is a result of the soil's difference in pore size, shape and conectivty or pore size distribution and arrangement (Hillel, 1998; Saxton and Rawls, 2006). During wetting micropores fill up first and during drying empty last whereas macropores fill up last during wetting and empty first during drying. As a result at any given matric suction, the soil water content during drying is always greater or equal to that of wetting (Saxton and Rawls, 2006).

2.2.3.1.1 Methods of determining soil water retention curve

Soil water retention function is one of the basic hydraulic properties and could be determined much easier from direct methods as compared to unsaturated hydraulic conductivity. Even though it is the most reliable method, direct measurement of soil water retention functions is expensive, laborious and time consuming and even sometimes impractical for larger scale applications (Guber *et al.*, 2006).

Direct measurements

Basically it is possible to get discrete (θ, ψ) data sets with either laboratory or field measurements in which both approaches yield discontinuous sets of θ–ψ data pairs within the range of suction heads used in the measurements (Khlosi *et al.*, 2008). In the field methods measurements are limited within 0 to 85 kPa. Under laboratory conditions the hanging water column and pressure plates are the basic procedures. In hanging water column experiment, the highest water content versus matric suction will be measured in laboratory which is <10 kPa. These procedures are discussed in detail by Dane and Hopmans (2002). For *in situ* measurements, tensiometers are installed at different depths of the profile to get θ-ψ datasets between 0 to 85 kPa. At lower water content and suction relations can be measured by the pressure plate apparatus which can measure between 10–1500 kPa. In pressure plate apparatus, the soil sample is kept at atmospheric pressure while an external gas pressure which is greater than the atmospheric pressure will be applied (Dane & Hopmans, 2002). The water inside the samples will be controlled by the external pressure applied. These methods are explained in detail by Dirksen (1999), Townend *et al.* (2001) and Reynolds and Topp (2008).

Indirect estimations

In this section two standard methods of indirect estimations of the soil water retention curve are explained. The first procedure that is gaining popularity in recent years is the pedotransfer functions (PTFs) and the second procedure is use of empirical/parametric models.

The soil water retention functions can be estimated by indirect methods from basic soil physical properties like texture classes, bulk density, water content and organic matter content which is known as pedotransfer functions (Vereecken *et al.*, 2010). Scheinost *et al.* (1997), Cornelis *et al.* (2005), Børgesen and Schaap (2005) and other reseachers evaluated the performance of pedo-transfer function and all have got reliable estimates. Therefore, the use of pedotransfer functions (PTFs) has been shown to be an efficient method for estimating hydraulic properties from readily available soil data. Many researchers tried to relate the van Genuchten hydraulic

model parameters to specific soil properties. For example: Rawls and Brakensiek (1985), Cornelis *et al.* (2005) and Børgesen and Schaap (2005) provided equations for the estimation of van Genuchten, parameters. The details are provided in Rawls and Brakensiek (1985) and Vereecken *et al.* (2010).

The main weakness of the use of direct measurements is that in these methods it is not possible get continuous values of the θ-ψ relations. Whereas in modelling soil water movement in the unsaturated zone, a continuous values and smooth representation of the soil water retention curve is preferred (Tuller and Or, 2004; Khlosi *et al.*, 2008). This can be found by fitting a closed-form analytical expression to a discrete data set. Therefore the use of empirical models is very important to get these continuous curves. These models use inverse methods that rely on mathematical models. Various mathematical models are proposed in the literature to represent the soil water retention functions (Gardner, 1958; Brooks & Corey, 1964; Campbell, 1974; van Genuchten, 1980; Kosugi, 1999; Omuto, 2009). Among these, the most commonly known is an equation proposed by Brooks and Corey (1964):

$$S_e = \left(\frac{\psi_a}{\psi} \right)^{\lambda}, \tag{2.13}$$

where S_e is normalized/dimensionless water content, i.e. $S_e = (\theta - \theta_r)/(\theta_s - \theta_r)$, θ_s and θ_r are the saturated and residual volumetric water contents respectively, ψ is the matric suction, ψ_a is the air entry value and λ the is pore size distribution index.

Another, commonly used model for the relationship between matric suction and the normalized water content was given by van Genuchten (1980):

$$S_e(\psi) = \theta_r + \frac{\theta_s - \theta_r}{\left[1 + |\alpha\psi|^n\right]^m}, \text{ for } \psi < 0, \tag{2.14}$$

$$S_e(\psi) = \theta_s, \text{ for } \psi > 0, \tag{2.15}$$

where α, n, and m are three different soil parameters, and $m=1 - 1/n$,

Equation (2.14) is more flexibility Equation (2.13). Equation (2.14) contains four independent parameters (θ_r, θ_s, α and n) that have to be determined from the water retention data (van Genuchten, 1980).

The corresponding isothermal hydraulic conductivity function, K_L (S_e) is:

$$K_L(S_e) = K_L S_e^{\,l}\left[1 - \left(1 - S_e^{1/m}\right)^m\right]^2, \text{ for } \psi < 0, \tag{2.16}$$

$$K_L(S_e) = K_s, \text{ for } \psi > 0, \tag{2.17}$$

in which K_s is a matching point at saturation or saturated hydraulic conductivity (cm d^{-1}), l is an empirical pore-connectivity parameter, and S_e is effective saturation.

S_e is also given by:

$$S_e(\psi) = \frac{\theta(\psi) - \theta_r}{\theta_s - \theta_r}, \tag{2.18}$$

whereas the modified Mualem-van Genuchten water retention function explained by Schaap and van Genuchten (2006) and proposed by Vogel and Cislerova (1988):

$$S_e(\psi) = \theta_r + \frac{\theta_m - \theta_r}{\left(1 + |\alpha\psi|^n\right)^m} \text{ for } \psi < \psi_s, \tag{2.19}$$

$$S_e(\psi) = \theta_s, \text{ for } \psi > \psi_s, \tag{2.20}$$

where $\theta_m = \theta_r + (\theta_s - \theta_r)(1 + |\alpha\psi_s|^n)^m$, and ψ_s is an introduced small capillary height.

Combining Equations (2.16) and (2.19) leads to the corresponding modified Mualem-van Genuchten (MMVG) model of hydraulic conductivity (Schaap and van Genuchten, 2006):

$$K_L(S_e) = \frac{K_s . S_e^l \left(1 - F(S_e)\right)}{\left(1 - F(1)\right)^2}, \text{ for } \psi < \psi_s, \tag{2.21}$$

$$K_L(S_e) = K_s, \text{ for } \psi > \psi_s, \tag{2.22}$$

where: $F(S_e) = \left(1 - S_e^{*1/m}\right)^m$ and also $S_e^* = S_e\,[\theta_s - \theta_r / \theta_m - \theta_r]$ (Vogel *et al.*, 2000; Schaap and van Genuchten, 2006).

Mathematical models that are used to estimate water retention in soils have been developed mostly for the wet range and hence they are ineffective for applications at the drier end while low water contents are still important (Rossi and Nimmo, 1994). Most models also assume that soil water pressure head is accredited to capillary forces only by ignoring the adsorptive forces relying on the oversimplified representation of medium pores as a bundle of cylindrical capillaries (Zhang, 2011). Similarly in residual soil water content it is often assumed that aqueous flow is negligible (Zhang, 2010).

All the mathematical models perform differently due to differences in the textural class and water content range of the soils. Under saturation conditions the van Genuchten (1980) model performed better than other five parameter models and Kosugi (1999) performed better in the four parameter models (Too *et al.*, 2014). On the other hand Campbell (1974) performed better in three parameter models. Generally the five parameter models performs better compared to those with few parameters in all water content ranges (Too *et al.*, 2014).

2.2.3.2 Saturated and unsaturated hydraulic conductivity

Saturated hydraulic conductivity (K_s) is the ability of the soil to transmit water at full saturation or at zero or positive capillary pressure whereas unsaturated hydraulic conductivity provides the water conductivity in terms of capillary pressure, $K_L(\psi)$, or water content or relative saturation $K_L(S_e)$ (Schaap *et al.*, 2003; Reynolds and Topp, 2008).

Hydraulic conductivity is the coefficient that depicts the permeability of porous media to water flow at various water contents (Ripple *et al.*, 1972; Elango, 2011). It is a major component of the general flow equation and under unity flow gradient it is assumed to be equal to flux. However, in practice this is not encouraged given the effect of matric suction on unsaturated soils. K_L is the most difficult hydraulic property to measure accurately. It differs over many orders of magnitude between different soils and within the same soil. The K_L could be determined as a function of either water content or matric suction (Mckenzie and Jacquier, 1958 and Dirksen,1999).

2.2.3.2.1 Determining saturated hydraulic conductivity

Currently there are a number of methods to determine saturated hydraulic conductivity (K_s). These methods can be directly measured either *in situ* or in laboratory. Some of the direct measurements include the Guelph permeameter (Reynolds and Elrick, 1986), constant-head permeameter (Klute, 1965), disk permeameter (Perroux and White, 1988), double tube method (Bouwer, 1964), velocity permeameter (Merva, 1987). Reynolds and Topp (2008) explained these methods in detail. Indirect methods include the development of mathematical models based on bulk density and other physical soil properties. A number of mathematical models have been developed to estimate K_s (Edoga, 2010).

2.2.3.2.2 Determining unsaturated hydraulic conductivity

Direct measurement methods

Fluid flow through porous media driven by gradients in water potential is highly sensitive to the structure and especially to the size and connectivity of the water-filled part of the pore space. This is why hydraulic conductivity is an extremely nonlinear function of the soil water content $K_L(\theta)$ or the related soil water potential $K_L(\psi)$. This nonlinearity and the sensitivity to the fluid configuration within the pore space make the unsaturated hydraulic conductivity difficult to measure directly (Schaap *et al.*, 2003; Weller *et al.*, 2011). Decrease in conductivity with reducing pressure is especially strong for pressures less than the air entry value or water contents smaller than the water content at the air-entry pressure (Schaap *et al.*, 2003). Therefore, in many applications $K_L(\psi)$ is derived from the water retention characteristic, $\theta(\psi)$, which is more easily measurable (Weller *et al.*, 2011). This is done by using mathematical models that use similar parameters as soil water retention curve uses.

Recent reviews of direct methods for measuring the hydraulic conductivity and diffusivity of unsaturated soils are given by Green *et al.* (1986), Klute and Dirksen (1986), and Reynolds and Topp (2008) for laboratory and field conditions. Some of the methods stated include tension/disk infiltrometer (both laboratory and field method), laboratory based evaporation method, instantaneous profile/the internal drainage method which measures K_L *in situ*.

Indirect estimations

Since soil hydraulic properties are critically important, *in situ* or direct measurements are preferred because they are highly sensitive and variable in space and time. However, direct measurement is not always possible. Hence the unsaturated hydraulic conductivity function can be predicted from the soil water retention curve (SWRC) with the use of parametric models that use similar parameters as the SWRC. For numerical models to accurately predict water flow in the unsaturated zone, parametric functions has to be determined accurately (Ruan and Illangasekare, 1999). Some of the well-known mathematical models to estimate K_L include the van Genuchten (1980) (Equation 2.16) and Modified van Genuchten-Mualem (Equation 2.21).

Many literatures show that there is no single procedure and model to estimate the hydraulic conductivity from full saturation to the oven dry condition. Common conceptual models for unsaturated flow assume the soil matric suction is accredited to the capillary force only; hence these mathematical models are effective at high to medium water contents but give poor results at lower water contents (Zhang, 2011).

2.3 Heat flow and temperature fluctuation

2.3.1 Theories of heat flow and temperature fluctuation

When two bodies that have different temperature come in contact to each other there will be an energy transfer from the hotter to the colder body and this is referred to as heat energy (Carslaw and Jaeger, 1959). Temperature is also defined as the thermal state of the body with respect to its ability to transfer heat, so temperature is the indicator of the driving force for heat flow (Lal and Shukla, 2004). There are three ways in which heat flows from one body to the other and these are dependent on their temperature (Carslaw and Jaeger, 1959; Hillel, 2004). Firstly, conduction; which is described as a process in which the heat transfers from one body to the other through the bodies themselves in contact by intermolecular forces. Secondly, convection; which is attributed to the relative motion of some part of the body carrying the heat. Thirdly, radiation; refers to the movement of heat energy in the form of electro-magnetic waves from all bodies above 0°K.

The governing equation for the movement of heat energy in a variably saturated rigid porous medium is given by the following energy conservation equation (Saito *et al.*, 2006):

$$\frac{\partial S_h}{\partial t} = \frac{\partial q_h}{\partial z} - Q, \tag{2.23}$$

where S_h is the storage of heat in the soil (J m^{-3}), q_h is the total heat flux density (J m^{-2} s^{-1}) and Q (J m^{-3} s^{-1}) accounts for sources and sinks of energy (de Vries, 1963; Saito *et al.*, 2006):

$$S_h = C_n T\theta_n + C_w T\theta_l + C_v T\theta_v + L_o\theta_v, \tag{2.24}$$

$$S_h = \left(C_n\theta_n + C_w\theta_l + C_v\theta_v\right)T + L_o\theta_v \quad , \tag{2.25}$$

$$S_h = CpT + L_o\theta_v, \tag{2.26}$$

where T is the given temperature (°K), θ_n is the volumetric fraction of solid phase (m^3 m^{-3}), C_n, C_w, C_v and C_p are volumetric heat capacities (Jm^{-3} K^{-1}) of the solid phase, liquid water, water vapour and moist soil, respectively, and L_o is the latent heat of vaporization of water (J m^{-3}).

The total heat flux density, q_h, is (de Vries, 1958):

$$q_h = -K_t\frac{\partial T}{\partial z} + C_w T q_L + C_v T q_v + L_o q_v, \tag{2.27}$$

where, K_t is the apparent thermal conductivity of soil (J m^{-1} s^{-1} K^{-1}), and q_L and q_v are the flux density of liquid water and water vapour (m s^{-1}), respectively.

By combining Equations (2.23), (2.24) and (2.27), the governing equation for heat movement becomes (Nassar and Horton, 1992; Fayer, 2000; Saito *et al.*, 2006):

$$\frac{\partial C_p T}{\partial t} + L_o \frac{\partial \theta_v}{\partial t} = \frac{\partial}{\partial z}\left((\theta) \frac{\partial T}{\partial z} \right) - C_w \frac{\partial q_L T}{\partial z} - L_o \frac{\partial q_v}{\partial z} - C_v \frac{\partial q_v T}{\partial z} - C_w S T \,, \qquad (2.28)$$

where $C_w ST$ represents a sink of energy associated with root water uptake.

2.3.2 Previous studies on soil heat flow and temperature distribution

Soil temperature and heat flow have been studied by a number of scholars (Idso *et al.*, 1975; Asaeda and Ca, 1993; Niu *et al.*, 1997; Popiel *et al.*, 2001; Florides and Kalogirou, 2005). Soil temperature distribution in the profile is affected by several factors. These include the structure and physical condition of the soil surface, type and density of surface cover and climate interaction. The latter is determined by air temperature, wind, solar radiation, air humidity and rainfall (Popiel *et al.*, 2001; Holmes *et al.*, 2008).

Soil water content has a great influence on the diurnal range of surface temperature especially on bare soils. This is because of the increase in evaporation, heat capacity and thermal conductivity of the soil (Arya, 2001). Nobel and Geller (1987) also explained that maximum soil surface temperature is influenced by short wave radiation, wind speed and the surrounding air temperature. A study conducted by Asaeda and Ca (1993) showed that the transport of water vapour inside the soil has an important effect on the subsurface distribution of temperature. This study also compared the temperature distribution on bare and mulched/covered surfaces. The temperature of the bare surface is much lower compared to covered surfaces. Temperature in covered surfaces is even higher than the air temperature during night time (Asaeda and Ca, 1993). Popiel *et al.* (2001) categorized the soil based on its temperature distribution as: (i) surface zone where the ground temperature is very sensitive to short time variations of weather, (ii) shallow zone where the ground temperature is almost constant and equals to the annual average temperature and (iii) deep zone where the temperature is practically constant but slowly increase with depth due to geothermal gradient. Based on their findings and classification, the surface, near surface and deep soil profile temperature distribution were classified to have a soil depth ranging from 0 to 1, 1 to 10 and >10 meter depths, respectively. Similar results were also showed by Shahran and Jadhav (2002) and Florides and Kalogirou (2005). Arya (2001) explained that the range of variability of daily soil surface temperature distribution decreases exponentially in depth and becomes insignificant around 1 meter depth.

Niu *et al.* (1997) regarded vapour phase transport to be more important than the liquid water flux for soil heat and water transport in drier soils. On the contrary, liquid water flux was still more significant than vapour transport in wet soils. Wetter soils exhibits lower surface temperatures compared to drier ones because of the greater loss of latent heat from the wet soils (Nobel and Geller, 1987).

Arya (2001) concluded that location (latitude), time of the year (season), net radiation at the surface, soil texture, ground cover and weather conditions are the major factors contributing to temperature distribution in soil profiles.

2.3.3 Soil thermal properties

Soil thermal properties, which includes thermal conductivity (K_t), volumetric heat capacity (C) and thermal diffusivity (D), are essential to conduct analysis and modelling related with numerous hydrological, agricultural and industrial applications (Smits *et al.*, 2009). These properties include thermal conductivity and resistivity, specific heat and thermal diffusivity. These essential soil properties are some of the elements determining mass-energy exchange processes occurring in the soil-plant-atmosphere system (Usowicz *et al.*, 1996).

2.3.3.1 Factors affecting soil thermal properties

Thermal properties are mostly influenced by water content, mineralogical composition, organic matter content and bulk density (Arya, 2001; Usowicz *et al.*, 2010). Thermal conductivity is mostly influenced by soil wetness and bulk density. It was also shown that differentiation in sand content has significant effect on spatial variability of the thermal conductivity (Usowicz *et al.*, 2010).

Many studies confirms that thermal properties are highly dependent on water content of soils (Misra *et al.* 1995; Smits *et al.*, 2009; Oladunjoye and Sanuade, 2012; Oladunjoye *et al.*, 2013; Busby, 2015). Generally these studies showed soil thermal properties increases with water content. Oladunjoye *et al.* (2013), Lydzba *et al.* (2014) and many other investigators confirmed that K_t, C and D increased with water content although other scholars pointed out that this is not true for some cases. For example, Sepaskhah and Boersma (1979) and Tarnawski and Leong (2000) concluded that K_t varies insignificantly at lower water contents around permanent wilting point. Misra *et al.* (1995) and Rubio (2013) also showed the increase of K_t in higher water contents, but the increase was insignificant closer to saturation which is true for D as well.

On the other hand the effect of temperature on thermal properties is complicated and it is not well studied and needs further research. Sawada (1977) conducted an experiment on frozen soils and showed that K_t and D increased with decreasing temperature and increasing water content. He also showed that the relation between D and soil water content is exponential and non-linear. Some investigators also ignore the effect of non-freezing temperature in influencing thermal properties and in developing mathematical models (e.g. Chung and Horton, 1987; Brandon and Mitchell, 1989).

2.3.3.2 Methods to determine soil thermal properties

2.3.3.2.1 Soil thermal conductivity

Thermal conductivity (K_t) describes the soil's ability to transfer heat mainly by conduction. It is understood to be the quantity of heat that flows through a unit area in a unit time under a unit temperature gradient (Bristow, 2002). The increasing use of soil thermal conductivity data input by simulation models requires procedures that can estimate or measure K_t for different soil conditions.

Direct measurement methods

Direct measurement of thermal conductivity can be done with single heat probe either in the field or laboratory. The equipment consists of a heater and a temperature sensor attached together in a thin needle-like probe (Bristow, 2002). After the probe is inserted to the soil, the temperature is measured during heating and cooling. Details on the operation of the single heat probe were described by Hanson *et al.* (2000). Heat flow on this instrument is measured by the probe's sensors response to temperature. The response rate of the heat sensors depicts the rate at which heat is conducted away from the probe and thus the thermal conductivity of the soil.

Predictive methods

De Vries (1952) proposed a modelling approach towards obtaining K_t of soils. The soil constituent could vary from liquid water, ice, air and minerals and organic matter. Based on de Vries's theory, the K_t of a porous medium does not only depend on its composition, but also on the pore size distribution and geometry. He approximated K_t by the following empirical formula:

$$K_t = \frac{\sum K_n X_n \lambda_n}{\sum K_n X_n}, \tag{2.29}$$

where K_n is weighting factor of the constituents, X_n volume fraction of the component of the media and λ_n is also the thermal conductivity of the fractional constituent.

Considering soil as the mixture of water, gas and minerals with volume fractions, X_w, X_a and X_m, and thermal conductivities of components λ_w, λ_a and λ_m respectively, then the overall thermal conductivity of the soil C_λ can be expressed as (de Vries, 1963):

$$K_t = \frac{K_w X_w \lambda_w + K_a X_a \lambda_a + K_m X_m \lambda_m}{K_w X_w + K_a X_a + K_m X_m}, \tag{2.30}$$

Where K_w, K_a, and K_m are weighting factors that enhance or dampen the influence of the soil constituents i.e. water, air, and an average value for the solids, respectively (Westermann, 2010).

On the other hand, de Vries (1963) and Hopmans *et al.* (2002) defined soil thermal conductivity (K_t) to be a function of mineral type and geometrical arrangement of the various constituents, as well as highly dependent on the water content of the soil. Based on this definition, Chung and Horton (1987) proposed the following mathematical model to predict K_t based on the water content of the soil:

$$K_t = b_o + b_1\theta + b_2\theta^{0.5}, \tag{2.31}$$

where θ is the volumetric soil water content and b_0, b_1, and b_2 are empirical constants dependent on soil textural compositions.

2.3.3.2.2 Volumetric heat capacity of soils

Volumetric heat capacity (C) is the amount in the change of a unit volume's heat content per unit change in temperature (Hillel, 2004). It depends on the composition of the soil's solid phase (mineral and organic components), bulk density, and on soil wetness.

Direct measurement

Heat capacity can be measured with the dual probe method in which one probe contains a heating part and the other one contains a thermocouple (Hanson *et al.*, 2000). Hanson *et al.* (2000) explained the way how this apparatus measures the heat capacity. The peak temperature change is indirectly related to heat capacity and both the peak temperature and the time required to reach the temperature show the thermal characteristic of the substance being investigated.

Indirect methods

Since water has a high heat capacity when compared to the solid and gas components of a soil, heat capacity and thermal diffusivity are extremely influenced by the water content of soils (Hanson *et al.*, 2000).

The heat capacity per unit volume of soil can be estimated by adding the heat capacities of the different soil components in one cm^3 (de Vries, 1963).

$$C = \sum \left(X_m C_s + X_w C_w + X_a C_a \right), \tag{2.32}$$

where C is the volumetric heat capacity of the soil, X_m, X_w and X_a denotes the volume fraction of the soil components (solids, liquid/water and gas/air respectively) and C_s, C_w and C_a are specific heat capacities of solids, liquids and gases, respectively.

2.3.3.2.3 Thermal diffusivity

Thermal diffusivity (D) is a change in temperature produced in a unit volume of medium depicted by the quantity of heat flowing through in a unit time under a unit temperature gradient (Hillel, 2004). It is also the ratio of thermal conductivity to the product of the specific heat and density:

$$D = \frac{K_t}{c\rho} = \frac{K_t}{C}, \tag{2.33}$$

where D is the thermal diffusivity ($m^2\ s^{-1}$), K_t is thermal conductivity ($W\ m^{-1}\ K^{-1}$), c is the specific heat capacity of the porous media ($J\ K^{-1}$, C is the volumetric heat capacity ($J\ m^{-3}\ K^{-1}$) and ρ is the density of the media ($kg\ m^{-3}$).

2.4 Bare surface evaporation in the presence of water table

2.4.1 Bare soil evaporation

Bare soil in this study refers to an arable land without any vegetation whereas bare soil evaporation is referring to the evaporation from such non-vegetated areas. Evaporation from bare soil surface in arid and semi-arid regions is characterized by vapour transport in the upper part and liquid transport in the lower part of the soil profile. Under such conditions, both phases must be taken into account to describe the movement of water and evaporation from soil above a water table. This requires location of the evaporation front, defined as the plane at which phase transformation occurs (Gowing *et al.*, 2006).

Three conditions are necessary for evaporation to occur and persist (Hillel, 1977; Rasheed *et al.*, 1989; Hillel, 2004). Firstly, there should be a continual supply of heat to meet the latent heat requirement of the liquid to be evaporated. Secondly, the vapour pressure in the

atmosphere over the evaporating body must remain lower than the vapour pressure at the surface of that body and thirdly, there must be a continual supply of water from or through the interior of the body to the site of evaporation. Under arid and semi-arid conditions where there is little or no rainfall and conditions are favourable for evaporation, a significant amount of soil water will be lost through this process. The first two conditions can be considered to be external to the porous body, as they are influenced by such meteorological factors as radiation, air temperature and humidity, and wind velocity, which together determine the atmospheric evaporativity. The third condition depends upon the content and potential of water in the porous body and upon its conductive properties, which determine the maximal rate at which the body can transmit water to the evaporation site (Hillel, 1977; Rasheed *et al.*, 1989; Hillel, 2004; Rose *et al.*, 2005). This shows that the rate of evaporation is determined by either the evaporativity of external environment or by the soil's ability to deliver water to the evaporation site or both. Hillel (2004) also stated that the rate of evaporation from bare surface will be more or less constant (steady state) under conditions of shallow water table. Since the ability of the soil to transmit water from the water table to the evaporation site (soil surface) is one of the main components that determines amount and rate of evaporation, the water flow and hydraulic properties are very important.

In arid and semi-arid areas where rainfall is very low and erratic, ground water is the primary source of fresh water (Gowing *et al.*, 2006; Jalili *et al.*, 2011). This water is abstracted mainly by borehole for human use. Shallow water table supplies water to plant roots for transpiration and the near soil surface zone to support evaporation. The ability of the soil to supply water to the site of evaporation is primarily dependent on the soil's physical properties and the depth of the water table. Researches show that the depth of water table has a significant effect on the rate of evaporation from shallow water tables (Gardner, 1958; Verma, 1974; Gowing *et al.*, 2006; Jalili *et al.*, 2011; Shokri and Salvucci, 2011; Assouline *et al.*, 2013; Hernández-López *et al.*, 2014). On the other hand, soil properties like soil texture, structure, density, porosity and other physical properties greatly affect the ability of the soil to transmit water upward from a water table (Lillak, 1969; Verma, 1974; Lewan and Jansson, 1996; Shokri and Salvucci, 2011; Li *et al.*, 2013).

2.4.2 Capillarity from shallow water table

Capillarity is the movement of fluids vertically inside narrow tubes of particles. The movement of water inside soil micro-pores is a very important phenomenon for a variety of environmental and agricultural uses like retention and movement of water and solutes through soils (Or and

Tuller, 2005). This upward movement is due to the existence of the capillary pressure at the interface of water molecules within a porous media (Smettem *et al.*, 2002). Or and Tuller (2005) explained that two opposite forces are responsible for capillarity from shallow water tables. These are adhesive forces between water molecules and the soil mineral particles and cohesive forces between the water molecules themselves.

The upward capillary water is dependent on soil properties, water and atmospheric parameters. Or and Tuller (2005) indicated that the capillarity phenomena is dependent of solid and the liquid inter-facial properties, like surface tension, contact angle of the water, soil surface roughness and geometry. Kramer & Boyer (1995) and Li *et al.* (2013) also explained the driving forces or causes of capillarity. Based on this, surface evaporation and removal of water from the root zone by plants are major driving forces. Soil texture and pore size distribution have also significant role in the upward movement of soil water from shallow water tables. The smaller the pore size distribution, the higher the upward movement of water flow (Li *et al.*, 2013). Again the pore size distribution is directly related with soil texture. Generally clay soils will have greater heights of capillarity than sandy and loam soils. But if a relatively course textured soil overlays on smaller sized textures like in some clay soils, the capillarity will be retarded due to formation of capillary barrier (Li *et al.*, 2013).

If the atmospheric evaporation demand is greater than the ability of the soil to supply water to the evaporation site in liquid phase, the phenomenon called evaporation front will be formed (Rose *et al.*, 2005; Or *et al.*, 2007; Jalili *et al.*, 2011). This is basically the development of hydraulic discontinuity between the water table and the evaporation site, i.e. ground surface and this affects the rate of evaporation significantly. During this time (during the formation of evaporation front), three soil water flow zones will be developed; a zone of liquid dominant flow above the water table, a zone of vapour dominated flow just below the ground surface and a mixed transition zone around the evaporation front (Rose *et al.*, 2005).

The maximum height that water can reach by capillarity in soils (h_{max}) can be estimated by using the Jurin equation (Hillel, 2004; Li *et al.*, 2013):

$$h_{max} = \frac{4\gamma \cos\beta}{dg\rho_w}, \tag{2.34}$$

where γ is the surface tension, d is the capillary diameter, ρ_w is the density of water, g is the gravitational acceleration, and β is the wetting angle.

Similarly Shokri and Salvucci (2011) proposed an equation to estimate h_{max} as:

$$h_{max} = \left(\frac{1}{\alpha} \frac{(n-1)}{n} \right)^{(1-2n)/n}, \quad (2.35)$$

where α and n are the fitting parameters of van Genuchten (1980) and related to the inverse of air entry value and pore size distribution, respectively. Equation (2.35) is used to calculate the maximum depth of water table hydraulically connected to the ground surface (h_{max}) when hydrostatic conditions are assumed and the viscous effect is ignored (Shokri and Salvucci, 2011).

Ehlers *et al.* (2003) also proposed an empirical equation to determine h_{max} from the relationship between capillarity and particle size distribution:

$$h_{max} = -0.3463(S_i + C_y)^2 + 24.525(S_i + C_y) + 484.47, \quad (2.36)$$

where h_{max} is the maximum depth/critical depth (mm), S_i is silt content (%) and C_y is clay content (%).

When the depth of the water table exceeds h_{max} for that soil, the rate of evaporation will be significantly lowered and evaporation front will be formed. This evaporation front moves downward in the first days and the rate of evaporation decreases significantly until the front reach h_{max}, where at this depth the evaporation front will be static and the rate of evaporation will be constant (Rose *et al.*, 2005; Gowing *et al.*, 2006; Shokri and Salvucci, 2011).

2.4.3 Estimation of bare soil water evaporation

2.4.3.1 Surface energy balance

Evaporation and sensible heat flux into the atmosphere require the availability of some form of energy at the earth atmosphere interface (Brutsaert, 1982). In places where there is no heating source from the interior earth, solar radiation becomes the only source of energy controlling the most micro-meteorological events in the layer of soil–atmosphere interface. Equations of the surface heat balance represent some particular cases of the basic law in physics, the law of energy conservation which states that the total energy of an isolated system remains constant or conserved over time. Therefore, to obtain an equation for the heat balance of the earth's surface, all the streams of the energy flowing between the element of the surface and the ambient space must be summarized (Budyko, 1958). For a bare soil surface, where energy storage is zero, surface energy balance at the soil–atmosphere interface can be quantitatively described as follows (Budyko, 1958; van Bavel and Hillel, 1976; Brutsaert, 1982; Qin *et al.*, 2002; Hillel, 2004; Saito *et al.*, 2006):

$$R_n = L_o E_s + H_s + G \tag{2.37}$$

This equation could be rearranged to solve E_s and be written as;

$$E_s = \frac{R_n - (H_s + G)}{L_o}, \tag{2.38}$$

where, R_n (w m^{-2}) designates the radiation flux of heat, H_s (w m^{-2}) for sensible heat flux density, G (w m^{-2}) soil surface heat flux density and L_oE (w m^{-2}) is the expenditure of heat for evaporation i.e. L_o (J kg^{-1}) for latent heat of evaporation and E_s (kg m^{-2} s^{-1}) stands for the evaporative flux.

2.4.3.2 Soil water balance

Bare surface evaporation is a key and one of the important components of soil water balance in dry land areas (Wythers *et al.*, 1999). Based on Hillel (2004), the change in water content in a soil profile (ΔW) is the difference between the total components under gains (W_{gains}) and losses (W_{losses}) of water in the soil profile:

$$\Delta W = W_{gains} - W_{losses} \tag{2.39}$$

By incorporating the components of gains and losses in the soil profile water balance, Equation (2.37) becomes (Hillel, 2004):

$$\Delta W = (P + I_s) - (R_o + D_r + E_s + T_r) \tag{2.40}$$

This function could be rearranged to solve E_s and be written as,

$$E_s = (P + I_s) - (\Delta W + R_o + D_r + T_r), \tag{2.41}$$

where P is the amount of precipitation, I_s is amount applied as irrigation, R_o is water loss as run off, D_r is water loss due to deep drainage, E_s is water loss due to evaporation from the bare surface, and T_r is the amount of water loss through transpiration.

2.4.3.3 Modelling

Models are some representations of the construction and working of some real events or systems under study whereas modelling is the process of building models (Maria, 1997; McHaney, 2009; Sokolowski and Banks, 2010). Similarly simulation is the act of executing, experimenting with or exercising a model or sets of models for a specific objective/intended

use. Hydrologic models are prominently used in characterizing and quantifying water flow in the vadose zone and sub-surface flows generally (Šimůnek *et al.*, 2012).

Computer aided modelling and simulations are becoming very important and getting a special attention nowadays. Models enable the user to manipulate the system's variables/parameters easily and helps to understand the interaction between variables easily that make up complex systems (Sokolowski and Banks, 2010; Sokolowski and Banks, 2011). Therefore models could be effective tools to understand complex processes if developed carefully and assisted by field collected data.

A lot of hydrological models are developed to simulate fluid flow in the unsaturated zone. Some of the models include:

The HYDRUS 1D/2D/3D

A numerical model used for simulating water, heat flow and solute transport in saturated and unsaturated soils (Simunek *et al.*, 1998). The Richard's and modified Richard's equations are solved in a mixed form by mass-lumped linear finite element discretization (Loukili *et al.*, 2008).

The Simultaneous Heat and Water (SHAW)

Simulates the freezing and thawing, simultaneous heat, water and solute transfer in one dimensional flow (Flerchinger, 2000). It uses initial conditions for soil temperature data, water content, daily or hourly weather data, parameters related with the vegetative cover, snow, residue and soil (Flerchinger, 2000).

The Canadian Land Surface Scheme (CLASS)

It is used to evaluate the vertical transfer of energy and water between the atmosphere and soil surface layers (Verseghy, 1991; Verseghy *et al.*, 1993).

The Hydrologic Evaluation of Landfill Performance (HELP)

This is a quasi-two-dimensional hydrologic model of water movement through landfills and accepts weather, soil and design data (Schroeder *et al.*, 1994). It estimates run off, evapotranspiration and drainage (Schroeder & Gibson, 1982).

2.4.4 Previous studies on bare soil evaporation

The process of evaporation in the presence of water tables has been studied by many investigators. Some of the most studied areas on bare evaporation included: soil properties and

evaporation (Hellwig, 1973; Rasheed *et al.*, 1989; Gowing *et al.*, 2006; Li *et al.*, 2013); dependence of E_s on atmospheric evaporative demand (Verma, 1974); critical water table depths and contribution to evaporation (Verma, 1974; Rasheed *et al.*, 1989; Rose *et al.*, 2005; Jalili *et al.*, 2011; Shokri and Salvucci, 2011; Li *et al.*, 2013; Assouline *et al.*, 2013). Little or no research has been conducted on bare soil evaporation from shallow water tables in South Africa, except some studies on evapotranspiration. Ehlers *et al.* (2003) and Haka (2010) studied evapotranspiration from shallow water tables on field crops while Zere (2005) studied the phenomena under veld grass. Based on Ehlers *et al.* (2003) findings, 30 to 65% of the crop water needs would be obtained from shallow water tables, whereas Haka (2010) showed that 12% and 27% of the evapotranspiration from canola and wheat under irrigation was bare soil evaporation, respectively. Zere (2005) also showed evapotranspiration on veld grass can vary from 50 to 90% of the total rain fall in driest and wettest areas respectively.

Based on Table 2.3 all of the studies showed that the rate of bare soil evaporation depends primarily on two major conditions, the atmospheric evaporation demand (AED) or potential evaporation and the ability of the soil to supply water to the evaporation zone. The rate of bare surface evaporation (E_s) depends on the atmospheric evaporation demand (AED) if the depth of water table is lower than the maximum height (h_{max}) that the water table is hydraulically connected to the surface (Philip, 1957; Gardner, 1958; Jalili *et al.*, 2011). On the other hand, if h_{max} is lower than the water table depth, E_s will be primarily dependent on the soil's physical characteristics.

Generally the evaporation rate decreases as the water table depth increases and vice versa. But there is no significant difference between AED and E_s when depth of water table is decreased until h_{max} (Rasheed *et al.*, 1989; Shokri and Salvucci, 2011). During high AED, the rate of bare surface evaporation (E_s) will not necessarily increase with decreasing water table depth due to the development of capillary barrier or surface crusting particularly if a fine textured soil underlies a course ones (Verma, 1974; Rasheed *et al.*, 1989; Li *et al.*, 2013). Saxena (1969) showed that in water table depths shallower than 600 mm, water is readily lost from most soils at a rate similar to that from a free water surface. Evaporation rates also decreased markedly as the water table is lowered to 2000 mm due to considerable reduction in capillary conductivity in the upper part of the soil column. Assouline *et al.* (2013) have also got a significant rate of evaporation up to 800 mm water table depth. A soil hydrological model developed by Chen and Hu (2004) showed that the soil water content in the first meter of the soil column with ground water was 21% greater than without ground water.

A non-steady state experiment by Jalili *et al.* (2011) showed maximum and minimum values of 3-7, 1.4-6.6 and 0.2-6.5 mm day^{-1}evaporation rates from 300, 500 and 800 mm water table depths with AED varying from 2.66-14.5 mm day^{-1}, respectively. Rose *et al.* (2005) have also got an evaporation rate of 1.3, 1.1 and 0.3 mm day^{-1} measured from water table depths of 300, 450 and 700 mm, respectively. Research by Gowing *et al.* (2006) indicated that the measured E_s was 1.1 and 0.97 mm day^{-1} for 450 and 700 mm water table depths, respectively.

A study by Shokri and Salvucci (2011) showed that the maximum height of capillary flow from the water table (h_{max}) was estimated to be 110, 200 and 380 mm for soil particle sizes of 1.02, 0.4 and 0.16 mm, respectively. The study also concluded that as long as the water table is below h_{max}, lowering the water table has no significant effect on total evaporation rate. Rasheed *et al.* (1989) also showed similar results. The higher the sand fraction, the deeper will be evaporation front formation. Keeping the water table below 300 mm below sand surface reduced E_s by 50% of the open water surfaces (Hellwig, 1973). The rate of evaporation even decreased rapidly by decreasing the content of very fine sand particles in the soil profile. Increasing the AED also increases h_{max} and at 1000 mm depth of water table, E_s is reduced by 37% of AED.

Table 2. 3 Summary of previous studies on evaporation under different water table depths and soil types

No.	Method	Water table depth (mm)	Soil textural class	Main focus of the study	Authors
1	Field lysimeter and numerical simulation	800	Fine sand	Critical water table depth and contribution to evaporation	Assouline *et al.* (2013)
2	Field lysimeter	300, 500, and 800	Clay-loam	The effect of water table depth on evaporation rate	Jalili *et al.* (2011)
3	Column experiment	300, 450 and 700	Sandy loam	Water table depth and rate of evaporation	Rose *et al.* (2005)
4	Column experiment	0 and 600	Sandy soil	Effects of textural constituents and arrangement on capillarity of water from ground water table.	Shokri & Salvucci (2011)
5	Numerical simulation	450 and 700	Sandy loam, Clay loam, Silt loam and Coarse sand	The relation between soil texture and capillarity for different water table depths	Gowing *et al.* (2006)
6	Field lysimeter	600	Sandy soil	Water table depth and texture contribution to evaporation	Hellwig (1973)
7	Column experiment	0 and 1200	loamy sand	The relation between *AED, $^{**}h_{max}$ and $^{***}E_s$	Verma (1974)
8	Field lysimeter	500, 750, 1000, 1250,1500 and 1750	Loamy sand, Silt loam, Sandy loam and Silt loam	h_{max}, water table depth and E_s	Rasheed *et al.* (1989)

*AED refers to the atmospheric evaporative demand $^{**}h_{max}$ refers to the maximum water table depth that is hydraulically connected to the surface $^{***}E_s$ refers to bare soil evaporation

2.5 Concluding remarks

In this chapter a review has been made on the process of soil water dynamics focusing on evaporation under a shallow water table condition. The impact of temperature and heat flow in soil water flow has also been assessed. Based on the review, soil water moves primarily due to difference in pressure potential. Particularly water flow from shallow water tables, which is capillarity, is due to a negative pressure potential or matric suction between the water table and the unsaturated soil above it. Even though some investigators ignored it, difference in temperature or thermal gradient has also significant contribution in water flow especially in arid and semi-arid areas.

This review also shows that generally the rate of soil water evaporation from bare surface (E_s) decreases as the water table depth increases. But this only occurs if the critical capillarity depth (h_{max}) is higher than the depth of water table. If h_{max} is equal to or lower than the water table depth, the evaporation rate will not be affected significantly. The textural composition of the soil significantly affects h_{max}. Generally as the fine textural composition increases, h_{max} increases and E_s will also increase. But in some cases, like in wetter soils, if fine textured soil underlies a course texture soil and at high temperature or high evaporation demand, E_s will decrease due to formation of capillary barrier or surface crusting.

A significant amount of ground and surface water is lost to the atmosphere by evaporation. The full understanding of this phenomenon is still a challenge especially the interaction between bare soil surfaces and shallow groundwater tables since evaporation is a complex process. Especially evaporation from ground water is a complicated process and it must be assisted by models to understand the process and its impacts on the water resources. Some of the models used in simulating water flow in soil include Hydrus 1D/2D/3D, SHAW, CLAAS and HELP.

Finally it can be concluded that evaporation and related soil water dynamics are based on sound scientific theories and principles. But the application and practice of theories in estimating bare soil water evaporation is relatively limited especially soil water evaporation from ground water is not well studied in South Africa; even though some works have been done in estimating evapotranspiration by some investigators. Even the effect of heat flow and temperature fluctuation will be ignored in the evaporation process. In calculating the evaporative flux, the amount of water as a vapour phase will be assumed insignificant while vapour flow is important in arid and semi-arid environments.

CHAPTER 3

CHARACTERISING HYDRAULIC PROPERTIES OF AEOLIAN SOILS

3.1 Introduction

Hydraulic properties are major determinants of water flow and storage in soil profiles and their knowledge is vital in agricultural and environmental water management. They govern the ability of soils to transmit, distribute and retain water and its dissolved constituents (van Genuchten and Pachepsky, 2011). In the case of soil water evaporation, the rate of water supply and delivery at the surface is determined by soils hydraulic properties especially under unsaturated conditions.

Therefore to quantify and characterize evaporation from soils, knowledge of the soil hydraulic properties will be crucial. On the other hand, many environmental studies on the conservation and sustainable use of soil and water resources usually use simulation models (Wösten *et al.*, 1999). The major obstacle to the wider application of these models is unavailability of accurate estimates of soil hydraulic properties. The study of soil hydraulic properties is therefore important in understanding and modeling of soil water movement and distribution in the unsaturated zone (van Genuchten *et al.*, 1991; Khlosi *et al.*, 2008; Weller *et al.*, 2011; Perkins, 2011).

Soil water retention curve (SWRC) is one of the important hydraulic properties and describes the relation between the water content and the matrix potential of the soil. Saturated and unsaturated hydraulic conductivity are also some of the important hydraulic properties in the determination of fluid flow in porous media. Particularly these properties are valuable for water resource development, agricultural water management, waste disposal strategies, planning regional water supply, ground water flow modelling and predicting effect of rainfall variability (Elango, 2011).

Hydraulic properties are dependent on many factors. Some of them are pore size distribution, connectedness of pore spaces and tortuosity of the soil. Again these factors are dependent on the physical properties of the soil like texture, structure and organic matter content (Tuller and Or, 2004; van Genuchten *et al.*, 1991). Hydraulic properties are also dependent on the behaviour of the fluid (fluid density and viscosity) (Hillel, 2004; Kumar and Mittal, 2007).

Many studies are conducted in the determination of hydraulic properties (Brooks and Coorey, 1964; Van Genuchten, 1980; Green *et al.,* 1986; Klute and Dirksen, 1986; van Genuchten *et*

al., 1992; Dane and Hopmans, 2002). Generally three approaches are proposed to determine hydraulic properties of soils; field measurements, laboratory measurements and mathematical models. But direct measurement methods are costly and tiresome. Especially measurement of the unsaturated hydraulic conductivity is sometimes even impractical since unsaturated hydraulic conductivity is highly non-linear (van Genuchten *et al.*, 1991; Schaap *et al.*, 2003). Thus cheaper and more convenient estimating methods are needed to implement better practices for managing water and chemicals in the vadose zone (van Genuchten *et al.*, 1991). In this regard simple and cost effective theoretical methods that are based on the statistical pore size distribution models are the primary options currently (van Genuchten *et al.*, 1991; Schaap *et al.*, 2003).

Some studies have been conducted on hydraulic properties of the study area (Ehlers *et al.,* 2003; Chimungu, 2009; Barnard *et al.,* 2010). Ehlers *et al.* (2003) emphasized on the effect of texture on capillarity and other hydraulic properties of soils. They didn't study all soil hydraulic characteristics of the study area. Chimungu (2009) characterized the SWRC, hydraulic conductivity and the classification of pores based on their size distribution but he didn't clarify the pores classification based on their function. Whereas Barnard (2010) studied the drainage properties only. Hence, in this study the full hydraulic data was determined and the classification of pores and pore volumes based on their functions and the influence on hydraulic properties was given attention. Especially the use of fixed boundary during pore size classification based on their functions is unacceptable as criticized in the literature (Tuller and Or, 2004; Kutilek *et al.*, 2006; Kutilek and Jendele, 2008).

Therefore this study was conducted to describe the physical properties of the two soils (Clovelly and Hutton). More specifically it focuses on the determination of: (a) bulk density and particle size (b) saturated hydraulic conductivity (c) soil water retention curve (d) unsaturated hydraulic conductivity and diffusivity (e) the relationship between soil pore volume-size distribution and hydraulic properties.

3.2 Materials and methods

3.2.1 Description of the study area

This study was conducted on the field-lysimeter facility of the University of the Free State, Department of Soil, Crop and Climate Science, located at Kenilworth near Bloemfontein, South Africa. The details on the description of the layout and management of the lysimeters are provided in Section 5.2.2. Briefly, the lysimeter facility contains a total of 30 lysimeters of which 15 was filled with Clovelly soil sampled at Hoopstad. The remaining lysimeters were

filled with a Bainsvlei soil sampled at Kenilworth Experimental Farm. Only the topsoil (Orthic A, named as Ap-horizon in Table 3.1) and red apedal B were sampled from the Bainsvlei soil, thus, creating a typical Hutton soil. Since the completion of the lysimeter facility in 2000, many soil water and salinity management experiments were conducted (Ehlers *et al.*, 2003; Ehlers *et al.*, 2007; Barnard *et al.*, 2010). But most of these experiments didn't consider the basic physical properties of the soils like saturated hydraulic conductivity, water retention curve and pore size distribution.

3.2.2 Soil sampling and preparation

Three replicates of undisturbed soil samples were collected from the master horizons, A_p-horizons (0–300 mm) and the B-horizons (300–1200 mm depth). A core sampler was mounted vertically on the soil surface and forced in using a hydraulic jack to ensure sampling with minimum disturbance. Immediately after taking the core samples both ends were trimmed carefully and sealed with masonite boards to prevent any soil disturbance during transportation. The undisturbed samples were used for the determination of bulk density and the water content to matric suction relation (θ-ψ) in laboratory.

3.2.3 Determination of soil physical properties

3.2.3.1 Bulk density and particle size analysis

The bulk densities of the soils were determined with the core sampler method of Blake (1965). The main activities of the sampling procedures are stated in Section 3.2.2. Whereas for particle size analysis, disturbed soil samples were obtained from the master horizons of the two soils and the pipette method of Robinson (1922) was used. The major procedures of this method are summarized as follows.

The bulk samples collected from field were sieved with a 2 mm sieve to separate gravels from the soil sample. Then 40 gram soil with 3 replications was measured from each horizon. Then the particle size analysis were done with two major procedures: (i) sedimentation to separate the sand particles by chemical and mechanical dispersion then decantation (ii) sampling from the soil suspension with automatic pipette to determine silt and clay content. All these procedures are described in detail in Robinson (1922).

3.2.3.2 Saturated hydraulic conductivity

In this study the saturated hydraulic conductivity (K_s) was measured *in situ* by the constant head permeameter method as described by Rehynolds (2002) and Eijkelkamp Agrisearch Equipment (2004). Accordingly, a well was drilled using a 75 mm bucket auger. Great care

was taken when drilling the well to keep the augering shaft vertical and homogeneous since excessive enlargement of the well hole would lead to erroneous measurements. Then the permeameter was assembled and mounted to keep it stable inside the hole during measurement. Cylinders with a capacity of 20 litres, graduated with 1 litres intervals, were filled with water and attached to the permeameter with a tube as shown in Figure 3.1. The cylinder was kept 1 meter high to allow water to enter to the permeameter easily.

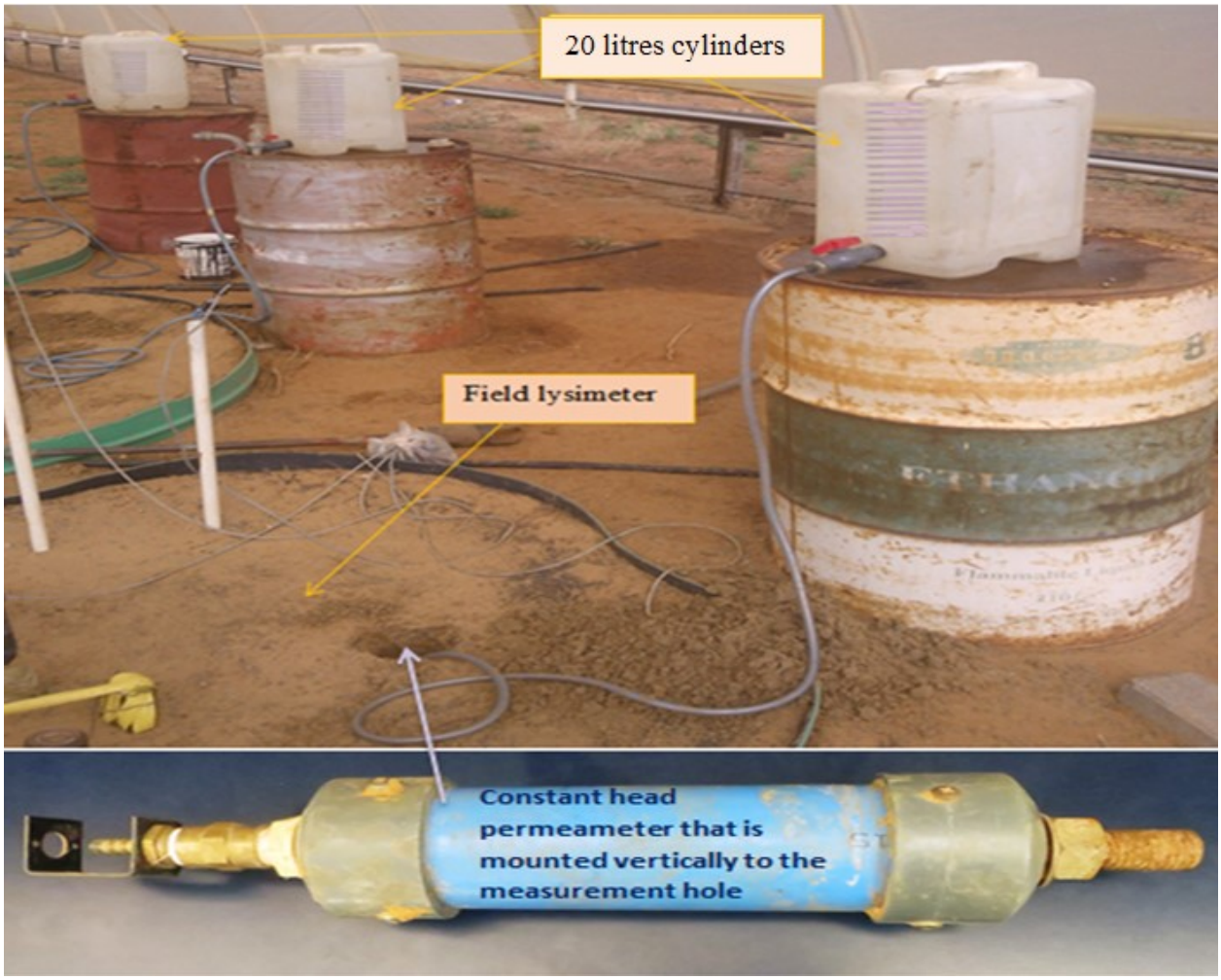

Figure 3.1 *In situ* measurement of the saturated hydraulic conductivity in the field lysimeter

The rate of water fall in the cylinders was measured using the described scale demarcated on the cylinder. The final infiltration rate (Q_I) was taken as the average of three consecutive readings at a steady state condition, i.e. when the difference in time was insignificant between consecutive readings. In this technique, the steady state flow rate or infiltration (Q_I) of water under a constant pressure (H) at the bottom of a cylindrical auger hole of radius (r) was measured, and the saturated hydraulic conductivity was calculated by measuring the change in the height of water in the reservoir with time (Amoozegar and Wilson, 1999):

$$K_s = \frac{C_f Q_I}{2\pi H^2}, \tag{3.1}$$

$$C_f = \sinh^{-1}\left(\frac{H}{r}\right) - \left[\left(\frac{r}{H}\right)^2 + 1\right]^{1/2} + \frac{r}{H}, \tag{3.2}$$

where K_s is the saturated hydraulic conductivity, Q_I is the steady state infiltration, H is the constant height of water (head of water), r is the radius of the well and C_f is a shape factor.

3.2.3.3 Soil water-matric suction relationships

In this study the soil water retention curve (SWRC) was measured with two laboratory procedures; the Hanging Water Column and the Pressure Plate Apparatus. The Hanging Water Column procedure of Buchner Funnel or Haines Apparatus was used to measure suction ranges (absolute values are used) from 0 to 10 kPa and it is based on the procedures explained in Dane and Hopmans (2002). The pressure plate apparatus was used to measure the SWRC from 10 to 1500 kPa suction ranges based on the procedures of Klute and Dirksen (1986) experiment.

For the experiments the undisturbed soil samples were saturated with de-aired water. This was accomplished by placing samples in suction chambers for 24 hours to get 100% saturation. Saturated samples were then transferred to the Hanging Water Column for measuring the SWRC at lower suction ranges. The samples were subjected to the following pressures; 0, 0.39, 2.55, 5.88 and 8.14 kPa. After completion of the lower suction experiment, the samples were transferred to the Pressure Plate Apparatus (Klute and Dirksen, 1986) where they were subjected to the following pressures; 10, 50, 100, 300, 500, 900 and 1250 kPa.

The observations from the two experiments were combined to construct the SWRC's using the van Genuchten (1980) model. This model was selected because it requires fewer parameters, and it is applicable to a wide range of textural soil classes (Too *et al.*, 2014) as given in Equation 2.14. To determine these parameters and fit the water retention curve, the RETC computer software was used by assuming m = 1 – 1/n (van Genuchten *et al.*, 1991).

3.2.3.4 Unsaturated hydraulic conductivity and diffusivity

Given the difficulty to measure the unsaturated hydraulic conductivity $K_L(\theta)$ and diffusivity $D_f(\theta)$ directly from *in situ* or laboratory, these important hydraulic properties were predicted from the SWRC using the van Genuchten-Mualem (1980) conductivity model which is available in the RETC computer program and given in Equation 2.16.

3.2.3.5 Pore volume and pore size relations

The pore size distribution was determined from the soil water retention curve. This was done by calculating the pore radius by using Equation 2.12 that relates pore radius with matric suction as it is explained in Section 2.2.3.1.

The pore sizes were also classified in relation to their function on plant growth based on the classification first proposed by Greenland (1977), but the thresholds of each category were adapted. The lower limits (LL) of the horizons were assumed to correspond to the residual water content which was already measured in laboratory. The drained upper limits (DUL) of the horizons were calculated from the silt and clay contents relationship to DUL which was proposed by van Rensburg (1988):

$$DUL = 0.0037\left(S_i + C_y\right) + 0.139\,, \tag{3.7}$$

Where DUL is the drained upper limit of the horizon ($mm^3\ mm^{-3}$), S_i is the silt content of the horizon, C_y is the clay content of the horizon. Then the corresponding pore sizes for DUL and LL were also determined from the pore volume-pore size response curve. The lower limit (LL) was assumed to be the upper and lower values of the residual and storage pores whereas the DUL was assumed to be the upper and lower values of the storage and transmission pores.

3.2.4 Statistical analysis

The deviation between measured θ-ψ values and those fitted by the van Genuchten model (van Genuchten, 1980) were assessed by Willmott (1982) statistics. The statistical parameters used for the assessment were: coefficient of determination (R^2); index of agreement (IOA); root mean square of error (RMSE) and the relationship to its unsystematic component (i.e. $RMSE_u$ and the ratio of $RMSE_u$ to RMSE). The difference in the soil water retention between the two soils was also compared by the t-statistics taking the water contents of the two soils at similar matric suction.

3.3 Results and discussions

3.3.1 Particle size distribution and bulk density

The physical properties concerning particle size distribution, bulk density and the saturated hydraulic conductivity of the Clovelly and the Hutton soils are summarized in Table 3.1. Despite the fact that both soils are of aeolian origin, the results showed that the physical properties differ considerably amongst the soils. Firstly, from the particle size distribution it

can be deducted that the Clovelly topsoil (A-horizon) and subsoil (B-horizon) belongs to a loamy-sand and sandy textural class, respectively. The Hutton soil has higher clay content in the top- and sub-soil and was classed as loamy-sand and sandy-loam, respectively. Both soils have a very fine sand grade, which is typical from the area where they were sampled (Bennie *et al.*, 1994). Aeolian soils, yellow brown and red apedal B's, are generally perceived to have a low chemical activity (Le Roux *et al.*, 2013).

Dunbar & Rodgers (1958) and Harmse (1963) are of opinion that the amount of clay content in aeolian sands will never be more than 5%, which is not the case in the soils under discussion. Harmse (1963) and Fey (2010) pointed out that the increase in clay content in the horizons of Clovelly and Hutton soils is neither a product of weathering nor inherent characteristics of the aeolian sands. Therefore the most probable processes accounted for the increase in clay content in the A_p horizon of Clovelly in the lysimeter would be the settlement of the wind-blown particles from the surrounding area and mixed to the top horizon. Whereas for Hutton B horizon, eluviation may have contributed to settle the clay particles and move down the profile with water and increased the clay content in the sub-soil. This change in particle sizes of the two soils will have a significant effect on the physical properties, like bulk density and saturated hydraulic conductivity, of the soils.

Table 3.1 Summary of the physical characteristics of the Clovelly and Hutton soils

Physical properties	Clovelly		Hutton	
	A_p	B	A_p	B
Particle sizes				
Total sand (%)	87.2	93.3	87.9	77.9
Coarse sand (%)	1.7	0.2	0.4	0.3
Medium sand (%)	10.3	6.0	7.3	5.4
Fine sand (%)	59.0	67.2	62.4	56.1
Very fine sand (%)	16.2	20.0	17.8	16.1
Silt (%)	6.5	3.0	4.1	4.0
Clay (%)	6.3	3.6	8.0	18.1
Bulk density (g cm^{-3})	1.3	1.5	1.4	1.7
K_s (mm hr^{-1})	63	80	60	26

The A_p-horizons of the two soils registered a lower bulk density than the B-horizons. Theoretically the bulk density of soils has a direct and positive correlation with the compaction of soils, which is highly affected by internal and external factors. As it is reported by Singer *et al.* (1981), Bennie and Krynauw (1985) and Chaudhari *et al.* (2013), the internal factors include

particle size distribution, organic matter content, mineralogy and water content of the soil. Whereas the external factors are mainly related to the compaction effect during farming activities. In this regard, the bulk density of Clovelly horizons increased down the profile similar as the findings of Aşkin and Özdemir (2003). However, in Hutton soil the bulk density increased down the profile which is inconsistent with the reports of Singer *et al.* (1981) and Bennie & Krynauw (1985). This could be due to a number of water and salinity management experiments that have been conducted on the experimental site (Ehlers *et al.*, 2003; Ehlers *et al.*, 2007; Barnard *et al.*, 2010 and Haka, 2010). During this experiment the profiles of the soils were subjected to shallow water tables for a long period of time. The shallow water table experiments would have created an external load to the sub-soil and increased the bulk density. These soils are also hydro-collapsible soils i.e. get compacted easily when some load is applied and their structure breaks easily as they get wet. These phenomena are well explained by Schwartz (1985) and El Howayek *et al.* (2011).

3.3.2 Soil water retention curve

Figures 3.2 and 3.3 depict the relationship between the average soil water content and matric potential of the combined data set (0-1500 kPa) for the corresponding horizons of the Clovelly and Hutton soils, respectively. The full hydraulic data that shows the measured θ-ψ, fitted θ-ψ, estimated K_L-θ and estimated D_f-θ of the two soils with their diagnostic horizons are also provided in Appendices 3.1-3.4.

Concerning the Clovelly soil, the soil water retention curves of the A_p and B horizons show that the soil water content ranged from 0.07 to 0.391 and from 0.05 to 0.4 mm^3 mm^{-3} for the respective horizons. It is clear that the B horizon held relatively higher water contents than the A_p horizon at lower suction ranges, approximately 0-8 kPa. The SWRC of the two horizons crossed near 8 kPa with the B- horizon maintaining a lower soil water content thereafter as matric suction is increased. This crossing of the SWRC suggests differences in pore size distribution of the two horizons. This result is consistent with the particle size distribution of the two soils with their diagnostic horizons.

Concerning the Hutton soil, the SWRC of the A_p and B horizons indicated that the soil water content varying from 0.091 to 0.374 and 0.095 to 0.366 over the 0 to 1500 kPa range, respectively. Due to the higher clay content (18%) and total sand fraction (88%) in the B- and A_p horizon, respectively, the SWRC of the B-horizon assumes a higher soil water regime at lower matric suction ranges, which is approximately 0-1 kPa. This result suggests that the B-horizon had a higher water retention and capillary pores compared to the A_p horizon.

Occupying a higher soil water regime A_p horizon from 0 to 1 kPa illustrates that it had a greater total sand fraction which have more non-capillary conducting pores resulting rapid release of water with increasing matric suction. A relatively more developed S-shaped SWRC was associated with Clovelly than Hutton soil form, an attribute explained by the high total sand fraction of the respective horizons.

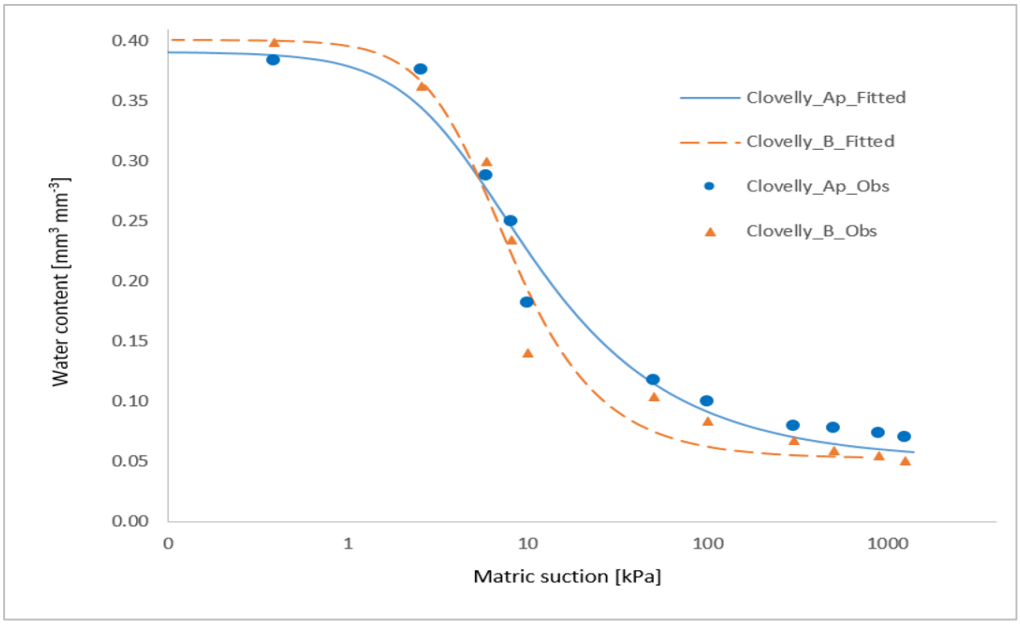

Figure 3.2 Comparison of observed and fitted SWRC for the two horizons of the Clovelly soil

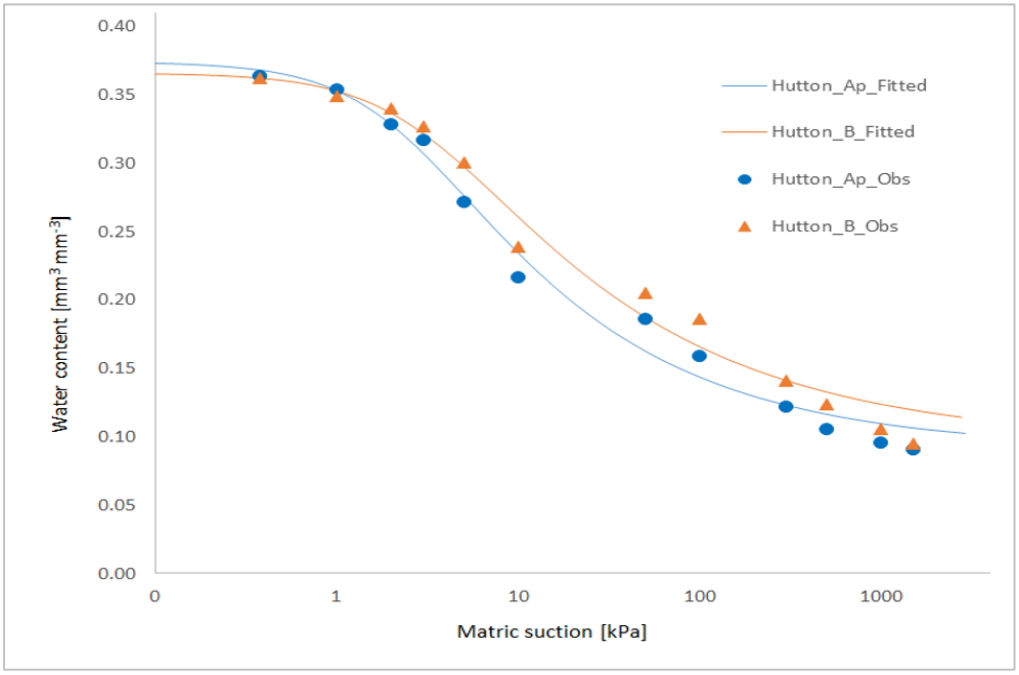

Figure 3.3 Comparison of observed and fitted SWRC for the two horizons of the Hutton soil

Table 3.2 summarizes the van Genuchten (1980) model parameters and their performance evaluation in fitting the SWRC of the two soils with their diagnostic horizons. The performance of the van Genuchten (1980) model was evaluated by the Willmott (1982) statistics. All the statistical parameters showed that the model estimated the SWRC of the two soils and their diagnostic horizons quiet well. This result corroborated with literature reports from various researchers (Vogel *et al.*, 2001; Abrisqueta *et al.*, 2006; Galage *et al.*, 2013).

The difference between the two horizons of Clovelly and Hutton soil forms were evaluated with a t-test. Based on the results of the t-statistics, there was a significant difference between the corresponding horizons of the two soils with a t-stat of 2.37 and 3.58, respectively (with a tabular value of 2.18 and alpha of 5%).

Table 3.2 Parameters of the van Genuchten model and the results of the Willmott statistics

Horizon	θ_r [mm mm^{-1}]	θ_s [mm mm^{-1}]	α	n	R^2	IOA	RMSE	RMSEs	RMSEu	$RMSE_u$ to RMSE
Cl-A_p	0.051	0.391	0.00370	2.063	0.98	1.00	0.017	0.005	0.019	1.115
Cl-B	0.045	0.401	0.00320	3.124	0.98	1.00	0.021	0.005	0.020	0.979
Hu-Ap	0.091	0.374	0.00330	2.102	0.99	1.00	0.011	0.003	0.011	1.002
Hu-B	0.095	0.366	0.00290	1.418	0.98	1.00	0.014	0.001	0.014	1.009

3.3.3 Hydraulic conductivity and diffusivity

Concerning the saturated hydraulic conductivity (K_s) of the two soils in Table 3.1, it is clear that the effect of the different textures was reflected on the soil's corresponding saturated hydraulic conductivity (K_s). The lowest K_s value came from the Hutton B horizon which had the highest clay content of 18%. Highest K_s value of 80 mm hr^{-1}, which is an increase of 68% than that of Hutton-B, was recorded by the B- horizon of the Clovelly soil which corresponded well with the high fine sand content (67%). Similar results are reported by Dec *et al.* (2008) and Mckenzie (2010).

The relationships between the unsaturated hydraulic conductivity (K_L) and hydraulic diffusivity (D_f) to soil water content (θ) for the two soils and their diagnostic horizons are illustrated in Figure 3.4 and 3.5, respectively.

The hydraulic conductivity and diffusivity of these soils and their diagnostic horizons increased with increasing water content and vice versa. The magnitude of K_L and D_f were higher in

horizons dominated by sandy fractions than clay plus silt. In this study, the properties of the curves below the residual water content are not shown. However, above the residual water content the behaviour of the K_L-θ and D_f-θ relationships could be distinguished into three categories. The first category starts from the residual water content up to the water content corresponding to the curve inflection point. In this category, K_L and D_f increases by several orders of magnitude for a per cent change in soil water content. In the second category, K_L and D_f start to increase in a decreasing rate as the soil water content is increased to approach the second inflection point. After the second inflection point further increase in soil water content i.e. in category three, the values of K_L and D_f start to increase in multiple orders of magnitude.

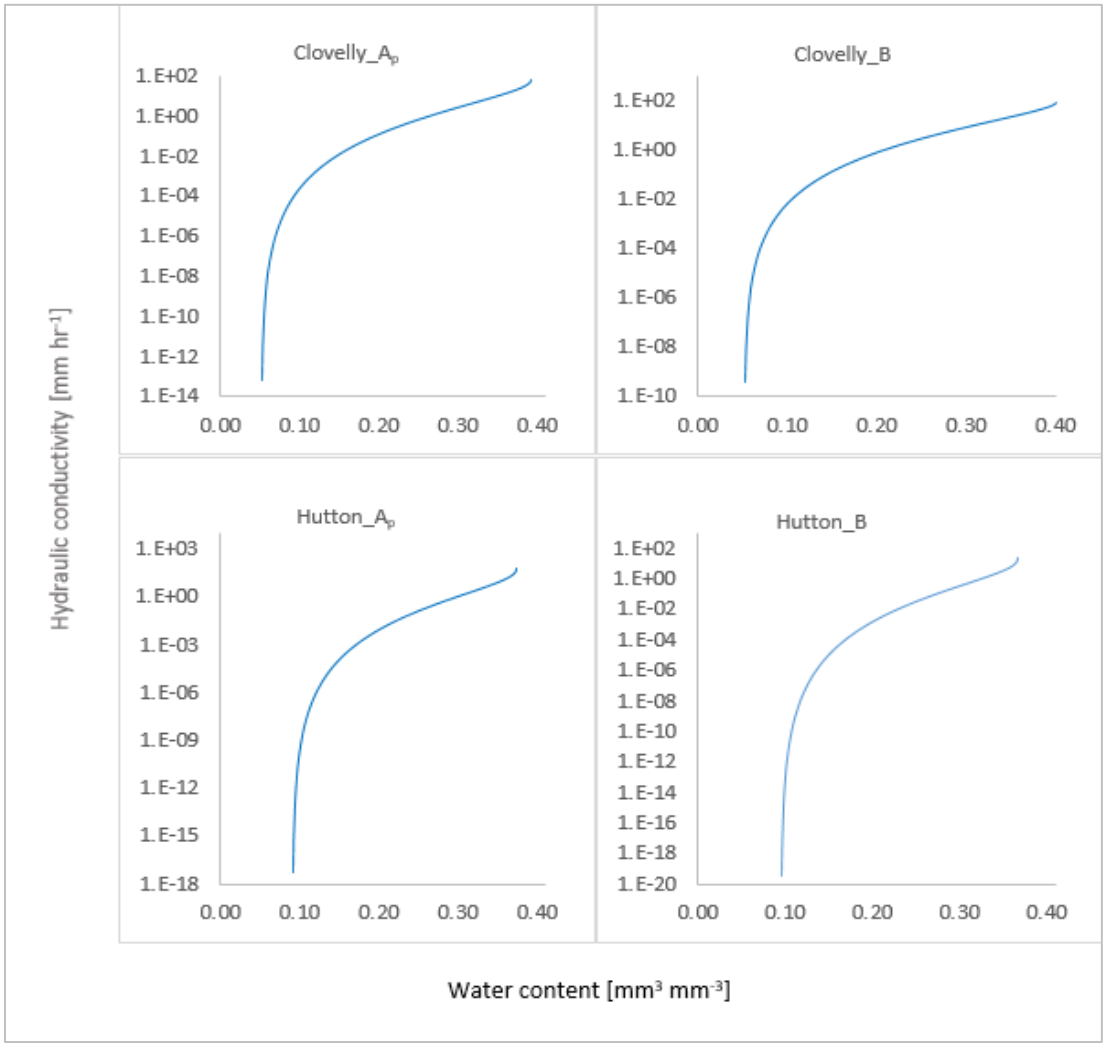

Figure 3.4 Hydraulic conductivity-water content relationships of the four horizons.

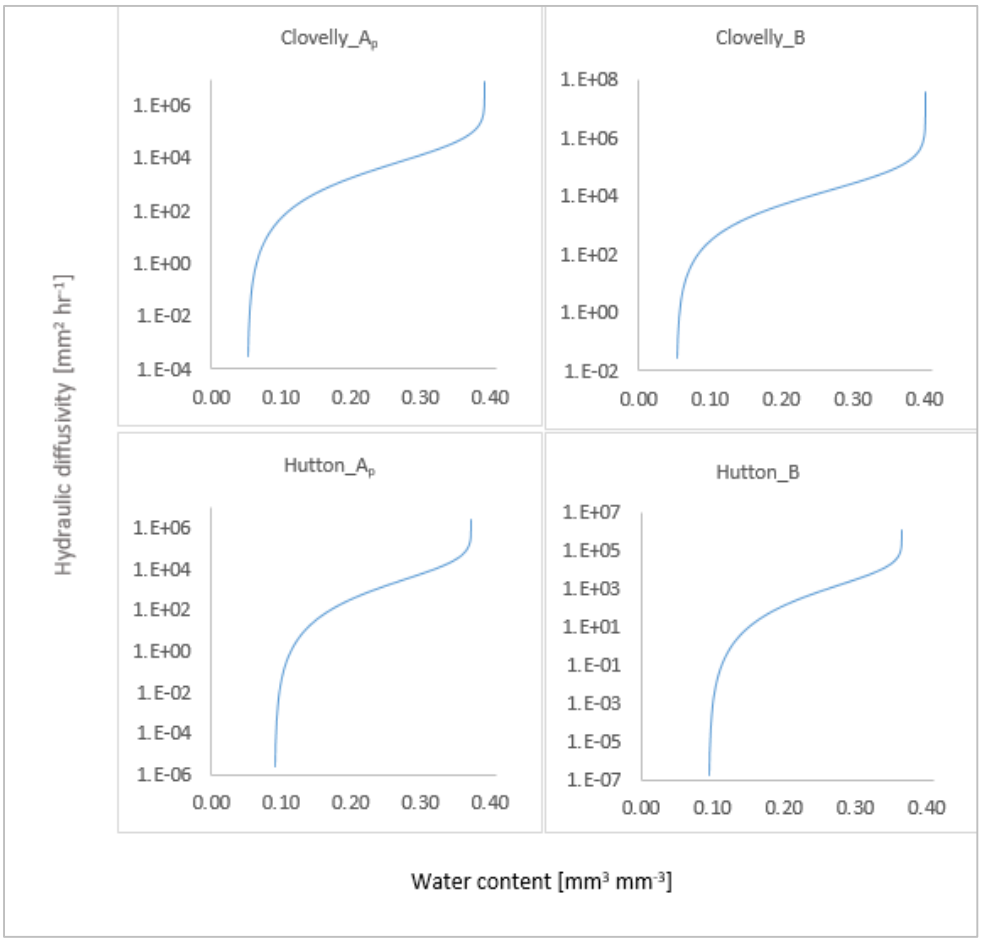

Figure 3.5 Hydraulic diffusivity-water content relationships of the four horizons.

In this category K_L kept up with the soil maximum infiltration capacity of the soil, which is also referred as K_s, while D_f increased with many orders of magnitude above K_s with smaller increase in water content above the air entry value.

A small variation in water content closer to saturation affected the $K_L(\theta)$ and $D_f(\theta)$ significantly as it is reported similarly by Vogel *et al.* (2001). The K_L and D_f of the two soils were higher in horizons dominated by sandy fractions than clay plus silt. This is because the hydraulic functions are influenced by structural and/or macro-pores at higher soil water contents (van Genuchten *et al.*, 1991; Vogel *et al.*, 2001; van Genuchten and Pachepsky, 2011). The van Genuchten model was also more sensitive near saturation for small changes in $\theta(\psi)$. Nevertheless, the van Genuchten-Mualem hydraulic conductivity model have shown to be reliable in estimating unsaturated hydraulic conductivity functions which corresponds with the reports of Chimungu (2009), Kadhim (2011), Perkins (2011) and Adhanom *et al.* (2012).

3.3.4 The effect of pore size distribution on hydraulic properties

The relationship between pore volume and pore size of the two soils with their diagnostic horizons are given in Figure 3.6.

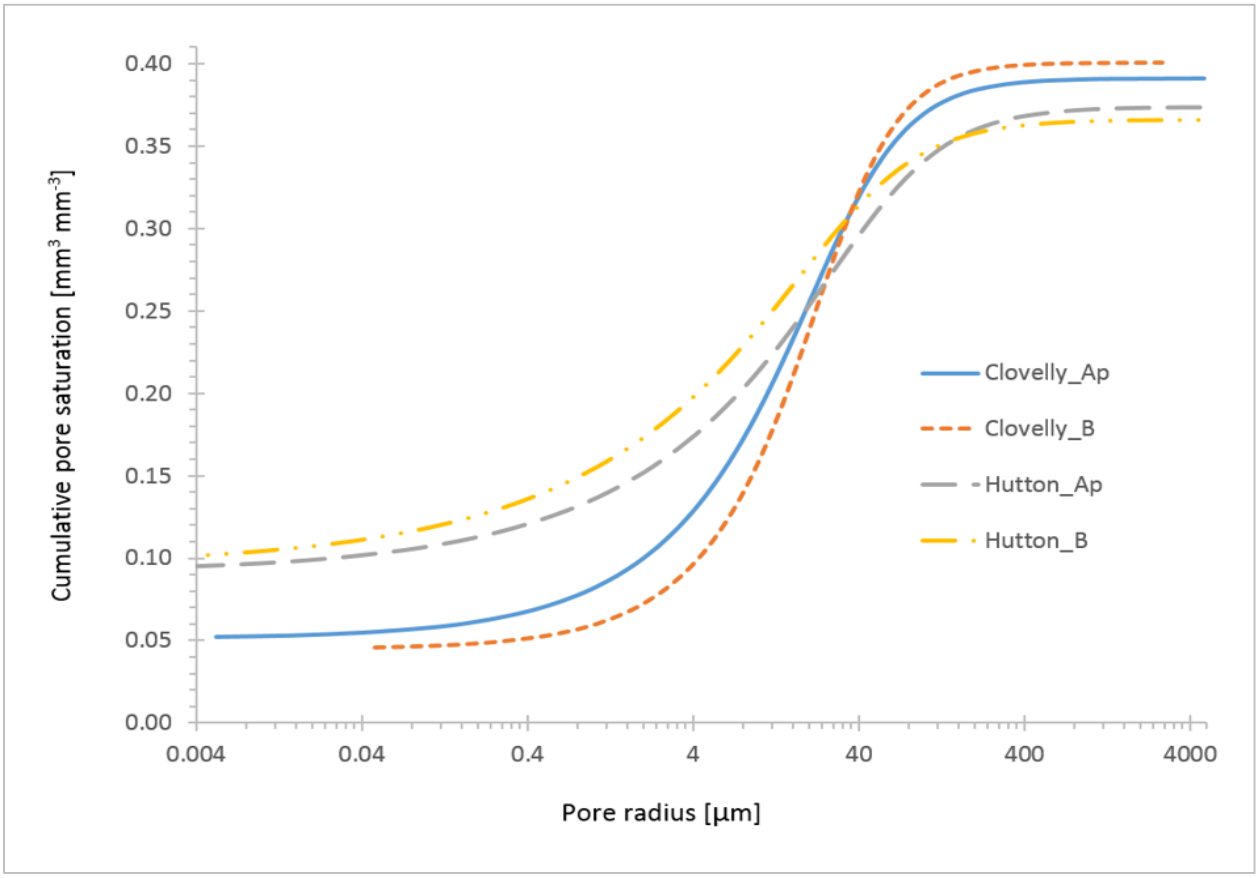

Figure 3.6 Pore volume-pore size response curve of the two soils and their diagnostic horizon

As it is evident from the pore volume-pore size response curve, the relationship between pore size and the corresponding cumulative pore volume was non-linear. Higher pore saturation could be observed from <35 µm for the Clovelly-A_p horizon, while in the B-horizon it was depicted from pore sizes greater than 35µm. Similarly, the B-horizon of Hutton had higher water content between pore sizes of 0-160 µm whereas the A_p horizon got higher water content greater than the 160 µm. This result could be explained by the different textural orientation of these soils horizons as observed earlier in this study. The increase in pore radius positively affected water content until the inflection point near saturation where further increase in pore size no longer increases pore saturation. This phenomenon could be explained by Loll and Moldrup (2000), Nimmo (2004), Heinemann (2005) and Kutilek and Jendele (2008).

The classification of soil porosity (Table 3.4) was developed depending on the concepts of field water capacity of the horizons (Hensely *et al.,* 2011) as summarized in Table 3.3. Based on

this, DUL was assumed to coincide with the lower and upper boundaries of the transmission and storage pores, respectively. Similarly, the LL values of the horizons were assumed to coincide to the lower and upper boundaries of the storage and residual/bonding pores, respectively.

Table 3.3 Critical water contents and their corresponding pore sizes that are important in the pore classification provided in Table 3.4 of the two soils with their diagnostic horizons

Horizon	DUL ($mm^3\ mm^{-3}$)	Pore radius (µm)	LL ($mm^3\ mm^{-3}$)	Pore radius (µm)
Clovelly-A_p	0.1864	9.44	0.057	0.098
Clovelly-B	0.1634	11.67	0.047	0.098
Hutton-A_p	0.1838	5.19	0.105	0.098
Hutton-B	0.2208	6.44	0.117	0.098

Table 3.4 Pore classification in relation to pore function among the horizons

Pore class	Pore radius [mµ]				Dominant functions
	Clovelly-A_p	Clovelly-B	Hutton-A_p	Hutton-B	
Transmission pores	> 9.44	> 11.67	> 5.19	> 6.44	Air movement and drainage of excess water
Storage pores	0.098-9.44	0.098-11.67	0.098-5.19	0.098-6.44	Retention of water against gravity and release
Residual and bonding pores	< 0.098	< 0.098	<0.098	<0.098	Retention and diffusion of ions in solutions, support major forces between soil particles

Soil porosity can be described depending on their number, sizes and shape. Especially the size and distribution rather than the total pore volume is very important (Lal and Shukla, 2004). Many researchers (Johnson *et al.*, 1960; Brewer, 1964; Greenland, 1977; Luxmoore, 1981) classified soil pores based on their size distribution. But all of these classifications were based up on fixed boundaries for all soil types to define the pore category. However, several studies (e.g. Tuller and Or, 2004; Kutilek *et al.*, 2006; Kutilek and Jendele, 2008) criticized the use of

fixed boundary in classifying the soil pore system. Therefore, from this analysis it should be noted that the use of fixed boundary in classification of the functions of porosity of soils is practically unacceptable.

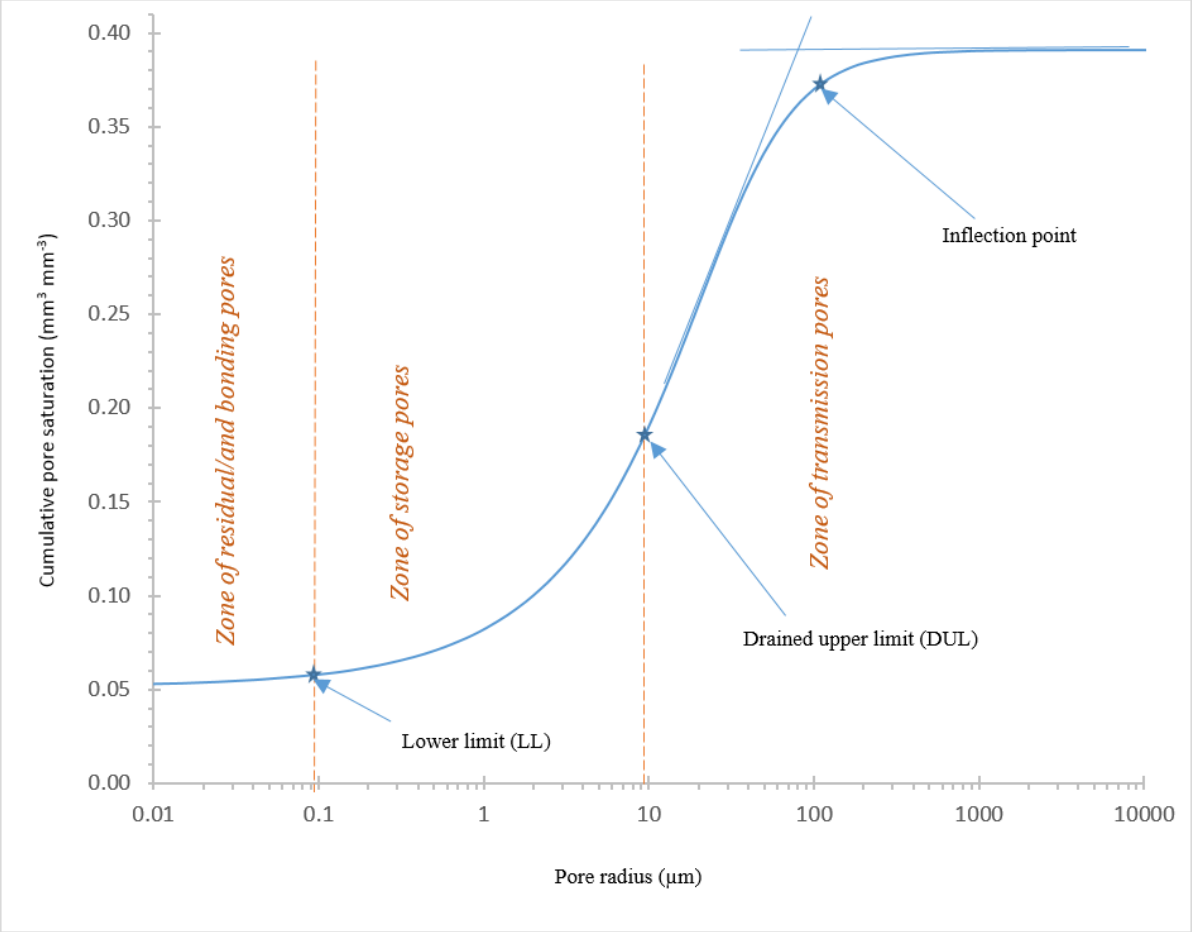

Figure 3.7 Functions of porosity classes in Clovelly-A_p horizon as a typical freely drained soil

The functions of the soil pores of Clovelly and Hutton soils with their diagnostic horizons are summarized in Table 3.4 for freely drained soils. The function of the pores can be further elaborated based on the pore volume-pore size response curve of Clovelly-A_p as a typical freely drained horizon as given in Figure 3.7. The transmission pores, which are responsible for the soil water beyond the DUL, are important for the movement of air and excess water in the profile (Luxmoore, 1981; Rowell, 2014; Lal and Shukla, 2004). In other words, these category of pores determine the saturated hydraulic conductivity and drainage of excess water. Whereas after the excess water in the saturated soil is removed by the force of gravity, then the water content of the soil is in the drained upper limit (DUL). The pores that are responsible for this stage of water content are called the storage pores which extends up to the lower limit of the soils. The water stored in these pores are available for plants and the evaporation and

transpiration processes are dependent on the availability of water in these pore classes. Below the lower limit of the storage pores, usually water in these pores is unavailable since it is strongly adsorbed in the micro-pores by the soil matrix. Therefore, knowledge of this pore classes and their function is very important for profile water management especially in irrigation scheduling.

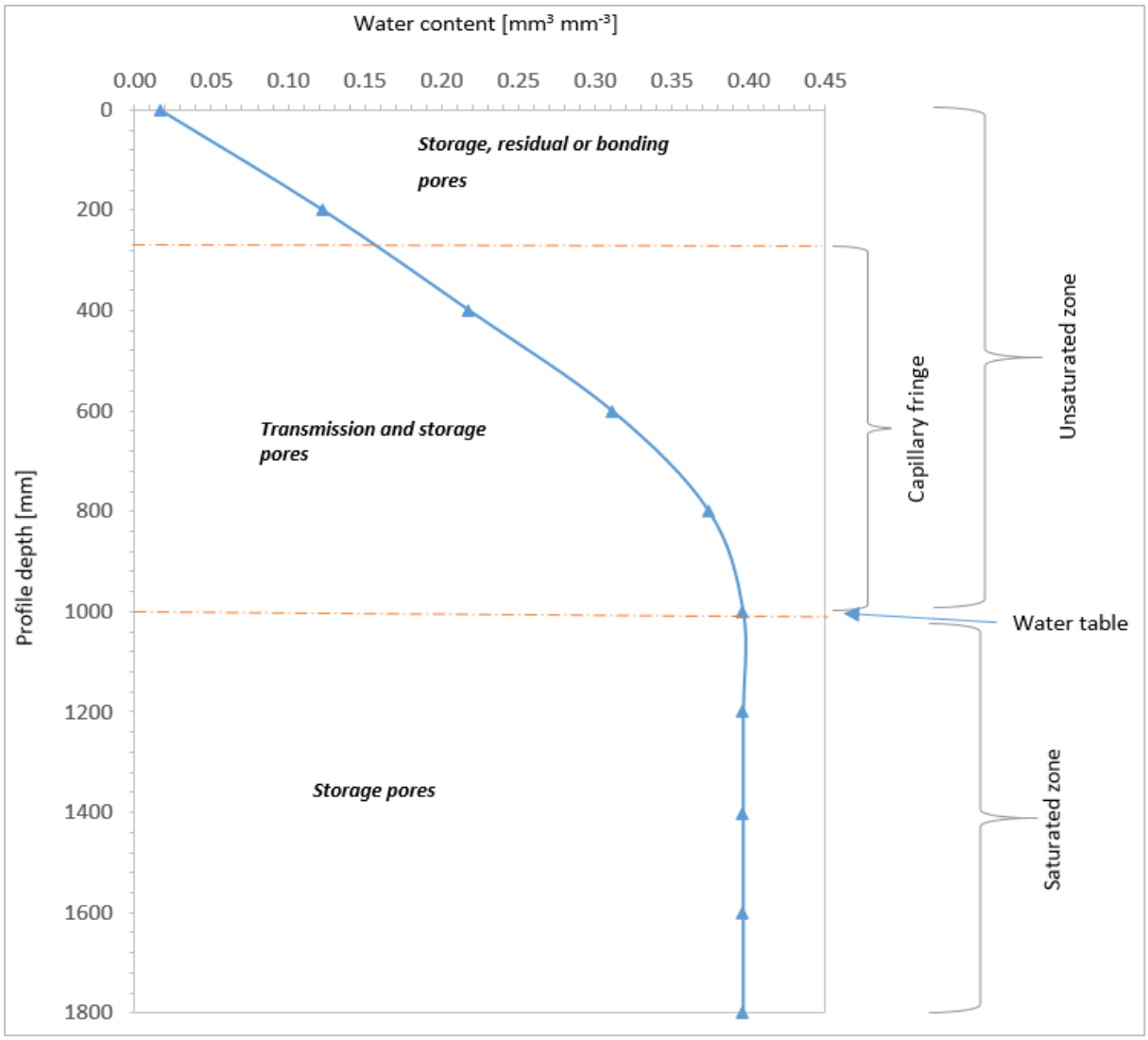

Figure 3.8 Functions of porosity classes in Hutton-B horizon with the presence of 1000 mm water table.

On the other hand, the function of pores in restricted drainage/water table soils is highly dependent on the depth of the water table. Figure 3.8 shows the function of Hutton-B horizon lodged in a field lysimeter with the presence of shallow water table (1000 mm). All the soil pores below the water table acts as storage pores since the soil and excess water is confined and forced to accumulate in the lysimeter. Immediately above the water table, there is a portion of soil with water content ranging from nearly saturated to DUL called the capillary fringe. In

this portion some part of the pores act like transmission pores to the drier end of the unsaturated zone above it other than acting as storage pores. However, the pores above the capillary fringe (the drier end of the unsaturated zone) will incorporate either storage, residual or bonding pores.

Generally, porosity is an important physical property describing the capacity and transport characteristics of soils (Drzal *et al.*, 1999; Nimmo, 2004; Kutilek and Jendele, 2008; Gonçalves *et al.*, 2010). The capacity characteristics include the ability to hold and release water which is the SWRC and availability of air in the soil. Whereas the transport characteristics include behaviour of water movement like hydraulic conductivity and drainage. Therefore all the hydraulic properties discussed in this chapter are highly dependent on the porosity (pore size, number and distribution) of the soils and their diagnostic horizons.

3.4 Conclusion

In this study, the basic physical properties of the two aeolian soils were characterised. The Clovelly and Hutton had bulk densities varying from 1.3 to 1.7 gm cm^{-3} and the same loamy sand texture in the A_p horizon. The Clovelly had lower bulk density in the upper and lower horizons. The two soils also differ in their textural class in their B-horizon, Clovelly categorized as sandy and Hutton as sandy-loam. The dominant sand fraction of the two soils were reflected in the SWRC and hydraulic conductivity. The Clovelly had a well-developed S-shape SWRC as evident to the high total sand fraction ranging from 87 to 93% compared to the range of 78 to 88% from the Hutton suggesting high permeability of the former. Consistent with this result was the higher saturated and unsaturated hydraulic conductivity from the Clovelly A_p and B horizons.

Relationship between pore size and cumulative pore volume was found to be nonlinear, a result that demonstrated the complex nature of particle and pore size distribution. This result also confirmed that classifying pore sizes using fixed boundaries was impractical given the overlapping nature of particle size distribution. In this study the pore size classification proposed by Greenland (1977) was modified based on the concepts of field water capacity. Therefore, the corresponding pore sizes of water contents less than the LL, between the LL and DUL and greater than DUL were functionally classified as residual/or bonding, storage and transmission pores, respectively. However the functionality of these pore classes were likely to change in the presence of a shallow water table or restricting horizon. Nevertheless, soil texture and particle size distribution played a key role in determining hydraulic properties, porosity in particular.

CHAPTER 4
THE EFFECT OF SOIL WATER AND TEMPERATURE ON THERMAL PROPERTIES OF AEOLIAN SOILS

4.1 Introduction

Thermal properties are physical properties that govern heat flow and retention processes in soils (Hanson *et al.*, 2000; Hillel, 2004). Their knowledge is key in understanding and modelling soil thermal regimes and mass-energy exchange processes occurring in the soil-plant-atmosphere system (Usowicz *et al.*, 1996). One of the major components of the mass-energy-exchange processes between the soil and the atmosphere is soil water evaporation. The major source of energy during evaporation is the solar radiation reaching the soil surface. When solar energy reaches the soil surface, it is either stored or transmitted down the profile or propagated as sensible heat back to the atmosphere in dry soil conditions. But in wet soil conditions, a considerable amount of the energy would be expended as latent heat of vaporization (Hillel, 2004). The amount of energy to be stored/transmitted to soils or propagated back to the atmosphere depends on the thermal properties of soils. Thermal properties are also crucial in many various fields of agriculture, environment and engineering applications.

Thermal properties of soils comprise of thermal conductivity (K_t), volumetric heat capacity (C) and thermal diffusivity (D). Thermal conductivity (K_t) describes the soil's ability to transfer heat mainly by conduction. It is the quantity of heat that flows through a unit area in a unit time under a unit temperature gradient (Bristow, 2002). Similarly, C explains the amount in heat change in a unit volume of soil per unit change in temperature (Hillel, 2004). Measurements concerning D reflect on how quickly a soil can change its temperature and are defined as the ratio of K_t to C (Hanson *et al.*, 2000). These properties depend heavily on soil physical properties such as bulk density, water content and temperature.

Concerning the effect of water content on thermal properties, literature (Willis and Raney, 1971; Misra *et al.*, 1995; Smits *et al.*, 2009; Oladunjoye and Sanuade, 2012; Oladunjoye *et al.*, 2013; Busby, 2015) suggested that thermal properties are significantly dependent on water content. However, the magnitude of the responses to water content was variable. Some researchers observed a linear increase in all thermal properties with an increase in water content (Fricke, 1992; Oladunjoye *et al.*, 2013; Lydzba *et al.*, 2014). A curve linear response was also observed (Willis and Raney, 1971; Sepaskhad and Boersma, 1979; Misra *et al.*, 1995; Tarnawski and Leong, 2000; Rubio, 2013). The curve linear response gives two types of critical

water contents for K_t. One is associated with a water content required for establishing sufficient contacts between solid particles for significant conductance of heat in unsaturated soils. The other critical water content is associated with water contents that give maximum heat conduction (Misra *et al.*, 1995; Rubio, 2013). For very dry soils all thermal properties of soils are governed by coordination number and quality of contacts between particles (Santamarina, 2012).

Literature study revealed that knowledge concerning the effect of soil temperature on thermal properties was very limited. Sawada (1977) indicated that K_t and D increased with decreasing temperature and increasing water content. Willis and Raney (1971) observed that K_t increases non-linearly over a temperature range stretching from 20ºC to 60ºC. They also demonstrated that the effect of temperature on soil thermal properties is insignificant at extremely low and high water contents. The relation between K_t and D with soil water content was shown to be non-linear (Willis and Raney, 1971; Sawada, 1977). Some investigators also ignored the effect of non-freezing temperature in influencing thermal properties (Chung and Horton, 1987; Brandon and Mitchell, 1989).

Thermal properties can be determined in various ways. The most popular methods are direct field measurement, laboratory procedures and predictive mathematical models. Direct determination methods are the most reliable but are expensive, time consuming and laborious as well as impracticable for large scale applications (Tombul *et al.*, 2004; Dashtaki *et al.*, 2010; Guber and Pachepsky, 2010; Vereecken *et al.*, 2010). Therefore, indirect estimation models that relate thermal properties to available or easily measureable soil physical properties like texture, bulk density, water content, organic matter content, soil temperature, etc. are important alternatives. These predictive empirical models are called pedotransfer functions.

Aeolian soils in South Africa were studied by many researchers, covering a wide range of disciplines, *viz.* geomorphology (Harmse and Hattingh, 2012), pedology and soil classification (Soil Classification Working Group, 1991; Le Roux *et al.*, 2013), studies related to sustainable crop production and environmental health (Bennie *et al.*, 1995; Barnard *et al.*, 2010; van Rensburg *et al.*, 2011; Verwey and Vermeulen, 2011). A number of researchers also studied hydro-physical properties of these soils. For example, Chimungu (2009) studied amongst other properties the pore size distribution, Haka (2010) reported on transpiration of field crops, Zerizghy *et al.* (2012) looked at rainfall-runoff properties, while Tesfuhuney (2012) concentrated on water storage under different runoff strip, runoff strip length and mulch cover for rainwater harvesting application. However, none of these studies addressed thermal

properties. Generally it is possible to say that there is insufficient information about thermal properties in literature. More so, very little is known about thermal properties of aelion soils in Southern Africa. Therefore, this study was conducted to determine the influence of soil water and temperature on thermal properties (K_t, C and D) of two important aeolian soils, namely Clovelly and Hutton soil forms. The study also aimed at developing a pedo-transfer function(s) that can estimate thermal properties of aeolian soils using relatively easily measureable soil physical properties.

4.2 Materials and methods

4.2.1 Description of the study area

Samples were collected from the field lysimetres constructed from Clovelly and a Hutton soil forms. The Clovelly samples were obtained from aeolian sandy deposits near Hoopstad, while the Hutton samples originated from the Kenilworth Experimental Farm of the University of the Free State, near Bloemfontein. The formation of Hutton soil form from the Bainsvlei soil is explained in Section 3.2.1.

4.2.2 Sample preparation and determination of soil thermal properties

Bulk samples were collected from the master horizons, A_p-horizons (0 – 300 mm) and the B-horizons (300 – 1200 mm depth). These bulk samples were first dried in a convection oven at 105^{o}C until the weights were constant and then re-packed at 10% gravimetrical water content in standard 110 mm PVC pipes with lengths of 75 mm. The mass of the samples were derived from the bulk densities that were predetermined using the core method as discussed in Chapter 3 of this thesis. The bulk densities for Clovelly were 1.32 and 1.52 g cm^{-3} and the Hutton were 1.40 and 1.68 g cm^{-3} for A_p and B horizons, respectively. During packing of the soil, care was taken to obtain the mentioned bulk densities as suggested by Dane & Hopmans (2002). After packing of the samples they were again oven-dried to be ready for the treatments.

The thermal properties, i.e. thermal conductivity, volumetric heat capacity and thermal diffusivity, were measured with the KD2-Pro thermal analyzer (SH-1 thermal sensor) developed by the Decagon Devices Inc. (2011) as can be seen in Figure 4.1. A pair of Shafts of about 30 mm in length were made in the soil samples using a 1 mm drill to insert the dual-needle probe (Decagon Devices Inc., 2011).

Figure 4.1 Measurement of thermal properties in laboratory: (a) Set up of the measurement process (b) the dual SH-1 sensor to measure thermal properties

4.2.3 Experimental design and management

This experiment was conducted in a simple randomized block design of two factor factorial experiment, however blocking doesn't have effect on treatments since it was conducted in laboratory. The four soil diagnostic horizons were treated independently. Each horizon was subjected to 5 soil water levels (0%, 8%, 16%, 22% and 39%) and 5 temperature levels (0.5^{o}C, 10^{o}C, 25^{o}C, 40^{o}C and 60^{o}C), replicated 4 times. The water levels, expressed in volumetric units, were achieved by equilibrating the soil samples with the equivalent gravimetric water content. The procedure comprised of adding pre-weighted water to the dried samples, wrapping the samples with plastic and then storage of them for a week at room temperature before measurements commenced. During storage the samples were turned upside down daily to ensure uniform distribution of soil water in the samples.

The equilibrated soil samples were subjected to the targeted temperatures using a climate control chamber, starting at the lowest temperature towards the highest. Three days were allowed for equilibrating samples at targeted temperature treatments.

4.2.4 Calibration of KD2 Pro Meter

Based on the manual of the KD2 Pro meter (Decagon Devices Inc., 2011), there is no special calibration procedure proposed. Only a simple performance verification was made on the Derlin block. Therefore, the SH-1 sensors were inserted to the two-hole Delrin block for 15 minutes for equilibration of temperature before taking measurement. The readings of the thermal conductivity, volumetric heat capacity and thermal diffusivity of the Derlin block were in the ranges of values proposed in the Quality Assurance Certificate.

4.2.5 Statistical analysis

As explained in Section 4.2.3, the experiment was laid out in a simple randomized block design of two factors or treatments (soil water and soil temperature) for each of the diagnostic horizons. The results were subjected to a statistical analysis; analysis of variances (ANOVA), coefficient of determination (R^2) as well as correlation and regression analysis. The analyses of variances (ANOVA) were done to evaluate the significance of each factor and whether there was an interaction between factors and carried out using SAS software version 9.4 (Muller & Fetterman, 2002; SAS Institute, 2013). However, the corresponding data of the thermal properties did not meet the requirements of normality or homogeneity tests as indicated by Peltier *et al.* (1998) and Osborne (2010), hence it was transformed using Equations 4.1, 4.2 and 4.3 for thermal conductivity, volumetric heat capacity and thermal diffusivity, respectively:

$$Log\_K_t = Log(K_t), \quad then, \; K_t = exp^{Log\_K_t} \tag{4.1}$$

$$Log\_C = Log(C), \; then, \; C = exp^{Log\_C} \tag{4.2}$$

$$Log\_D = Log(D), \; then, \; D = exp^{Log\_D} \tag{4.3}$$

where Log_K_t, Log_C and Log_D are the values of the log-transformed data sets of thermal conductivity, volumetric heat capacity and thermal diffusivity of the two soil forms, respectively.

The above mentioned data were further subjected to statistical analysis to explain the combined effect of water and temperature on the thermal properties, C, K_t and D. The t-test revealed that there was no significant difference between the two soils, therefore the datasets of the two soils were combined and presented as water content groups (A to E) and temperature groups (A to E). Further details on the t-statistics are provided in Appendix 4.4 for the three thermal properties. Appendices 4.1, 4.2 and 4.3 were dedicated to the least significant difference

method (LSD) to sort out which treatment means were significantly different for K_t, C and D, respectively.

Non-linear multiple regression analysis (with stepwise process) was used for the development of models to estimate thermal properties from soil physical properties. In this study the Clovelly soil data were used to develop mathematical models whereas the Hutton soil data sets were used to validate the model performance.

4.3 Results

4.3.1 Effects of soil water and temperature on thermal properties

4.3.1.1 Volumetric heat capacity

The results of the ANOVA of volumetric heat capacity of the two soils analysed along their diagnostic horizons are summarized in Table 4.1. The least significant difference (LSD) to examine the differences between the means of C at different treatments combinations of soil water and temperature are also provided in Appendix 4.1.

Table 4.1 Summary of the analysis of variance of volumetric heat capacity for the four horizons

Horizon code	Sources of variation	DF	Anova SS	Mean Square	F Value	Pr > F
Cl-A_p	Replication	3	0.00697	0.002323	0.16	0.9216
	Water	4	6.038336	1.509584	105.24	<.0001
	Temperature	4	1.061599	0.2654	18.5	<.0001
	Water*Temperature	16	1.079664	0.067479	4.7	<.0001
	Error	72	1.032773	0.014344		
	Corrected total	99	9.219342			
Cl-B	Replication	3	0.036089	0.01203	1.01	0.3943
	Water	4	8.124197	2.031049	170.2	<.0001
	Temperature	4	1.421206	0.355301	29.77	<.0001
	Water*Temperature	16	2.129508	0.133094	11.15	<.0001
	Error	72	0.859203	0.011933		
	Corrected total	99	12.5702			
Hu-A_p	Replication	3	0.101874	0.033958	2.66	0.0543
	Water	4	10.36111	2.590277	203.16	<.0001
	Temperature	4	0.417786	0.104447	8.19	<.0001
	Water*Temperature	16	0.82665	0.051666	4.05	<.0001
	Error	72	0.918005	0.01275		
	Corrected total	99	12.62542			

Hu-B	Replication	3	0.09033	0.03011	1.95	0.1297
	Water	4	7.160653	1.790163	115.76	<.0001
	Temperature	4	2.118743	0.529686	34.25	<.0001
	Water*Temperature	16	1.13078	0.070674	4.57	<.0001
	Error	72	1.113468	0.015465		
	Corrected total	99	11.61397			

The analyses of variances shows that there was a highly significant difference between treatment means of C due to a difference in soil water content, temperature and their combination which is true for all the horizons. Since the interaction was highly significant, the analysis and discussion will only focus on the combined effects of soil conditions induced by water and temperature. Further analysis, as mentioned in the materials and methods, indicated that there was no significant difference between the two soils with t-statistic of -0.35. Therefore the datasets of the horizons were combined and divided into five temperature groups (A to E in Figure 4.2a) as well as five water groups (A to E in Figure 4.2b). The temperature groups quantify the relationship between C and water content, while the water groups give the C-temperature relationship. The statistical results are summarised in Tables 4.2 and 4.3 for the temperature and water groups, respectively.

Considering the relationship between heat capacity and water content at the different temperature levels (Group A-E), it is clear that the response was curve-linear in all the groups, implicating an increase in heat capacity with an increase in water content from dry (0 mm^3 mm^{-3}) to saturation (0.39 mm^3 mm^{-3}). However, there is a clear difference between the heat capacity-water content relationship between Groups A and B. Under these conditions the heat capacity of Group A (solid phase) was significantly higher than B (liquid phase), illustrating the effect of temperature upon freezing and thawing of soils. With regard to the groups in the liquid phase (Groups B-E), it seems that the shape of the curves changed along the temperature groups. As the temperature increases from Group B towards Group E, the shape of the curves became progressively linear. This indicates that there was a change in the heat capacity-water content relationship between DUL and saturation. Another important change in the heat capacity-water content relationship of the liquid phase groups, is the increase of the intercept along the groups, which excelled from 1.3 to about 2.3 MJ (m^{-3} K^{-1}) with the addition of water.

With regard to the heat capacity-temperature relationship, the regression results for the different water levels (Group A–E) in Table 4.3 were calculated without the 0°C (solid phase) dataset, because it differed significantly from the rest of the datasets which represents a liquid

phase. All the slopes were positive, indicating that the heat capacity increased with an increase in temperature from 10 to 60 ºC. Of note is the change in the heat capacity between Group A and Group B where an initially dry soil is slightly wetted. In this case the slope at the dry soil was more positive than the wet soil, while the intercept was higher in the wet soil than the dry soil, indicating that temperature affected the heat capacity more in the dry soil than the wet soil. Another important phenomenon is the fact that the intercepts of the regression functions increased with an increase in water levels from Group A (0.76 MJ (m^{-3} K^{-1}) to Group D (2.34 MJ (m^{-3} K^{-1}), which corresponds with the drained upper limit of the soils. Adding of water beyond this point did not affect the intercept, it actually started to decrease slightly toward 2.25 M J (m^{-3} K^{-1}).

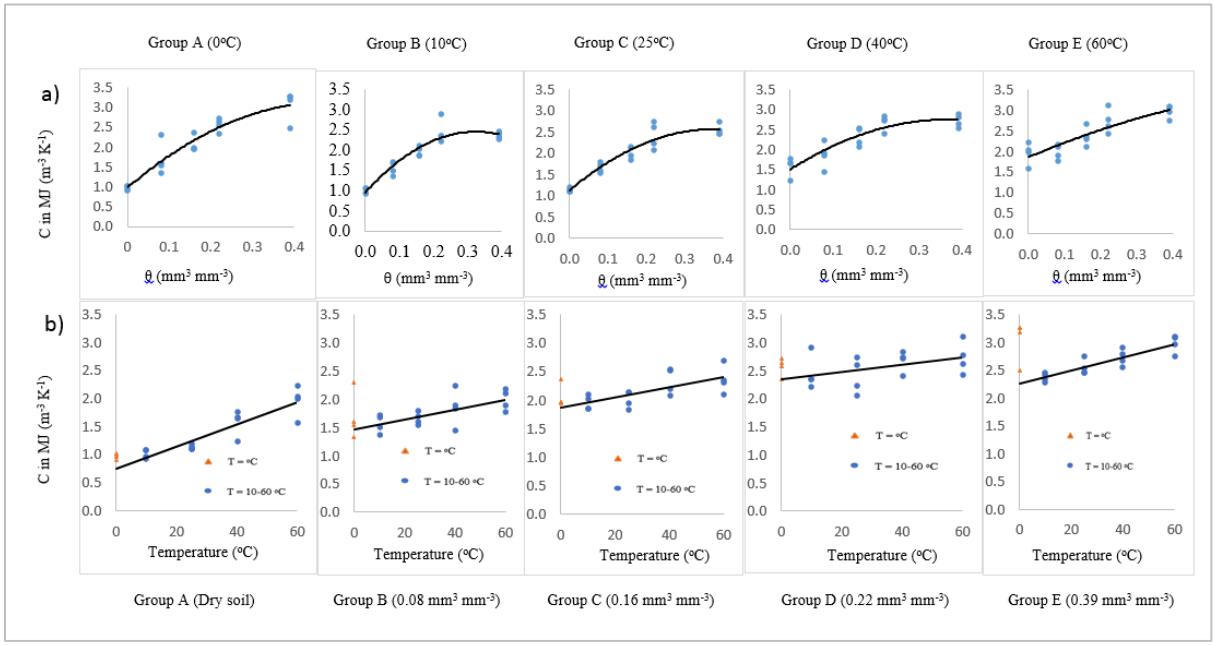

Figure 4.2 Comparison of the effect of soil water (a) and temperature (b) on C amongst the five groups (A-E).

Table 4.2 Descriptive statistics for the C-water content relationships in five temperature groups

Group	Slope	Y-intercept	R^2	P-value	Min	Max	Mean
A	5.2535	1.1744	0.89	<0.001	0.91275	3.2645	2.067488
B	3.5494	1.2695	0.9	<0.001	0.93	2.904	1.87289
C	3.6136	1.3392	0.81	<0.001	1.107	2.749	1.95346
D	3.117	1.7034	0.8	<0.001	1.23375	2.89575	2.23329
E	2.9333	1.9014	0.74	<0.001	1.56275	3.1105	2.400063

Table 4.3 Descriptive statistics of the C-temperature relationships for five water content groups

Group	Slope	Y-intercept	R^2	P-value	Min	Max	Mean
A	0.0197	0.7562	0.81	<0.001	0.93	2.21675	1.42125
B	0.0088	1.4677	0.44	0.0050	1.35925	2.23525	1.764672
C	0.009	1.86211	0.45	0.0040	1.834	2.6905	2.164547
D	0.0067	2.3429	0.19	0.0870	2.06025	3.1105	2.567906
E	0.012	2.2499	0.78	<0.001	2.28025	3.10325	2.65625

4.3.1.2 Thermal conductivity

The statistical results concerning soil water content and temperature treatments on K_t for the individual diagnostic horizons are presented in Table 4.4. The pairwise comparison between treatment means is also provided in Appendix 4.2.

Table 4.4 Summary of the analysis of variance concerning K_t in the four diagnostic horizons (A_p and B horizons) of the Clovelly and Hutton soils

Horizon code	Sources of variation	DF	Anova SS	Mean Square	F Value	Pr > F
Cl-A_p	Replication	3	0.02135351	0.00711784	1.13	0.3415
	Water	4	74.8448224	18.7112056	2978.52	<.0001
	Temperature	4	0.41428957	0.10357239	16.49	<.0001
	Water*Temperature	16	1.40225257	0.08764079	13.95	<.0001
	Error	72	0.45230679	0.00628204		
	Corrected total	99	77.1350248			
Cl-B	Replication	3	0.04643623	0.01547874	2.27	0.0878
	Water	4	68.7313853	17.1828463	2518.25	<.0001
	Temperature	4	1.11545447	0.27886362	40.87	<.0001
	Water*Temperature	16	2.92649056	0.18290566	26.81	<.0001
	Error	72	0.49127949	0.00682333		
	Corrected total	99	73.3110461			
Hu-A_p	Replication	3	0.07191502	0.02397167	3	0.0361
	Water	4	72.6109485	18.1527371	2272.29	<.0001
	Temperature	4	0.70371105	0.17592776	22.02	<.0001
	Water*Temperature	16	1.68207979	0.10512999	13.16	<.0001
	Error	72	0.57519033	0.00798875		
	Corrected total	99	75.6438447			

Hu-B	Replication	3	0.07329223	0.02443074	3.47	0.0204
	Water	4	71.5732637	17.8933159	2542.89	<.0001
	Temperature	4	0.83143842	0.2078596	29.54	<.0001
	Water*Temperature	16	2.18379827	0.13648739	19.4	<.0001
	Error	72	0.50663507	0.0070366		
	Corrected total	99	75.1684277			

The analyses of variances in Table 4.4 shows that there was a highly significant difference between treatment means of K_t due to a difference in soil water content, temperature and their combination which is true for all the horizons. Since the interaction was highly significant, the analysis and discussion will only focus on the combined effects of soil conditions induced by water and temperature. Further analysis, as mentioned in the material and methods, showed that there was no significant difference between the two soils with t-statistics of 0.4598. As a result, the datasets of the horizons were combined as one soil for further analysis by dividing in to five water content and temperature groups. The temperature groups (A to E in Figure 4.3a) quantify the relationship between K_t-water content whereas the water groups (A to E in Figure 4.3b) show the K_t-temperature relationship. The statistical results are summarised in Tables 4.5 and 4.6 for the temperature and water groups, respectively.

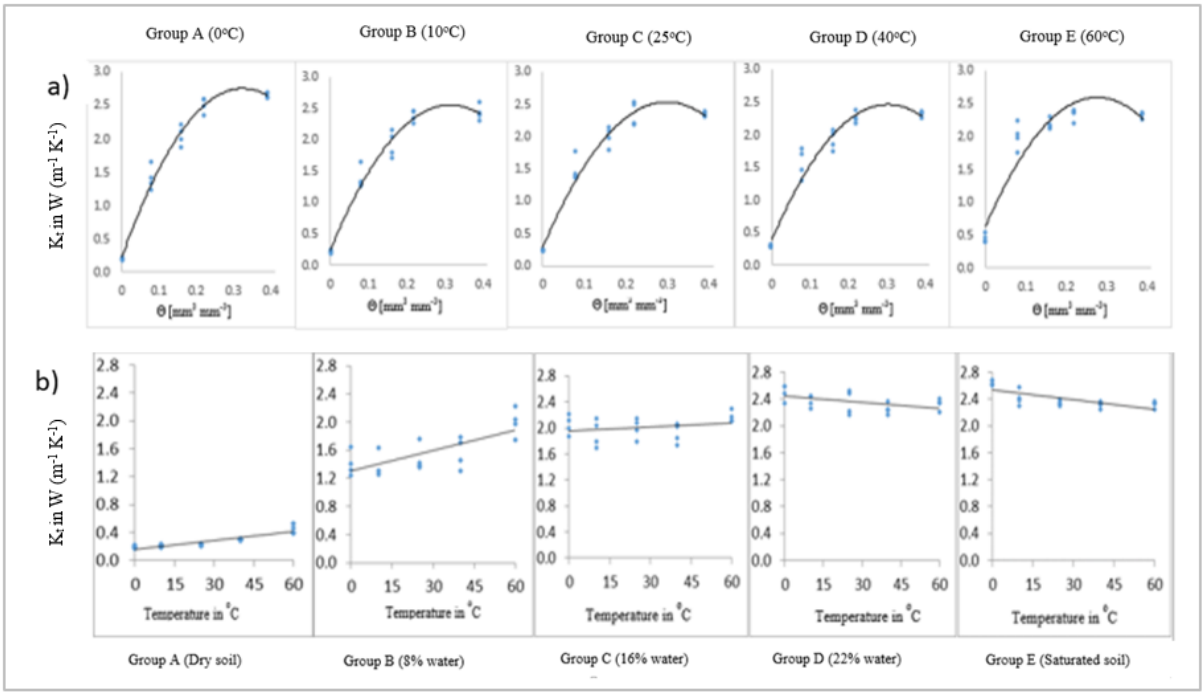

Figure 4.3 Comparison of the effect of a soil water (a) and temperature (b) on K_t amongst the five groups (A-E)

Table 4.5 Descriptive statistics for K_t-water content relationships in the five temperature groups

Group	Slope	Y-intercept	R^2	P-value	Min	Max	Mean
A	6.0116	0.7382	0.98	<0.001	0.174	2.6875	1.76015
B	5.3689	0.7436	0.97	<0.001	0.18875	2.576	1.656325
C	5.0116	0.824	0.97	<0.001	0.23125	2.52275	1.675975
D	4.6689	0.8736	0.95	<0.001	0.2985	2.36775	1.667275
E	3.9614	1.1799	0.89	<0.001	0.39025	2.3995	1.851325

Table 4.6 Descriptive statistics for K_t-temperature relationships of the five water content groups

Group	Slope	Y-intercept	R^2	P-value	Min	Max	Mean
A	0.0041	0.1622	0.80	<0.001	0.1740	0.5325	0.2727
B	0.0097	1.3030	0.54	<0.001	1.2380	2.2303	1.5636
C	0.0022	1.9486	0.08	0.233	1.6948	2.2948	2.0070
D	-0.0029	2.4397	0.23	0.034	2.1660	2.5963	2.3610
E	-0.0048	2.5362	0.53	<0.001	2.2423	2.6875	2.4068

Considering the relationship between K_t and water content at different temperature groups, it is evident that the response was curve-linear in all the groups as it was true for C. This implicates that K_t will increase with an increase in water content up to a maximum point where after it will decrease with further addition of water. In all cases the linear part of the curve is associated with water contents below the drained upper limit (DUL), while the curvature part reflects on water content beyond DUL up to saturation. Generally, the results suggested that K_t will increase from about 0.174 for dry soils to 2.36775 W (m^{-1} K^{-1}) at DUL, where after it change very little with further increase in water content up to saturation (2.3995 W (m^{-1} K^{-1}). The K_t-water relationship differed visually from the K_t-temperature relationship. The effect of freezing and thawing relationship here was lower as compared to the C-water relationship mentioned in the previous section.

Focusing on the results how K_t was influenced by soil temperature (Group A-E), it should be mentioned that all the data were included in the regression analysis as freezing did not influence the results as in the case of the C-water relationship discussed in the previous section. Accordingly the general relationship between K_t and temperature (0 - 60 °C) was linear amongst the different water levels. However, judging the slopes of the lines suggested that the

relationship is changed positively from a dry soil (Group A) towards DUL and then turned negative from Group D towards saturation (Group E). The intercept increased along the groups, with a prominent increase of 1.14 W (m^{-1} K^{-1}) from Group A to B. This implicates that the wetting of dry soils up to 0.08 mm^3 mm^{-3} improved K_t significantly; the intercept of Group B was 1.303 W/(m.K) compared to the 0.1622 W (m^{-1} K^{-1}) of Group A, while the slope of Group B is more positive than that of Group A.

4.3.1.3 Thermal diffusivity

The ANOVA of the thermal diffusivity (D) of the two soils with their diagnostic horizons is given in Table 4.7. The pairwise comparison of the mean D with the LSD method is also summarized in Appendix 4.3.

Table 4.7 Summary of the analysis of variances for thermal diffusivity in the four soil horizons

Horizon code	Sources of variation	DF	Anova SS	Mean Square	F Value	Pr > F
Cl-A_p	Replication	3	0.009303	0.003101	0.22	0.8791
	Water	4	43.77087	10.94272	791.84	<.0001
	Temperature	4	0.249922	0.06248	4.52	0.0026
	Water*Temperature	16	0.342675	0.021417	1.55	0.1062
	Error	72	0.994989	0.013819		
	Corrected total	99	45.36776			
Cl-B	Replication	3	0.032687	0.010896	1.03	0.3849
	Water	4	35.29609	8.824023	833.42	<.0001
	Temperature	4	0.333767	0.083442	7.88	<.0001
	Water*Temperature	16	0.915235	0.057202	5.4	<.0001
	Error	72	0.76232	0.010588		
	Corrected total	99	37.3401			
Hu-A_p	Replication	3	0.075475	0.025158	1.71	0.1716
	Water	4	33.7629	8.440725	575.36	<.0001
	Temperature	4	0.178141	0.044535	3.04	0.0227
	Water*Temperature	16	0.975038	0.06094	4.15	<.0001
	Error	72	1.056265	0.01467		
	Corrected total	99	36.04782			
Hu-B	Replication	3	0.064729	0.021576	1.36	0.2618
	Water	4	34.78675	8.696687	548.32	<.0001
	Temperature	4	0.863153	0.215788	13.61	<.0001
	Water*Temperature	16	0.577937	0.036121	2.28	0.0094

	Error	72	1.141968	0.015861
	Corrected total	99	37.43454	

The results show that water content and temperature has a significant effect on the means of thermal diffusivity both as main effects and in an interactive way in all the horizons (exceptionally, there was not significant interaction in Cl-A_p). Since the interaction of water and temperature is significant, the analysis is based on the interaction effects only. The difference in means between the two soils was not significant (a t-statistics of -0.2793). As a result the datasets of the horizons are merged keeping the treatments as before for further discussion. The details of the t-statistics are given in Appendix 4.6.

The temperature groups (in Figure 4.4a from A to E) quantify the relationships between D to water content, whereas the water groups (Figure 4.4b from A to E) depicts the D-temperature relationships. The statistical results are also summarized in Table 4.8 and 4.9 for the temperature and water groups, respectively.

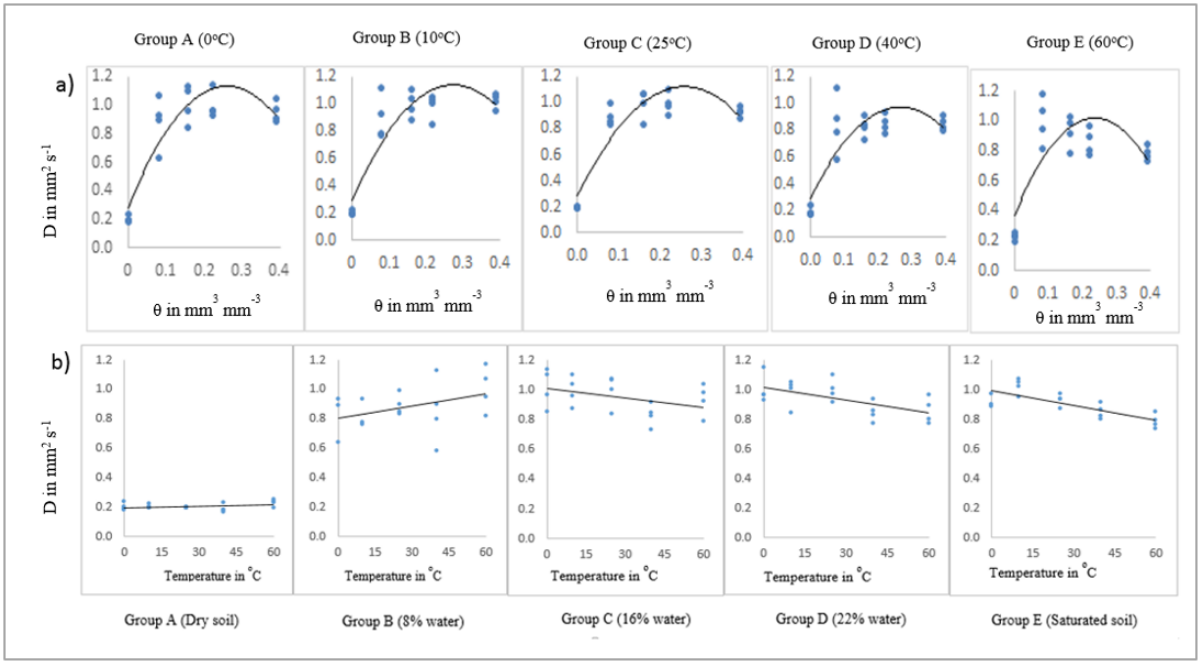

Figure 4.4 Comparison of the effect of a soil water content (a) and temperature (b) on D amongst the five temperature groups (A-E)

Table 4.8 Descriptive statistics for the D-water content relationships of the five temperature groups

Group	Slope	Y-intercept	R^2	P-value	Min	Max	Mean
A	1.5465	0.5485	0.82	0.003	0.18225	1.15125	0.81135
B	1.6967	0.5325	0.82	<0.001	0.1955	1.11175	0.820963
C	1.4847	0.5503	0.86	0.003	0.191	1.09975	0.802725
D	1.2836	0.4963	0.7	0.004	0.18	1.128	0.714488
E	0.8749	0.613	0.63	0.078	0.197	1.175	0.76175

Table 4.9 Descriptive statistics for the D-temperature relationships of the five water content groups

Group	Slope	Y-intercept	R^2	P-value	Min	Max	Mean
A	0.0003	0.1947	0.095	0.1862	0.169	0.254	0.2036
B	0.0014	0.8678	0.0399	0.3988	0.5848	1.175	0.9065
C	-0.0021	1.0097	0.1521	0.0891	0.7328	1.1363	0.9535
D	-0.0028	1.0149	0.348	0.0062	0.7728	1.1513	0.9387
E	-0.0035	1.0043	0.6191	<0.001	0.735	1.0715	0.9091

With reference to the D-water content relationship at different temperature levels (Group A-E), the general response was similar to that of K_t. However, the curves bend more between DUL and saturation than observed with K_t. As in the case of K_t, the linear part of the curve in Groups A to E is associated with water contents below the drained upper limit (DUL), while the curvature part reflects on water content beyond DUL up to saturation. Generally, the results suggested that D will increase from about 0.18225 for dry soils to 1.128 ($mm^2\ S^{-1}$) at DUL, where after it didn't change considerably with further increase in water up to saturation (1.175 $mm^2\ S^{-1}$), irrespective of temperature. The effect of freezing and thawing relationship was lower just like the K_t-water content relationship as compared to the C-water content relationships.

Focusing on the D-temperature relationship, it reveals that all the relationships were linear. However, the slope of the functions changed along the water levels. It was positive for the first two water levels, where after it became negative with further addition of water up to saturation. This result implies that D at both the dry and slightly wetted soil increased with warming of soils from 0 to 60 ^oC, while further wetting of the soils results in a decrease in D with increasing temperature. As can be seen from the intercepts of the different water levels (Group A-E), there

is a significant increase in the slopes of Group B (0.8678 mm^2 S^{-1}) compared to Group A (0.1947 mm^2 S^{-1}) as witnessed for K_t as well. The maximum D value (1.14 mm^2 S^{-1}) corresponds with 0°C at Group C.

4.3.2 Development of mathematical models

From this study it was realized that there was a non-linear relationship between thermal properties and the interactive effect of selected soil physical properties (soil water content and temperature). Empirical mathematical models were developed using linear polynomial regression with exponential curve fitting for the three thermal properties. In this regression analysis, stepwise linear regression process with 8 main effects (θ, θ^2, θ^3, θ^4, T, T^2, T^3 and T4) and 16 two factor interactions were tested in SAS v9.4 software (SAS Institute, 2013). In this case θ is water content and T is the soil temperature, whereas θ^2, θ^3 and θ^4 are water content squared, cubed and the fourth power, respectively. Similarly, T^2, T^3 and T^4 are the soil temperature squared, cubed and the fourth power, respectively. Those main and interaction effects showing a significant effect ($P<0.10$) on the dependent variables were selected and incorporated in the model. Note that in the selection procedure the principle of marginality was observed, whereby a lower order effect was removed from the model only all higher order effects involving the lower order effects were not significant. Consequently, the final model might contain non-significant effects, when a higher order effect involving the non-significant effect was found to be significant.

4.3.2.1 Volumetric heat capacity

After performing the stepwise regression procedure, the variable and parameter combinations that have a significant influence on C were determined and summarized in Table 4.10.

Table 4.10 Parameters selected for volumetric heat capacity

Variable	DF	Parameter Estimate	Standard Error	t Value	Pr > |t|
Intercept	1	0.02744	0.07010	0.39	0.6977
θ	1	3.51645	1.22697	2.87	0.0068
θ^2	1	7.15707	7.16068	1.00	0.3240
θ^3	1	-22.65014	12.00230	-1.89	0.0670
T	1	-0.01125	0.01279	-0.88	0.3845

T^2	1	0.00101	0.00053863	1.87	0.0692
T^3	1	-0.00001051	0.00000584	-1.80	0.0799
θ T	1	0.18964	0.15486	1.22	0.2284
θ T^2	1	-0.01157	0.00652	-1.77	0.0844
θ T^3	1	0.00012084	0.00007066	1.71	0.0956
θ ^{2}T	1	-0.63953	0.37063	-1.73	0.0928
θ $^2T^2$	1	0.03119	0.01561	2.00	0.0531
θ $^2T^3$	1	-0.00031451	0.00016913	-1.86	0.0709

Finally, Equation 4.4 was developed with a high R^2 value of 0.92 and a very low root mean squared error (RMSE = 0.10232).

$$C = \exp\left[\begin{array}{l} 0.02274+3.51645\theta+7.15707\theta^2-22.65\theta^3-0.0113T+0.00101T^2-0.00001051T^3+0.18964\theta T \\ -0.01157\theta T^2+0.0012084\theta T^3-0.63953\theta^2 T+0.03119\theta^2 T^2-0.00031451\theta^2 T^3 \end{array}\right] \quad (4.4)$$

Where C is the volumetric heat capacity in MJ (m^{-3} K^{-1}), θ represents volumetric water content (mm^3 mm^{-3}), T is the soil temperature in ^{O}C.

The plots of the curve fitting and model validation procedures are illustrated in Figure 4.5 and 4.6, respectively. The model validation procedure (R^2 = 0.72) indicated that Equation 4.4 can be used to predict fairly good values of volumetric heat capacity of aeolian soils with similar condition.

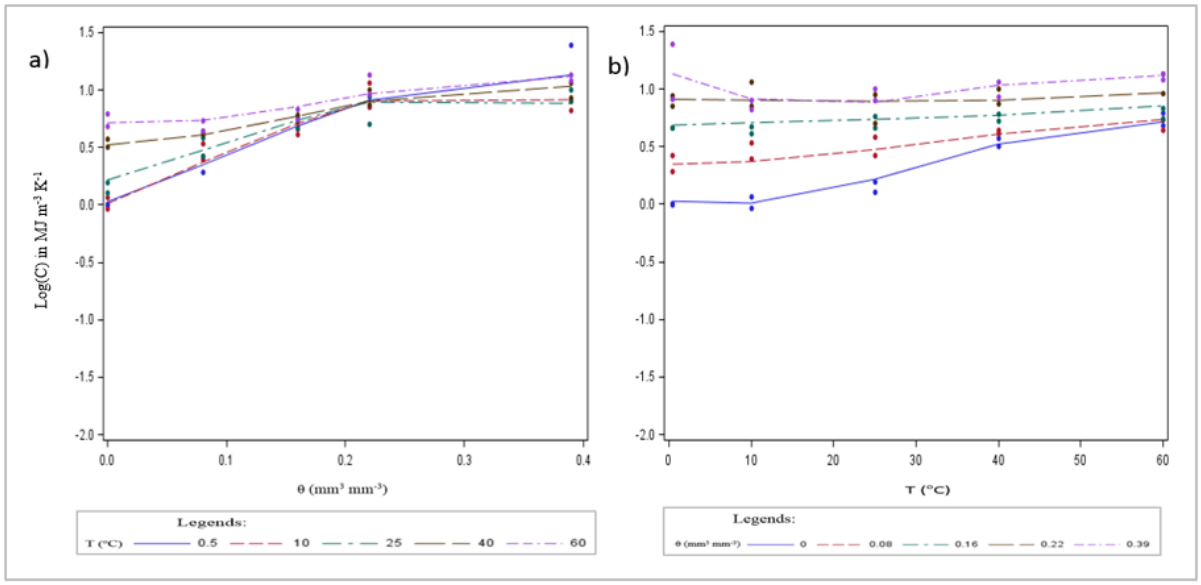

Figure 4.5 Comparison of the observed and fitted values of the mean C on Clovelly soil form: (a) Effect of soil water content on C keeping the temperature values constant (b) Effect of temperature on C keeping the soil water content constant.

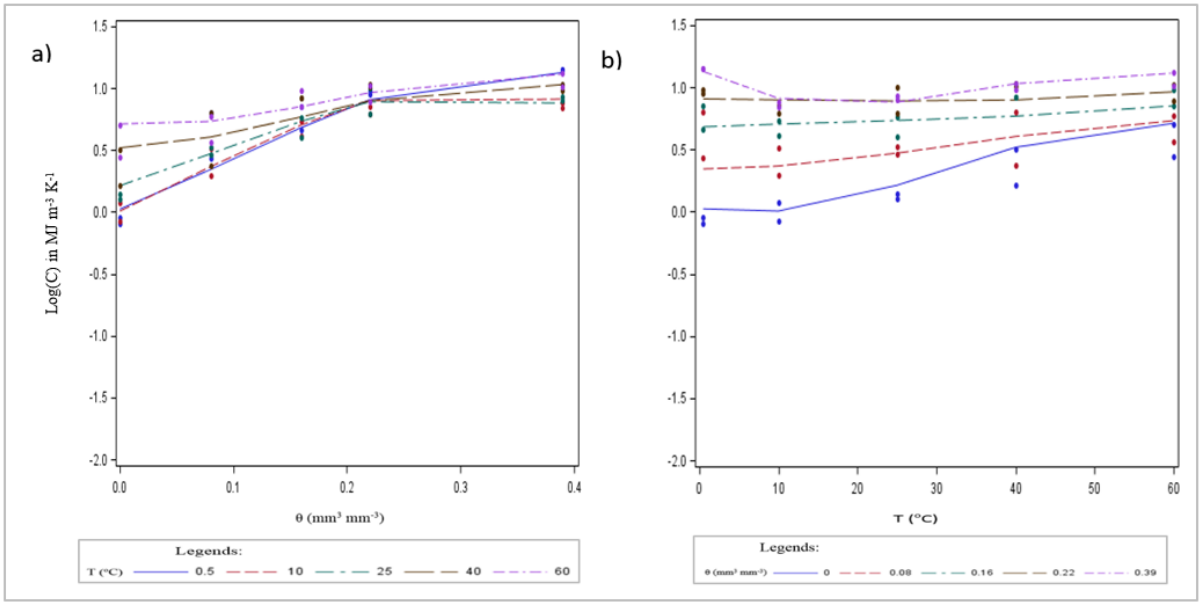

Figure 4.6 Validation of the C model based on Hutton data sets: (a) Effect of soil water content on C keeping the temperature values constant (b) Effect of temperature on C keeping the soil water content constant.

4.3.2.1 Thermal conductivity

The same procedure as in the case of C was applied and the parameters shown in Table 4.11 found to be the best estimates in the development of a model (Equation 4.5) for predicting thermal conductivity of aeolian soils.

Table 4.11 Parameter estimates of the thermal conductivity model

Variable	DF	Parameter estimate	Standard error	t Value	Pr > |t|
Intercept	1	-1.63656	0.07373	-22.2	<.0001
θ	1	33.676	1.49534	22.52	<.0001
θ^2	1	-142.57795	9.78948	-14.56	<.0001
θ^3	1	189.9755	16.74567	11.34	<.0001
T	1	0.00595	0.00383	1.55	0.128
T^2	1	0.00013472	5.459E-05	2.47	0.018
θ T	1	-0.10929	0.02373	-4.61	<.0001
θ^2T	1	0.16434	0.0568	2.89	0.006

$$K_t = \exp\left[\begin{array}{l} -1.63656+33.676\theta-142.578\theta^2+189.9755\theta^3 \\ +0.00595T+0.000135T^2-0.10929\theta T+0.16434\theta^2 T) \end{array}\right] \quad (4.5)$$

Where K_t is a soil thermal conductivity in W (m^{-1} K^{-1}), θ represents volumetric water content (mm^3 mm^{-3}), T is the soil temperature in ^{O}C.

The presence of a higher coefficient of determination approaching to unity (R^2 = 0.97) and lower value of Root Mean Square of Error closer to zero (RMSE = 0.14276) shows the goodness of fit of the regression procedure (Figure 4.7). The performance of the model to estimate K_t was also independently evaluated against the Hutton soil. The results for the variables water and temperature inputs are depicted in Figure 4.8. Accordingly, there was a good agreement between the observed and predicted values of K_t (R^2 = 0.92) showing the model can predict K_t in statistically acceptable values.

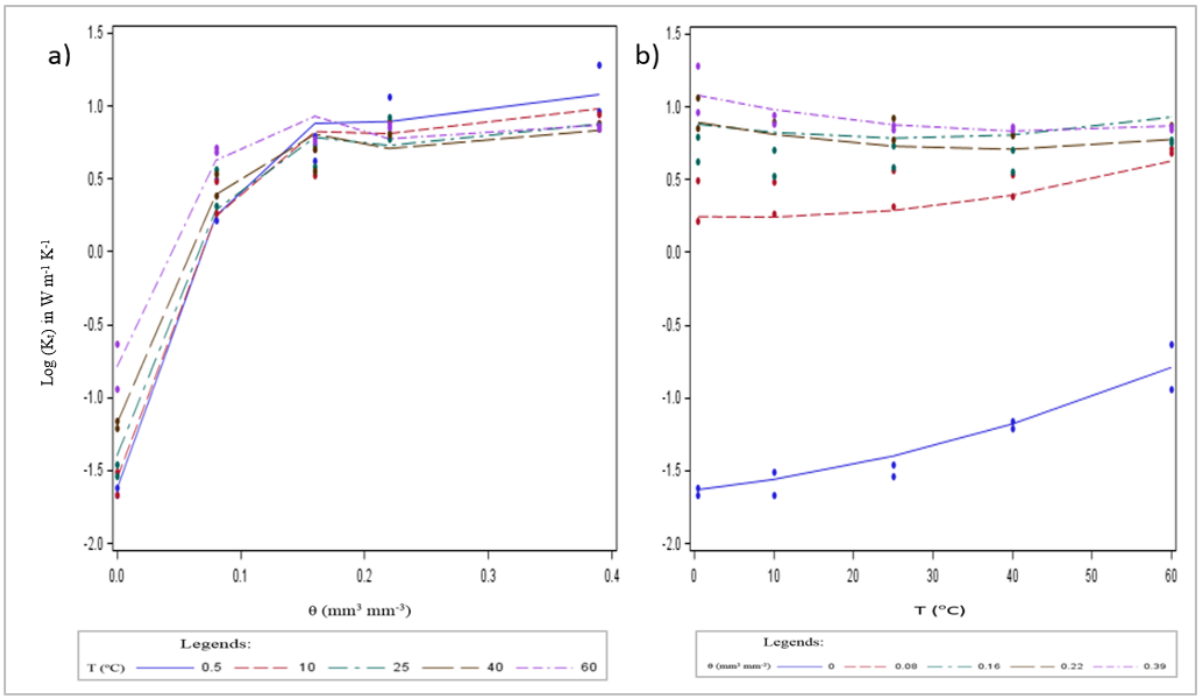

Figure 4.7 Observed and fitted values of the mean K_t: (a) Effect of soil water on K_t keeping the temperature values constant (b) Effect of temperature on K_t keeping the soil water content constant.

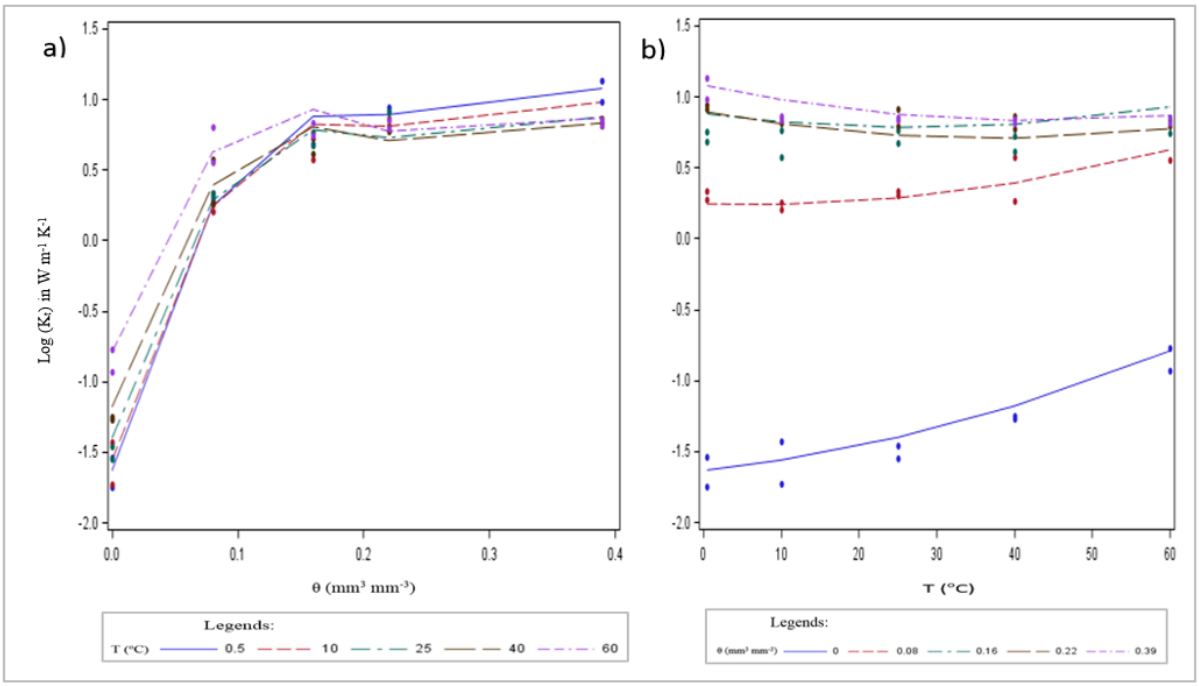

Figure 4.8 Validation of the K_t model based on Hutton data sets: (a) Observed and predicted values of the K_t against water content keeping the temperature values constant (b) Observed and predicted values of the mean K_t against soil temperature values keeping the water content constant

4.3.2.3 Thermal diffusivity

In the stepwise-regression process of thermal properties, thermal diffusivity had relatively fewer parameter and variable combinations as shown in Table 4.12. The model fitting and validation plots are also shown in Figure 4.9 and 4.10, respectively. All the statistical parameters show the model fitting and validation procedures were successful. The effectiveness of the model fitting procedure is supported with acceptable statistical parameters (R^2 = 0.93 and RMSE = 0.16). Similarly the statistically acceptable value of the coefficient of determination (R^2 = 0.75) indicates that Equation 4.6 can be used to predict fairly good values of the thermal diffusivity of similar soils.

Table 4.12 Parameters estimated for thermal diffusivity model

Variable	DF	Parameter Estimate	Standard Error	t value	Pr > |t|
Intercept	1	-1.61814	0.06874	-23.54	<.0001
θ	1	25.90759	1.52830	16.95	<.0001
θ^2	1	-126.29705	10.83317	-11.66	<.0001
θ^3	1	180.77644	18.76439	9.63	<.0001
T	1	0.00250	0.00173	1.44	0.1561
θ T	1	-0.01739	0.00803	-2.17	0.0358

$$D = \exp\left[\begin{array}{l} -1.61814 + 25.90759\theta - 126.29705\theta^2 \\ +180.77644\theta^3 + 0.00250 - 0.01739\theta T \end{array}\right] \quad (4.6)$$

Where D is a soil thermal diffusivity ($mm^2\ s^{-1}$), θ represents volumetric water content ($mm^3\ mm^{-3}$), T is the soil temperature in ^{O}C.

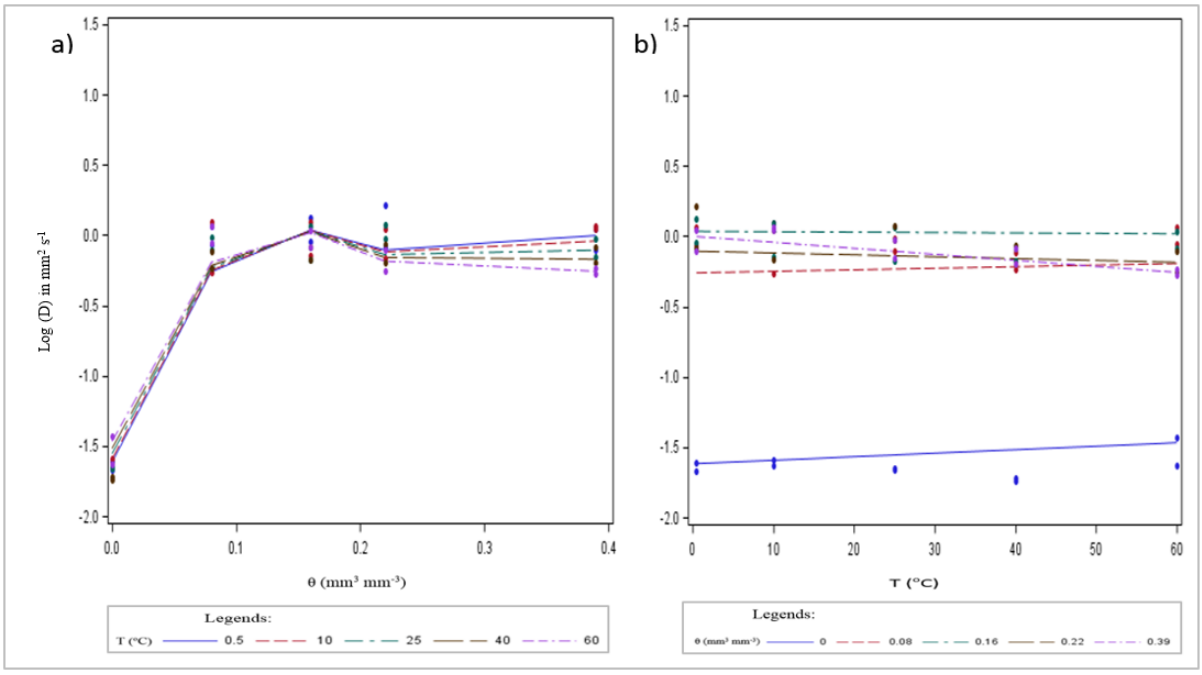

Figure 4.9 Comparison of the observed and fitted values of the mean D on Clovelly soil form: (a) Effect of soil water content on C keeping the temperature values constant (b) Effect of temperature on C keeping the soil water content constant.

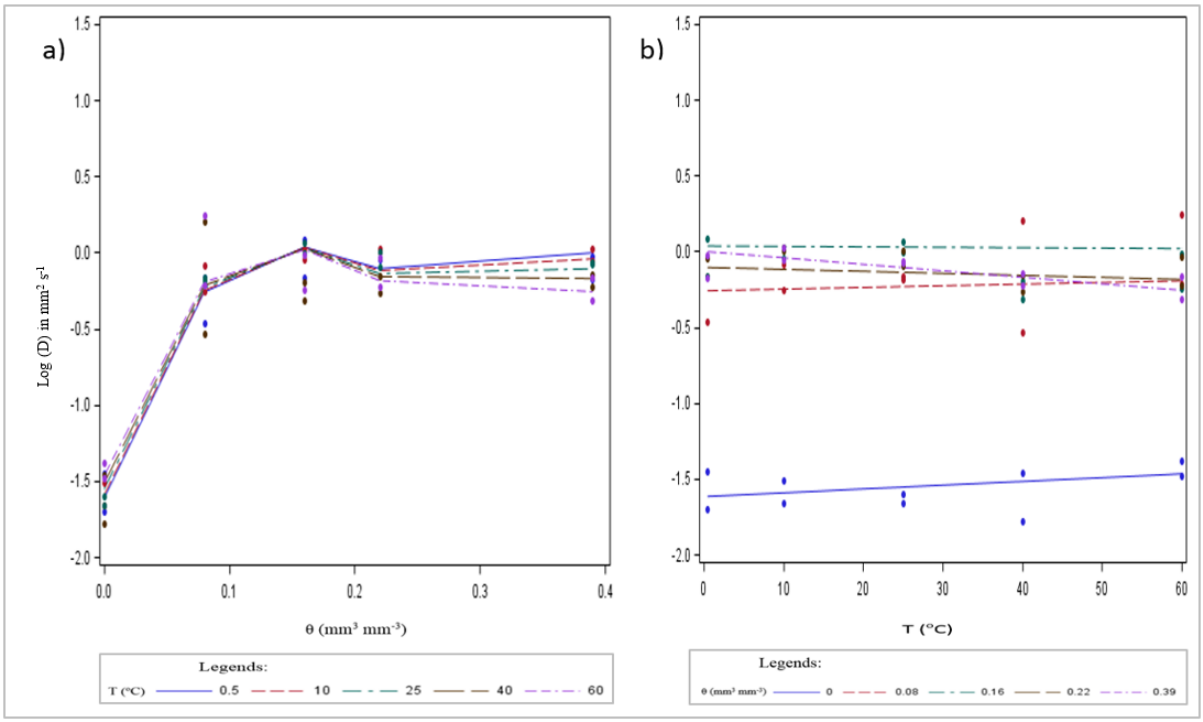

Figure 4.10 Validation of the D model based on Hutton data sets: (a) Observed and predicted values of the D against water content keeping the temperature values constant (b) Observed and predicted values of the mean D against soil temperature values keeping the water content constant

4.4 Discussion

4.4.1 Effect of soil conditions on thermal properties

This study succeeded in showing three soil conditions of importance for managing thermal properties *viz,* wetting of dry soils, freezing and thawing and excessive wetting of soils above DUL towards saturation. The interaction effects of water and temperature on the thermal properties are depicted in Figure 4.4 a-c.

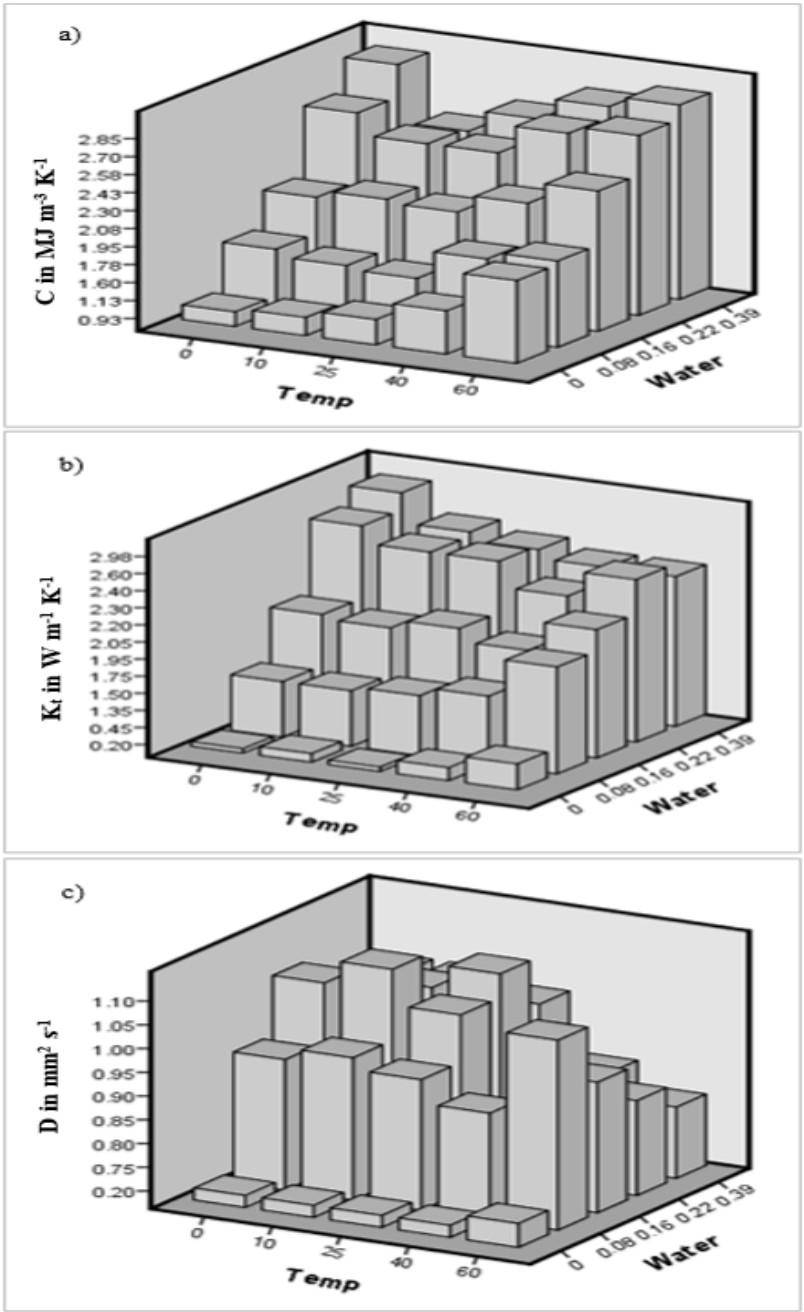

Figure 4.11 The interaction between thermal properties and the two factors, namely water and temperature: (a) Volumetric heat capacity (C), (b) Thermal conductivity (K_t) and (c) Thermal diffusivity (D).

4.4.1.1 Wetting of dry soils under rising soil temperatures

This condition refers to the 0 and 0.08 mm^3 mm^{-3} water content treatments in combination with the 0 to 60°C treatments as displayed in Figure 4.4a-c. Supportive evidence of the interaction effect of water and temperature on the thermal properties can be deducted from the intercepts and slopes, respectively, reported for groups A and B in Tables 4.3, 4.6 and 4.9. The intercepts of C, K_t and D suggests that water affected thermal properties significantly, more so in K_t and D. However, the slopes indicate that a rise in temperature of the soils affected K_t positively but there is no clear trend for C and D. Thus, water affected the thermal properties relatively more than temperature in this particular section.

Basically, wetting of a dry soil with little water apparently means replacing the air in the micro pores with water. This will assist in the formation of water bridges between soil particles hence increases the quality of contacts between particles. As a result, all the thermal properties mentioned above will increase. Therefore, the micro pores play a great role at lower water contents. Similar results are reported by Farouki (1981), Bristow (1998), Hiraiwa & Kasubuchi (2000), Tarnawski & Leong (2000), dos Santos (2003) and Smits *et al.* (2009).

The increase in K_t due to the warming of soils can be attributed to the basic mechanisms of heat transfer in materials as discussed by Callister (2001). Accordingly there are two ways namely, movement of electrons and molecular vibration. In non-metallic substances the second way of heat conduction is common. In this case the response of K_t to soil temperature can be explained by the increase in the molecular vibrations in the soil particles due to increased temperatures, and as the vibration increases K_t will also increases (Tritt, 2004; Lamond and Pielert, 2006).

4.4.1.2 Freezing and thawing

This condition of the experiment consists of the soil samples with water content from 0 to 0.39 mm^3 mm^{-3} in combination with the freezing (0°C) and thawing temperatures (10°C). The statistical evidences of this soil conditions are summarized in Table 4.2, 4.5 and 4.8 under Groups A & B for C, K_t and D, respectively. The experimental results in this specific condition clearly revealed that there was a significant change in the volumetric heat capacity of soils between the two temperature levels especially at higher water contents. As the water content increased from dry soil towards saturation, the C of the soils was almost similar in water contents lower than DUL. However, the heat capacity of the soils was higher in the freezing temperature (0°C) than the values at 10°C after DUL towards saturation. But the effect of freezing and thawing temperature levels was lower in both K_t and D as compared to the C-

temperature relationships. Especially, the effect of freezing and thawing was inconsiderable in the change in D of soils in these temperature groups.

In the freezing temperature (0ºC), the soil sample consists of the three phases of matter, namely solid (frozen soil particles and smaller ice crystals), unfrozen water and water vapour and air at lower water contents. Therefore, the volumetric heat capacity (which is called the apparent heat capacity in this condition) of the soils will be the sum of the heat capacity of the components and the latent heat of fusion of ice (Anderson and Morgenstern, 1973; Hanson *et al.*, 2004). On the other hand, in the case of the thawing temperature (10ºC), the C of the samples will be the sum of C of the components only since there is no ice formation. Therefore, the increase in C of the samples in the freezing temperature would be due to the latent heat of fusion during phase change from liquid water to ice. This result is consistent with the reports of Anderson and Morgenstern (1973), Sawada (1977) and Farouki (1981).

Regarding the effect of freezing temperature on K_t, the increase especially at higher water contents would be due to the phase change of water to ice. Farouki (1981) explained that the thermal conductivity of ice is four times greater than liquid water. Similar results are reported by Sawada (1977), Farouki (1981) and Hanson *et al.*, (2004).

4.4.1.3 Excessive wetting

The soil conditions under this category includes the treatment combinations of higher water contents between 0.16 mm^3 mm^{-3} and saturation (0.39 mm^3 mm^{-3}) with temperature values between room temperature (25ºC) and 60ºC. As discussed in the previous sections, thermal properties responded differently for this condition of soils. All the statistical evidences for this soil conditions are summarized in Tables 4.3, 4.6 and 4.9 for C, K_t and D, respectively. In this regard, the volumetric heat capacity of the soils increased with increasing water content irrespective of the soil temperature. However, thermal conductivity and diffusivity showed different responses with water than C. The results suggested that K_t will increase from dry soils to DUL, where after it change very little with further increase in water up to saturation. In the case of thermal diffusivity, it attains its maximum at 0.16 mm^3 mm^{-3} where after the increase in water content did not affect D. This was what was exactly shown by Willis & Raney (1971). On the other hand, judging the slopes of the K_t and D curves, the relationship between these two properties and temperature was changing positively from a dry soil (Group A) towards their maximum value and then turned negative towards saturation (Group E) with increasing temperature from 25ºC up to 60ºC.

As the water content of the soil increases, the pore space filled with air would be replaced with water. Therefore the increase in C due to water content could be due to the higher thermal storage capacity of water than air. On the other hand, the influence of temperature would be due to the increase in the vibrational energy of the atoms in soil particles. As the vibration of atoms increase the ability of the particles to store or transmit energy increases (Callister, 2001). The influence of soil water content and temperature on C was similarly reported by Farouki (1981), Callister (2001), Santos (2003), Yu *et al.* (2015).

In this condition of soils, the soil is sufficiently wet for the formation of water bridges and increases the quality of contacts between soil particles. Therefore, K_t increased with water content from dry soil up to DUL. But the increase in K_t with a further increase of soil water beyond DUL was not considerable. This is because as the water content of the soil increases after DUL, the order and binding of the water from the particle surfaces will decrease as its distance from the soil particle surfaces increases. As a result the water will be free to move and do not contribute in the thermal conductivity (Farouki, 1981). This result is consistent with the reports of Bristow (1998), Hiraiwa and Kasubuchi (2000), Tarnawski and Leong (2000), Santos (2003) and Smits *et al.* (2009).

On the other hand, the increase of K_t with lower and medium water contents due to temperature would be due to the increase in the molecular vibrations in the soil particles with temperature as explained above. But at higher water contents, the increase in temperature showed a considerable decrease in K_t. This could be due to the increase of the fluidity of the water and decrease of both the surface tension and viscosity of water with the increase in temperature. These physical properties as a functions of temperature will affect the thermal bridging of the water. A rise in temperature will also decrease the volume of the water bridge at each contact point, which will cause the decrease in the conduction of heat. A similar result is reported by Willis and Raney (1971), Campbell *et al.* (1994), Hiraiwa and Kasubuchi (2000) and Yu *et al.* (2015).

The effect of water content on the thermal diffusivity of soils was higher at lower and medium water content ranges. On the other hand, there was a considerable influence of soil temperature throughout the groups except the dry soil in which its influence was insignificant. As it is well explained in the literature (Section 2.3.3.2.3), thermal diffusivity is the ratio of thermal conductivity and volumetric heat capacity. As a result any change in both properties affects thermal diffusivity directly. Therefore, the decrease of D in higher water contents could be related to the faster increase of C than K_t in the given water content and temperature ranges.

This result is similar to the reports of Willis and Raney (1971), Sawada (1977), dos Santos (2003); Omer and Omer (2014) and Yu *et al.* (2015).

4.4.2 Thermal pedotransfer functions

Empirical equations were developed to predict thermal properties based on the relationship between thermal properties and soil water, temperature and their interactions as given in Equation 4.4 for C, Equation 4.5 for K_t and Equation 4.6 for D. The analysis that was performed on thermal properties of the soils show that differences in soil water content, temperature and their interaction have significant effects on the three thermal properties. Comparisons between experimental and predicted values also revealed that the proposed models can be applied to determine soil thermal properties with similar soil conditions.

Although thermal properties play a vital role in various applications, sufficient information is not available in the literature especially the area covered by sandy deposits in Africa, south of the equator. Since direct determination are expensive, time consuming, laborious and sometimes impractical for large scale applications (Tombul *et al.*, 2004; Dashtaki *et al.*, 2010), the use of pedotransfer functions are important alternatives.

Many mathematical equations have been proposed in the literature (Kersten, 1949; Johnson, 1977; Côté and Konrad, 2005; Chen, 2008) to estimate thermal properties of soils, but none of them considered the effect of temperature and its interaction with water content. Most of the models considered the relationships of thermal properties with water content, bulk density, porosity, mineralogy, etc. As it is evident from this study, soil water and temperature influence thermal properties both as main effects and in interactive manner. As a result the incorporation of temperature in the empirical equation will enable the models to predict effectively.

The three models were tested with data collected from separate soil samples and reliable results have been observed. However, additional datasets should be collected or gained from literature for validation of these equations so that to apply in all types of aeolian soils in the semi-arid climates of Africa, south of the equator.

4.5 Conclusion

The objective of this chapter was to describe the influence of soil water and temperature on thermal properties, namely volumetric heat capacity (C), thermal conductivity (K_t) and thermal diffusivity (D) of two aeolian soils (Clovelly and Hutton). It was also aimed at developing pedotransfer functions to estimate C, K_t and D of aeolian soils.

This study succeeded in showing three important water-temperature combinations, i.e. wetting of dry soil under rising temperature, freezing and thawing and excessive wetting of soils. Wetting of dry soils up to 0.08 mm^3 mm^{-3} improved all thermal properties of aeolian soils. Hence, a 94, 703 and 346% increase in C, K_t and D was observed between dry and slightly wetted soils. On the other hand, C was decreased by 55%, K_t and D were increased by 137% and 367%, respectively with increasing temperature.

Freezing (0ºC) and thawing (10ºC) temperatures had a significant influence in the volumetric heat capacity of the soils. There was an average 8% increase in C as the temperature changed from 0 to 10ºC while a 42% decrease was recorded due to water content. Even though the effect of these temperatures was negligible, K_t decreased by 11% and D increased by 10% due to an increase in water content from 0 to 0.39 mm^3 mm^{-3}.

Volumetric heat capacity and thermal conductivity increased at a decreasing rate with addition of water up to DUL. On the other hand thermal diffusivity increased remarkably with increasing water content up to 0.16 mm^3 mm^{-3}. Volumetric heat capacity at all water contents increased with temperature. Thermal conductivity and diffusivity also increased with temperature up to DUL and 0.16 mm^3 mm^{-3}, respectively where after decreased with increasing temperature.

Pedo-transfer functions (PTF) provided reasonable estimates for all the thermal properties with R^2 ranging from 0.72 to 0.92. Although the development of the pedo-tranfer functions was a first step towards understanding relationships between physical and thermal properties of aeolian soils it could provide insight to researchers on how thermal properties influence temperature fluctuations under different soil water regimes. A comprehensive model in this regard could be developed when a detailed account of thermal-physical property relationships and interactions is researched on aeolian soils under different land use.

CHAPTER 5

CHARACTERIZING THE EFFECT OF SHALLOW WATER TABLES ON SOIL WATER EVAPORATION AND TEMPERATURE DISTRIBUTION

5.1 Introduction

Evaporation is a water loss from the soil water balance to the atmosphere and its proliferation over and above precipitation is associated with dry soil water regimes, fall in a water table levels and desertification. Globally an annual amount of 7.2×10^{13} m^3 of water is lost through evapo-transpiration (Babkin, 2009). Under South African conditions, Bennie and Hensley (2001) and Jovanovic *et al.* (2015) reported that on average 65% of the annual precipitation is lost through evapo-transpiration. Evaporation is not a means of water loss only, it is also one of the major means of loosing energy during the conversion of liquid water to vapour. As Babkin (2009) estimated that evaporation uses 25% (which is about 1.26×10^{24} joules) of the total energy reaching the earth's surface. Therefore evaporation is a very important process that influence water and energy balances between the earth's surface and the atmosphere. Hence, accurate determintion of evaporation is a very important task in arid and semi-arid environments.

South Africa is generally a water scarce country and this is attributed to the higher potential evapotranspiration with aridity between 0.2 to 0.5 (Bennie and Hensely, 2000). On the other hand, most of the dry land and irrigated crop productions are practiced in arid and semi-arid areas (Bennie and Hensely, 2000; Harmse and Hattingh, 2012). Therefore, the most important factor limiting agricultural production in South Africa is the unavailability of water (Benhin, 2006). Hence water management and governance is required to ensure the sustainable use of this precious resource. To achieve the sustainability of this resource, unproductive water losses, like evaporation, drainage and runoff must be quantified accurately and methods should be devised to minimize it.

Soils developed from aeolian sands, e.g. Clovelly and Hutton soil forms, are characterized by weak soil structure caused by relatively higher sand fraction (Harmse and Hattingh, 2012; Le Roux *et al.*, 2013). In some cases the sands are deposited on impermeable parent material, which enables the soils to hold appreciable water during irrigation or rainfall. Due to high incidence of fine silt and sand fraction, water will also be taken up by the capillary action during the incidence of shallow water tables. However, the water stored in the pores is not strongly adsorbed as in the case of clayey soils (Harmse and Hattingh, 2012). Most importantly, the area

is characterised by the high radiation and prolonged sunshine hours. As a result, the stored water near the soil's surface is more vulnerable to E_s. Hence, evaporation accounts for the highest losses of surface and ground water. The drying front has also been observed to advance deeper into the soil profile, up to 1m in arid and semi-arid environments (Hensley *et al*, 2000; Hillel, 2004). Bare soil evaporation could also be exacerbated in shallow soil profiles or by the activities of shallow water tables (Ripple *et al.*, 1972; Chari *et al.*, 2012). Specifically evaporation under shallow water table has got great attention in arid and semi-arid areas since the contribution of shallow water table to evaporation is significant (Chen and Hu, 2004; Bargahi and Moosavi, 2006; Young *et al.*, 2007). On the other hand ground water is the major water resource in dry climates (Sen, 2015). Therefore water management especially managing evaporation is a key practice to sustain life in dry areas.

On the other hand, the solar energy reaching the earth's surface has an important effect on the surface energy fluxes. This energy will be stored in the soil, reflected back to the atmosphere as sensible heat or will be lost as latent heat during evaporation (Arya, 2001; Hillel, 2004; Saito *et al.*, 2006). Therefore, as the profile water content increases, the soil water evaporation will increase and a considerable amount of heat energy will be lost as latent heat. As a result, the profile soil temperature will decrease (Saito *et al.*, 2006; Maxwell *et al.*, 2007; Alkahier *et al.*, 2012). Generally, soils with shallow water tables will have higher water contents than deep water table soils, hence it will have lower surface temperature due to a higher loss of energy through evaporation.

Even though the presence of a shallow water table is important in arid and semi-arid climates, it has other influences unless it is properly managed and used. Especially when the land is used for irrigated agriculture, the problem will be hazardous and it will cause severe degradation since such dry areas are mostly saline naturally (Umali, 1993). Improper application of irrigation water and poor drainage will cause the water level to rise with its soluble salts. This will cause salinization and the problem will be severe if the rate of evaporation is very high (Hillel, 1998). For example Ojo (2013) estimated that after 15 years (from 2005 to 2020), 46% of the total irrigation area in Vaal Harts Irrigation Scheme (Free State Province, South Africa) will have visible signs of salinity on its surface.

Many researches have been conducted on evapo-transpiration (Ehlers *et al.*, 2003; Haka, 2010; Nhlabatsi, 2010), however, the study of soil water evaporation is still an active area of research. Especially the contribution of shallow water table to evaporation from bare soils have got great attention since shallow water tables are the only fresh water resources in arid and semi-arid

areas. The study by Ehlers *et al.* (2003) was concentrated on contribution of shallow water table to evapo-transpiration while Haka (2010) was on partitioning of evapotranspiration in to its components. Whereas the study by Nhlabatsi, 2010) was conducted without water table. As a result this study would be important to quantify evaporation from shallow water tables and understand the effect of water tables to the distribution of temperature in soil profiles.

This chapter aimed at quantifying the contribution of shallow water table towards bare surface evaporation in two typical aeolian soil groups, namely Clovelly and Hutton. The following objectives were the focus of this section: (i) quantifying the daily rate and cumulative evaporation from different water table depths and soil type (ii) characterizing the effect of different water table depths on the temperature distribution of the two soil profiles.

5.2 Material and methods

5.2.1 Description of the experimental site

This research was conducted at Kenilworth Research Farm, Department of Soil, Crop and Climate Sciences, University of the Free State, near Bloemfontein, South Africa. The research site is equipped with field lysimeters (30 round static lysimeters 1,800 mm diameter and 2,000 mm deep) arranged in two parallel rows of 15 each, with their rims 50 mm above the bordering soil surface (Figure 5.1). One row of lysimeters are filled with Clovelly soil, an aeolian sand deposit originated from Hoopstad while the other row is filled with Hutton, another aeolian soil originated from the Kenilworth Experimental Farm of the University of the Free State. The formation of the typical Hutton soil from Bainsvlei that is collected from the experimental farm in Kenilworth is explained in Chapter 3, Section 3.2.1.

Figure 5.1 Kenilworth Research Farm

The lysimeters were covered with a mobile rain shelter (Figure 5.1) that can be moved into place when a rainfall event occurs.

5.2.2 Experimental treatments and management of lysimeters

Five water table depths or treatments were distributed randomly for the rows (soil types) as shown in Table 5.1 and Figure 5.2. Artificial water tables were created in the field lysimeters with different water table depths based on the treatment allocation. The bottom of each lysimeters was connected to a clear hydraulic tube (to monitor the depth of water table) and a 10 litre bucket that was used to replace the amount of water lost through evaporation so as to maintain the water table at constant depth (Figure 5.3). The water table was checked every day and a measured amount of water was refilled to each lysimeter based on the daily decrease in height of water table read from the manometer (Figure 5.4). For each lysimeter a 1.2 meter soil moisture probe that was developed by DFM Software was installed. During installation, a hole was made by using a hand drilling machine. The diameter of the hole was made similar to the size of the DFM probe so that it would be tight and have enough contact to the soil. The first sensor was kept just below the soil surface (2–3 cm) so as to measure ground surface temperatures.

Table 5.1 Treatments and replications.

No.	Treatment codes	Explanation	No. of replications
1	WT_1	Water table with 0 mm depth	3
2	WT_2	Water table with 500 cm depth	3
3	WT_3	Water table with 1000 mm depth	3
4	WT_4	Water table with 1500 mm depth	3
5	WT_5	No water table (control)	3

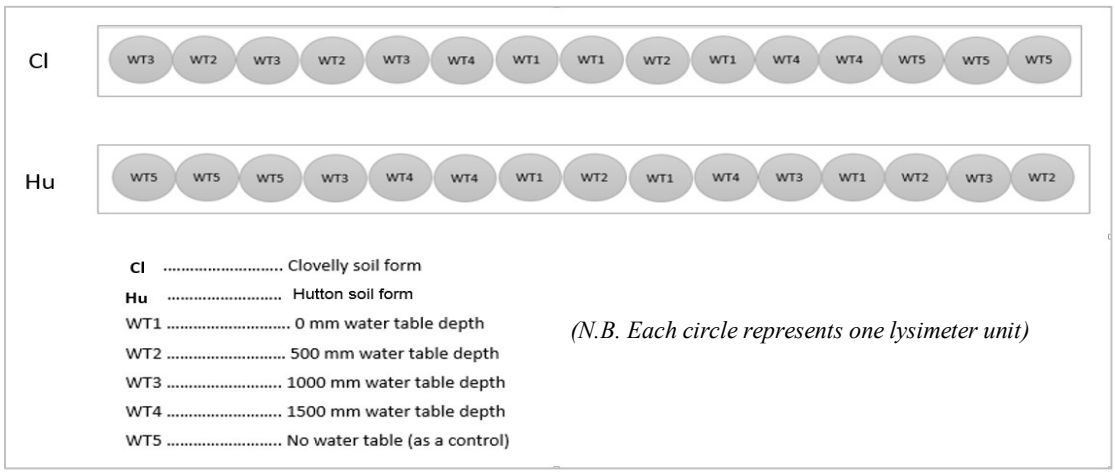

Figure 5.2 Field lay out of the experiment.

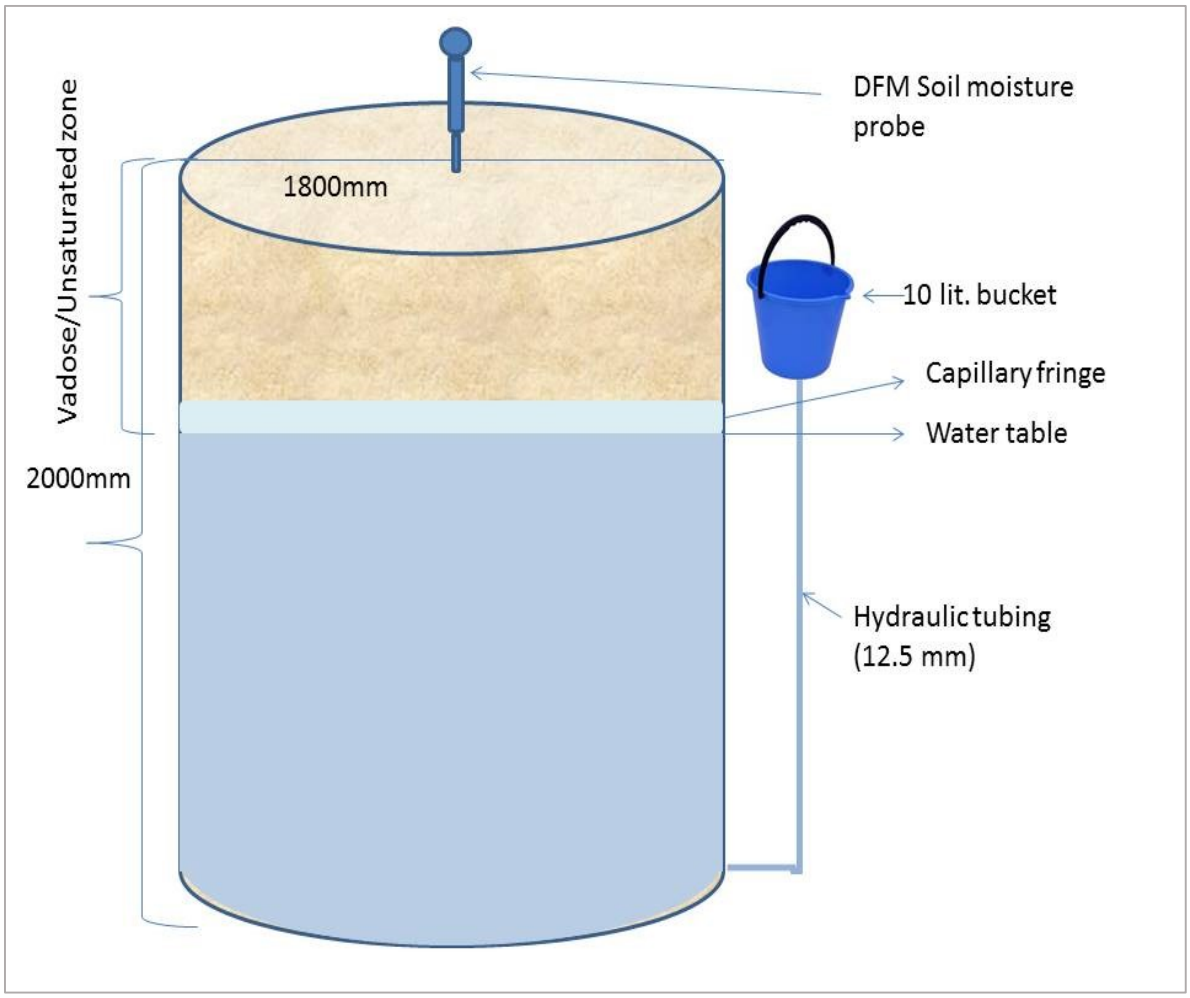

Figure 5.3 A typical lysimeter unit showing the major components during preparation of the site for experiment.

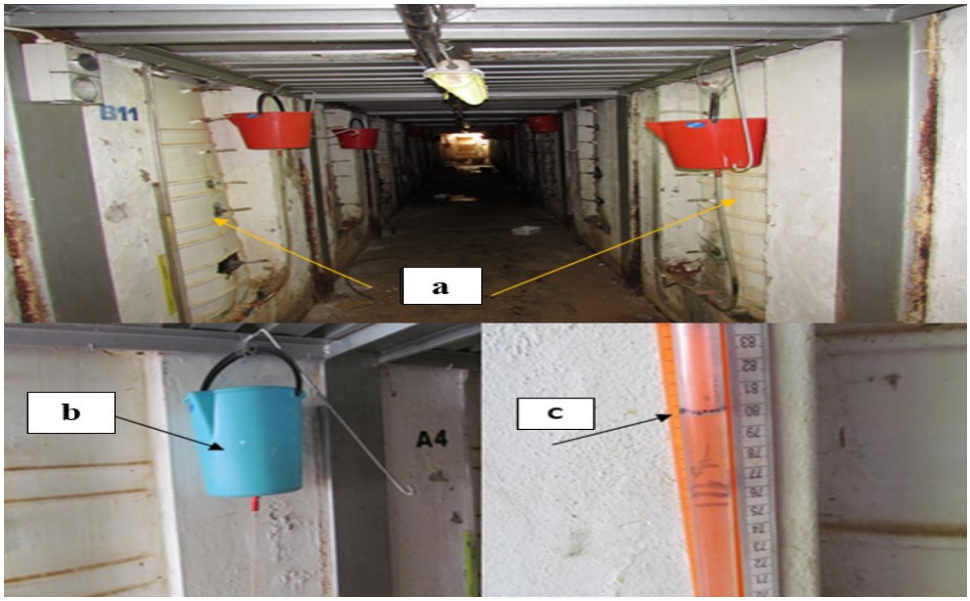

Figure 5.4 Preparation of the experimental cite: (a) Lysimeters constructed below the ground surface (b) 10 litre bucket (c) Manometer showing the water table depth.

5.2.3 Measurements

5.2.3.1 Recharge of the water tables

During the whole experimental period, a measured amount of water was added every day to each lysimeter based on the treatments (water table depths) and daily weather conditions of the area. This measured amount of water was part of the water balance during calculation of E_s.

5.2.3.2 Soil water content

Time series soil water content in the soil profile was measured using DFM soil moisture probes in two cycles. The first cycle representing the time from November 01, 2014 to December 02, 2014 while the second cycle represents January 8, 2015 to February 5, 2015. Each DFM probe measured 6 data points at different depths (with 200 mm interval) at a time. The soil surface water content was also measured gravimetrically from each lysimeter on daily basis.

DFM moisture probes were calibrated in the filed lysimeters. Three soil water content readings were taken with the DFM probes at the six depths as well as the gravimetric water content at the same depth and time. All the lysimeters were irrigated until the soil become fully saturated. The first readings were taken immediately at saturated water content after which the water releasing valves of the lysimeters were opened for 3 days in order for the soil to reach field capacity, where after the second measurements were taken. The last measurements were taken when the soil was completely dried out. This was achieved by planting sunflower. The sunflower was irrigated for the first 2-3 weeks and then allowed to grow on the stored soil water in the lysimetres. Measurements commenced after the plant showed signs of severe water stress. Figure 5.5 shows the different stages of sun flower during the calibration process.

The readings from the DFM moisture sensors versus the gravimetric water contents were regressed to get calibration equations for soil water content. Some of the plots and the calibration equations of the water sensors are given in Appendix 5.1.

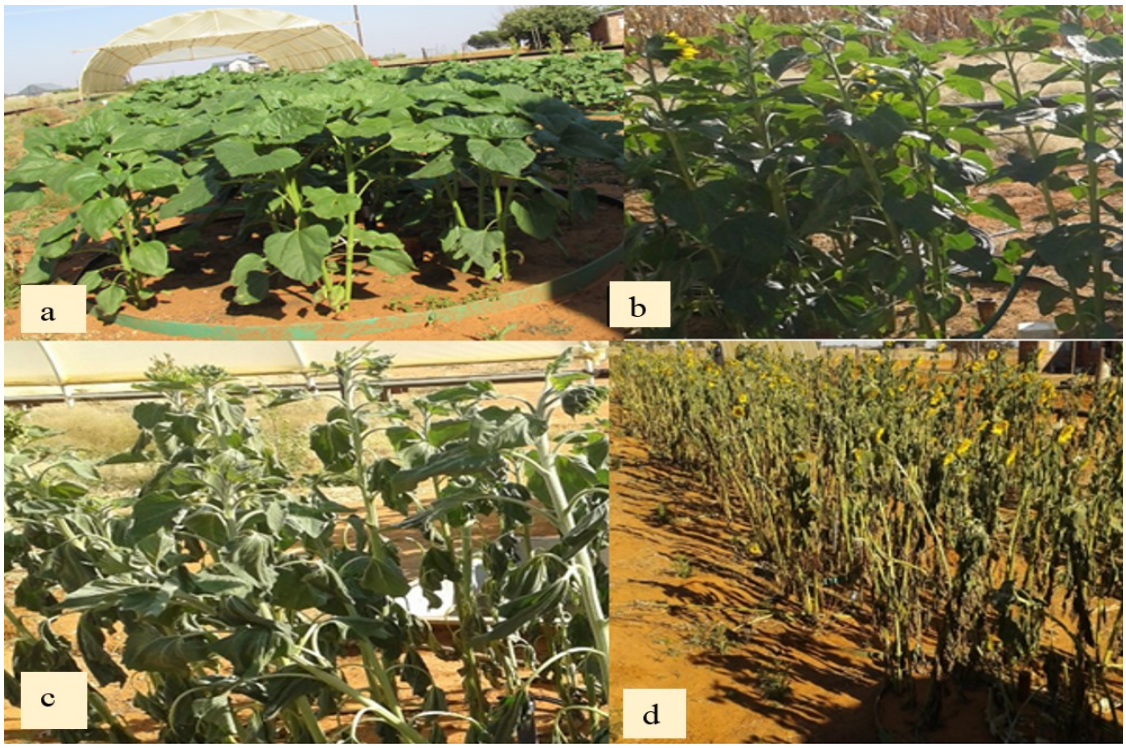

Figure 5.5 Different development stages of Sunflower crop during calibration of DFM probes: (a) and (b) the crop looks in good stand (c) the crop started to wilt (d) the crop started dying

5.2.3.3 Potential evaporation

The potential evaporation of the study area during the experimental period was provided by the South African Weather Service in daily basis.

5.2.3.4 Determination of soil water evaporation

The rate of surface evaporation from different water table depths was estimated from the water balance equation as given in Equation 2.41.

For Equation 2.41, the effect of precipitation was nullified by using a movable shelter, then P = 0; since P = 0 and there was no surface irrigation, $R_o = 0$; the lysimeter was confined in all sides except in its top side, so $D_r = 0$; since the soil surface was free of any crops or weeds, $T_r = 0$. ΔW was calculated as the change in volumetric water content in the profile. I_s was the measured amount of water added daily to recharge the lysimeters so that the water table would be at constant depth. So the water balance equation could be shortened as:

$$E_s = I_s - \Delta W \,, \tag{5.1}$$

The critical depth h_{max}(mm) at which the water table is hydraulically connected to the surface of the soil was determined from the empirical relationship to the clay plus silt content (S_i+C_y, %) as proposed by Ehlers *et al.* (2003):

$$h_{\max} = -0.3463\left(S_i + C_y\right)^2 + 24.525\,(S_i + C_y) + 484.47, \qquad (5.2)$$

5.2.3.5 Soil temperature

The temperature sensors in the DFM probes were used to measure soil temperature hourly at the six depths. The effect of variations in soil, water table and measurement depths to temperature distribution in the profile were investigated. The experimental mean, water table mean and daytime amplitude temperatures were calculated as indicators of variation in the soil temperature. In this study the experimental mean was the mean temperature for the whole measurement period without considering the treatments. Whereas, the water table mean was the mean of all observations in the same water table treatment only. The daytime amplitude was calculated by subtracting the experimental mean temperature from the mean maximum temperature during the measurement period for each treatment. In the soil temperature analysis, only the 2nd cycle of measurements were considered.

The temperature sensors were calibrated in the Soil Physics Laboratory, in the Department of Soil, Crop, and Climate Science, University of the Free State. The probes were immersed in a temperature regulator bath filled with distilled water. The probes were set to take measurements at intervals of 1 minute. The water in the bath was stirred using a wire plunger for even temperature distribution before taking readings. The temperature readings were taken using three mercury thermometers, set at different depths in the water bath. The thermometers were to confirm the homogeneity of the temperature in the water bath. The temperature in the water bath was gradually increased from 10 to 50˚C. The thermometer readings were taken in 10-minute time intervals, with a total of 15 observations.

The readings from the DFM temperature sensors versus the thermometric readings were regressed to get calibration equations that was used for the data collected from the field. Some of the plots and the calibration equations of the temperature sensors are given in Appendix 5.2.

5.2.4 Statistical analysis

This experiment was conducted on 2 soil types (Clovelly and Hutton) with 5 water table depths (0, 500, 1000, 1500 mm depths and No water table as a control) and 3 replications each arranged in a completely randomized block design. ANOVA was used to indicate the presence

of statistical differences between the means of the cumulative evaporation ($\sum E_s$) from soils, from the water table depths or their interactions. A regression analysis was performed to demonstrate the relationship between the water table depth, soil type and potential evaporation to the daily rates of evaporation.

Regarding the temperature, ANOVA have been done considering the daytime amplitude temperature as a major indicator of variation in temperature in the soil profiles. Hence, the two soils were evaluated with their six measurement depths (MD) and with four replications each arranged in simple random block design. The four water tables (WT), excluding the 0 mm, were combined with the six measurement depths (MD) in two replications each arranged in a similar design to see the influence of water table and measurement depths on the temperature distribution in the soil profiles.

5.3 Results

5.3.1 Daily rates and cumulative evaporation

The daily rates of soil water evaporation from the two soils (Clovelly and Hutton) and two measurement cycles (1st cycle from November 01, 2014 to December 02, 2014) and 2nd cycle (from January 08, 2015 to February 5, 2015) with five shallow water tables kept in steady state conditions are depicted in Figure 5.6. The data reflects on the variation in E_s as affected by water table depth with each soil type and the two cycles of measurement. It is clear that the two factors (soil and water table depth) influenced E_s. The statistical proof to what extent these two factors had influenced E_s can be denude from the ANOVA tables (Tables 5.2 and 5.3), accordingly.

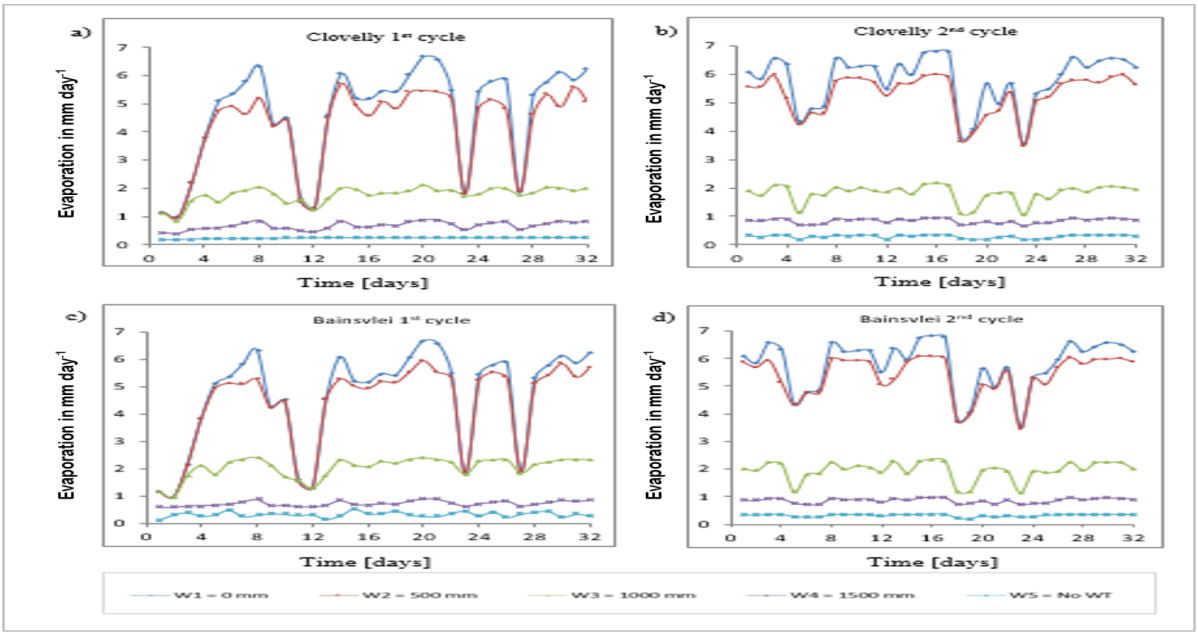

Figure 5.6 The daily rates of soil water evaporation from: a) Clovelly 1st cycle of measurement, b) Clovelly in the 2nd cycle of measurement, c) Hutton in the 1st cycle of measurement and d) Hutton in the 2nd cycle of measurement.

The analysis of variances on the effect of soil types and water table depths on the cumulative evaporation ($\sum E_s$) measured in 1st and 2nd cycle of measurement were summarized in Table 5.2. The pairwise comparison of $\sum E_s$ using the LSD method between the soil groups and water table depths is also given in Table 5.3 for both cycles of measurements.

Table 5.2 ANOVA for the interaction effect of water table depth (WT) with soil type on $\sum E_s$ in both cycles

Source	DF	1st cycle				2nd cycle			
		Sum of Square	Mean Square	F Value	Pr > F	Sum of Square	Mean Square	F Value	Pr > F
Rep	2	15.52	7.76	1.55	0.2387	2.2154	1.1077	0.46	0.639
Soil	1	109.75	109.75	21.97	0.0002	22.7418	22.7418	9.43	0.007
WT	4	99908.55	24977.14	4999.41	<.0001	162081.14	40520.284	16805	<.0001
Soil*WT	4	68.63	17.16	3.43	0.0297	17.2358	4.309	1.79	0.175
Error	18	89.93	5			43.4021	2.4112		
Total	29	100192.38				162166.73			

Table 5.3 Comparison of cumulative evaporation ($\sum E_s$) among the two soils and five water table depths

Treatments		Mean $\sum E_s$ (mm) comparison	
		1st cycle	2nd cycle
Soils	Clovelly	73.74^{b}	89.9467^{b}
	Hutton	77.5653^{a}	91.688^{a}
Water table depths	0 mm	149.14^{a}	185.46^{a}
	500 mm	136.838^{b}	171.39^{b}
	1000 mm	61.013^{c}	60.36^{c}
	1500 mm	22.307^{d}	27.39^{d}
	No WT	8.965^{e}	9.49^{e}

The analysis of variance confirms the overall trend in Figure 5.6 that the cumulative evaporation was highly significant due to a difference in water table depth, soil type or both factors. Even though the interactions between water table depth and soil type was significant in the 1st cycle, its effect in the 2nd cycle of measurement was not significant. Therefore, due to lack of consistency of the results, the interaction is ignored for further discussion. The pairwise comparison between the water table depths and soils show that all the water table and soil groups are significantly different from each other in both measurement cycles.

The results of the relationships between the cumulative evaporation ($\sum E_s$) and the cumulative potential evaporation ($\sum PE$) of the study area are depicted in Figures 5.7 and 5.8 for the two soils and the five water table depths, respectively.

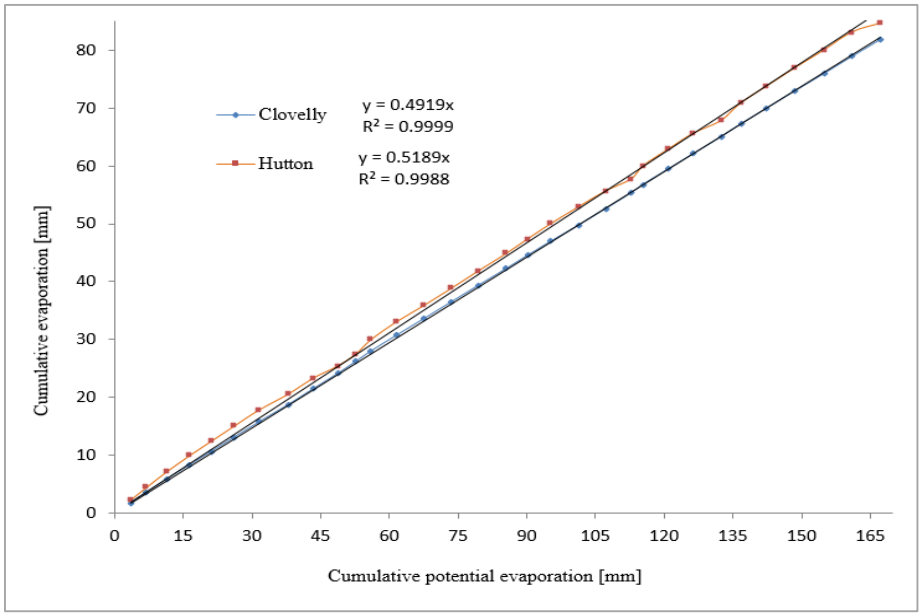

Figure 5.7 Comparison of the cumulative evaporation in the two soil types.

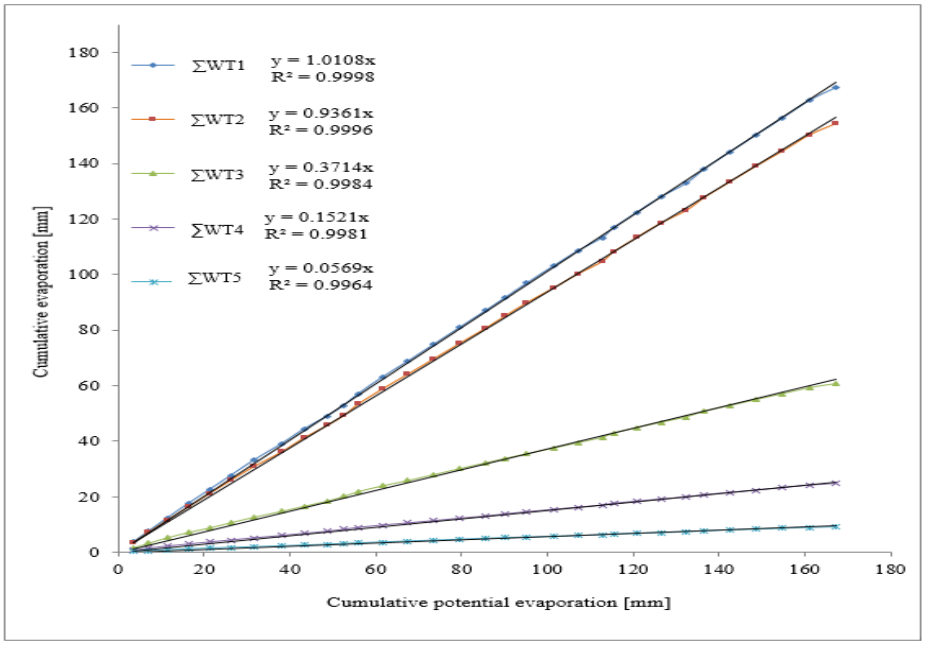

Figure 5.8 Comparison of the cumulative evaporation in the five water table depths.

Cumulative evaporation increased linearly as the cumulative potential evaporation increased for both soils and water table depths. But the rate of increase in Hutton (0.52 mm mm^{-1}) profile was slightly higher than Clovelly (0.49 mm mm^{-1}) as it is evident from the slopes of the lines in Figure 5.7. Regarding the effect of water table depth, $\sum E_s$ generally increased as the water table decreased, but the rate of increase in $\sum E_s$ with the increase in $\sum PE$ differs among the water tables. In other words, the response of the water tables for an increase in potential evaporation was highly dependent on the depth of the water table. E_s from shallow water tables were highly increased with potential evaporation compared to the relatively deep and no water table treatments. This rate of change in $\sum E_s$ is indicated by the slope of each treatment (Figure 5.8) with the 0 mm and no water table treatments recorded the maximum and minimum slopes, respectively.

The comparison of relative profile water loss from different water table depths from the two soils is given in Table 5.4.

Table 5.4 Comparison of relative profile water loss through bare soil evaporation from different water table depths along two soil types

No.	Water table depth in mm	Clovelly		Hutton	
		ΣE_s	% loss	ΣE_s	% loss
1	0	167.3	100	167.3	100
2	500	151.95	90.75	156.3	93.45
3	1000	57.55	34.75	63.8	38.7
4	1500	24.3	14.5	25.45	15.2
5	No WT	8.15	4.85	10.3	6.25

No WT refers to treatment with no water table

This is the relative contribution of each water table treatment to the atmosphere. Taking the averages between the soil types, the 0 mm and no water table depth were the highest and lowest contributors with average values of 100% and 5.55%, respectively. Similarly 500 mm, 1000 mm and 1500 mm water table depths contributed 92.1%, 36.7% and 14.9% of the atmospheric evaporative demand or potential evaporation, respectively.

5.3.2 The influence of water table depth to temperature distribution on the soil profiles

The ANOVAs of the mean daytime amplitude of the 32 days of measurement between the two soils and four shallow water table depths were summarized in Table 5.5 and 5.6, respectively.

Table 5.5 ANOVA for the effect of soil type and measurement depth (MD) in the daytime amplitude as an indicator for the difference in temperature distribution in soils

Source	DF	Sum of Square	Mean Square	F Value	Pr > F
Rep	3	13.38	4.46	2.11	0.118
Soil	1	0.39	0.39	0.18	0.672
MD	5	383.29	76.66	36.22	<.0001
Soil*MD	5	0.29	0.06	0.03	0.9996
Error	33	69.84	2.12		
Total	47	467.19			

Table 5.6 ANOVA for the effect of shallow water tables and depths of measurement in the daytime amplitude as an indicator for the difference in temperature distribution

Source	DF	Sum of Square	Mean Square	F Value	Pr > F
Rep	1	0.388	0.388	3.3	0.08
WT	3	13.383	4.461	37.95	<.0001
MD	5	383.291	76.658	652.19	<.0001
WT*MD	15	67.423	4.495	38.24	<.0001
Error	23	2.703	0.118		
Total	47	467.188			

The ANOVA shows that there was no significant difference between the amplitude due to the variation between the two soils. But, both the water table and measurement depths and their interaction was highly significantly influencing the amplitude of the temperature indicating that the distribution of temperature in soils are affected by the water table and measurement depth. The effect of the interaction is further explained by the separation of the mean amplitude by the LSD method as summarized in Table 5.7. This pairwise comparison of the mean amplitude shows that generally lower water tables with shallower measurement depths had greater amplitudes which indicates the presence of higher soil temperature. The reverse was true for shallow water tables and deeper measurement depths.

Table 5.7 Comparison of the mean daytime amplitude temperature by the interaction between water table depth and measurement depth

Water table Depth (mm)	Depth of Measurement (mm)	Mean of amplitude (^{o}C)	Tukey grouping
1500	0	12.01	a
No WT	0	9.91	b
1000	0	9.09	b
500	0	4.01	c
1000	200	3.44	cd
No WT	200	3.14	d
1500	200	2.64	de
500	1000	1.65	e
1000	400	1.60	e
No WT	400	1.49	e
500	800	1.47	e
500	600	1.29	e
1500	1000	1.24	e
1000	1000	1.17	e
1500	400	1.16	e
No WT	1000	1.01	e

No WT	800	0.82	e
500	200	0.80	e
500	400	0.77	e
No WT	800	0.66	e
1500	800	0.59	e
1000	600	0.59	e
1000	800	0.54	e
1500	600	0.45	e

The interactive effect of the 5 water table depths with 6 depths of measurements on the diurnal variation of temperature is depicted in Figure 5.9. As the depth of measurement increased from the surface down the profile, the variation of temperature decreased within the diurnal cycle. This was what exactly shown by the decrease of the daytime amplitude as an indicator of diurnal temperature variation in the analysis of variance. On the other hand, as the measurement depth increased from the surface down the profile, the difference between the mean daily temperatures, the experimental mean (mean of the 32 days of the whole experiment) and the water table means (means of the water table treatments only) decreased gradually and finally all seems to converge to a single value. Especially the mean daily temperature and the water table mean converged to a single value after the fourth measurement depth in the 500 mm water table depth (WT2). The variation between the mean daily temperatures, the experimental mean and the water table means even decreased as the water table depth was increased, but in this case the experimental mean was closer to the mean daily temperature unlike in the 500 mm water table depth.

Regarding the impact of water table depth, as the water table was lowered, the daily variation of temperature increased. This is indicated by the increase in amplitude and the presence of higher gaps in the minimum and maximum temperatures (Table 5.8). Comparison of the water table mean revealed that in the 500 mm water table depth, the water table mean was always less than the experimental mean whereas in 1000, 1500 mm and No WT depth, the water table mean was greater or equal to the experimental mean showing the profile temperature is increasing.

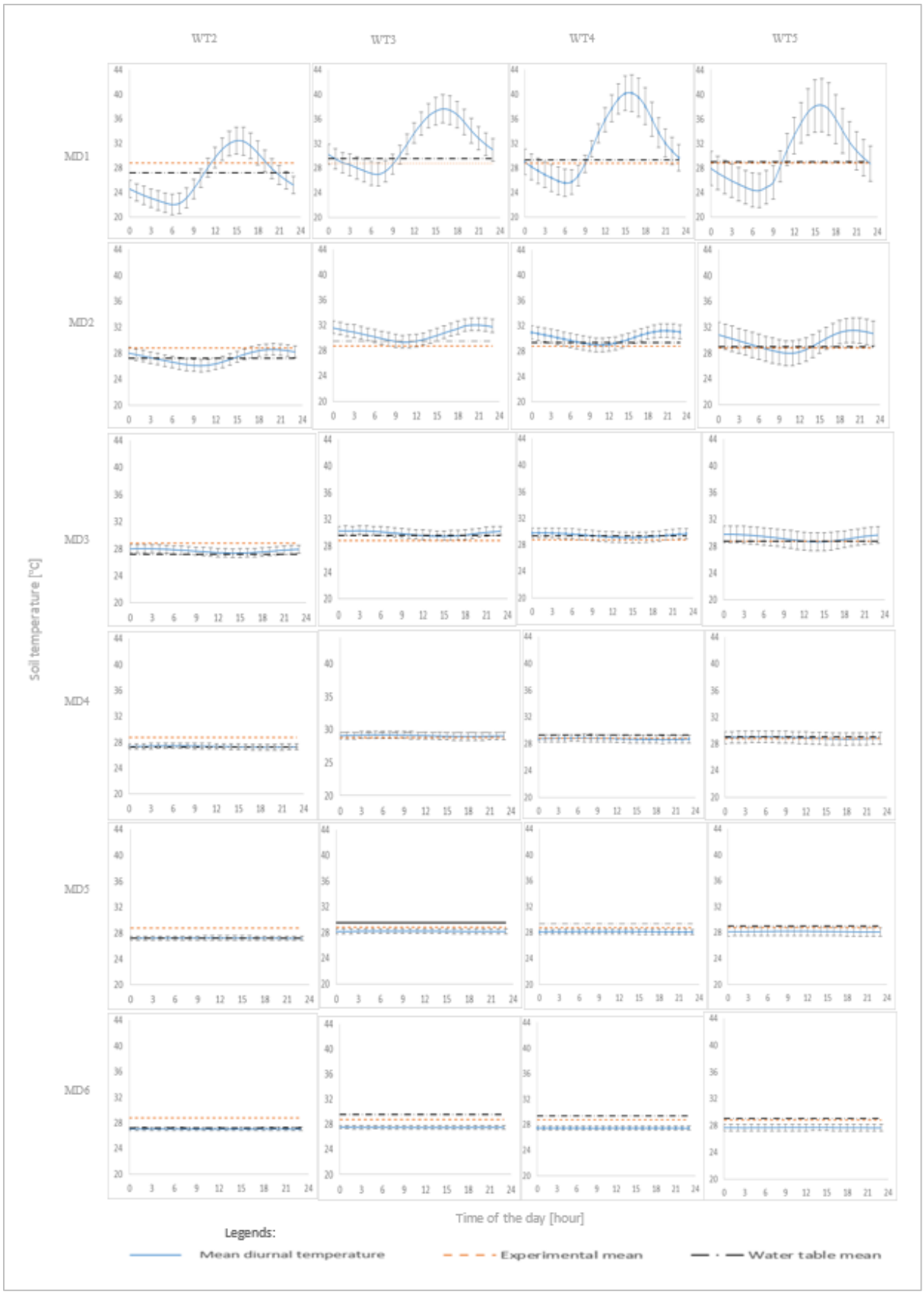

Figure 5.9 The interactive effect of different water table depth (WT) and measurement depth (MD) on the mean diurnal temperature of 32 measuring days of the 2nd evaporation cycle

Table 5.8 The effect of water table and measurement depths on the minimum, maximum and amplitude of temperature in the soil profile

Water table depths [mm]	Parameters	Measurement depths in the soil profile (mm)					
		0	200	400	600	800	1000
500	Minimum [ºC]	21.95	26.04	27.34	27.20	27.14	26.99
	Maximum [ºC]	32.76	28.72	28.11	27.48	27.31	27.12
	Amplitude [ºC]	4.01	0.80	0.77	1.29	1.47	1.65
1000	Minimum [ºC]	26.96	29.33	29.47	28.95	28.11	27.47
	Maximum [ºC]	37.86	32.21	30.38	29.26	28.27	27.61
	Amplitude [ºC]	9.09	3.44	1.60	0.59	0.54	1.17
1500	Minimum [ºC]	25.45	28.95	29.04	28.59	28.03	27.38
	Maximum [ºC]	40.78	31.41	29.86	28.88	28.21	27.53
	Amplitude [ºC]	12.01	2.64	1.16	0.45	0.59	1.24
No WT	Minimum [ºC]	24.13	27.95	28.63	28.65	27.99	27.57
	Maximum [ºC]	38.68	31.80	29.96	29.09	28.25	27.76
	Amplitude [ºC]	9.91	3.14	1.49	0.82	0.66	1.01

The time of occurrence of minimum and maximum temperature was also affected by both the water table and measurement depths (Table 5.9). Especially as the measurement depth increased from the surface, the time of recording of the minimum and maximum temperature varies highly between the successive measurements.

Table 5.9 The temporal distribution of the daily minimum and maximum temperature along the water tables and measurement depths

Water table depth [mm]	Parameters	Measurement depths [mm]					
		0	200	400	600	800	1000
500	Min	06:00-09:00	09:00-12:00	15:00-18:00	21:00-00:00	18:00-21:00	18:00-21:00
	Max	15:00-18:00	18:00-21:00	00:00-03:00	06:00-09:00	06:00-09:00	06:00-09:00
1000	Min	06:00-09:00	09:00-12:00	15:00-18:00	18:00-21:00	15:00-18:00	15:00-18:00
	Max	15:00-18:00	21:00-00:00	00:00-03:00	03:00-06:00	03:00-06:00	03:00-06:00

1500	Min	06:00-09:00	09:00-12:00	15:00-18:00	18:00-21:00	21:00-00:00	21:00-00:00
	Max	15:00-18:00	21:00-00:00	00:00-03:00	06:00-09:00	06:00-09:00	06:00-09:00
No WT	Min	06:00-09:00	09:00-12:00	12:00-15:00	18:00-21:00	21:00-00:00	21:00-00:00
	Max	15:00-18:00	18:00-21:00	00:00-03:00	06:00-09:00	09:00-12:00	15:00-18:00

5.4 Discussion

5.4.1 Evaporation from shallow water tables

The effects of shallow water table and soil type to evaporation is shown in the analysis of variances in Tables 5.2 and 5.3. Figures 5.7 and 5.8 also show the relationships between $\sum E_s$ and $\sum PE$ on the two soils and the five water tables, respectively. The relationships between the daily evaporation (E_s) and the potential evaporation (PE) of the two soils and the five water table depths are given in Figure 5.7 and 5.8, respectively. As it is already stated, both the water table depths and soil types have highly influenced both the cumulative and daily rates of evaporation. The rate of evaporation increased with decreasing water table and was also higher in the Hutton soil than the Clovelly soil profile. On the other hand, the contribution of each water table to the potential evaporation differs highly on the depth of water table and the potential evaporation itself (shown in Table 5.9). As the water table decreased, there was a possibility that the atmospheric evaporation demand (potential evaporation) could be met by the water table. But, as the water table depth increased, the possibility of meeting the atmospheric evaporation demand would be very low. Especially at deeper water table depths and higher evaporation demand, there will be a lower contribution from the water table.

The rate of bare surface evaporation with the presence water tables mainly depend on three important conditions (Gardner, 1958; Verma, 1974; Rasheed *et al.*, 1989; Hillel, 2004; Gowing *et al.*, 2006): i) The potential evaporation or the atmospheric evaporative demand, which is the ability of the atmosphere to convert liquid water to vapour and loose it without the limitations of water in the site of evaporation. It is mainly dependent on daily weather condition (temperature, wind speed, precipitation, cloud cover, humidity, etc.). The potential evaporation (PE) is a combined term showing the effect of different weather conditions on E_s as shown in Figures 5.7 and 5.8 for the two soils and five water tables, respectively. (ii) The depth of water table: as the depth of the water table is closer to the site of evaporation, then E_s and ΣE_s will

increase up to a maximum of the PE. (iii) Hydraulic properties of the soil: if the supply of water in the site of evaporation is limited due to deeper water tables, then E_s and ΣE_s will depend on the hydraulic properties of the soil. In this case the particle size distribution plays a great role. Soils with higher clay plus silt content will have a higher capillarity than sandy soils (Shokri & Salvucci, 2011; Li *et al.*, 2013).

Generally, the increase in E_s and ΣE_s with decreasing the water table depth is related with the increase of water content to the site of evaporation, usually the ground surface which is consistent to the reports of Ripple *et al.* (1972), Hellwig (1973), Hillel (2004), Rose *et al.* (2005), Gowing *et al.* (2006), Shokri & Salvucci (2011), Assouline *et al.* (2013). Therefore capillarity plays a great role here. The increase in the E_s and ΣE_s from the Hutton profile is due to the presence of higher capillarity in Hutton soil than the Clovelly which is also associated with the presence of higher silt plus clay content in it (Figure 5.7). This result is consistent with the reports of Shokri & Salvucci (2011) and Li *et al.* (2013).

Bare surface evaporation with the presence of shallow water table is characterized by its steady state condition. During the evaporation process, water will rise up through the profile by capillarity towards the soil surface. But the water may not reach the site of evaporation, usually the soil surface, during deeper water tables. Hence, the evaporation front is formed below the soil surface and that position is the maximum height that water can rise up and called the critical depth or maximum capillary height (Table 5.10). If the water table depth is equal or lower than this critical depth the rate of evaporation will be similar as evaporation from free water surfaces (Rose *et al.*, 2005; Shokri & Salvucci, 2011; Li *et al.*, 2013). Therefore, the evaporation process will be dependent on the potential evaporation. If the water table depth is greater than the critical depth, the rate of evaporation will be significantly lower and said to be a soil limited evaporation (Rasheed *et al.*, 1989; Hillel, 2004; Gowing *et al.*, 2006). As a result, the rate of evaporation will primarily depend on the ability of the soil to supply water to the evaporation zone.

Table 5.10 Calculated values of the height of capillary fringe and position of the evaporation front (EF)

Water table depth [mm]	Clovelly		Hutton	
	h_{max} [mm]	Depth of the EF [mm]	h_{max} [mm]	Depth of the EF [mm]
0	742	0	731	0
500	742	0	731	0
1000	631	369	857	143
1500	631	869	857	643
No WT	-	No EF	-	No EF

a) h_{max} refers to the maximum height of capillary fringe

b) No EF refers to no formation of evaporation front

Regarding the maximum capillary fringe, the results in Table 5.10 shows that there is no significant difference between the 0 and 500 mm water tables. However, the ANOVA (Table 5.5) indicated that there was a significant difference between these water tables. The dependence of the rate of evaporation on the potential evaporation also depends on the depth of the water table. For example in this experiment, water tables shallower than 1000 mm were highly affected by the potential evaporation. Whereas the difference in E_s for water tables deeper than 1000 mm decreases. Therefore, at very low potential evaporation (closer to zero), the difference between E_s from the different water tables will decrease. Similar results are reported by Ripple *et al.* (1972) and Hillel (2004). The dependence of E_s on the daily potential evaporation is illustrated in Figures 5.10 and 5.11 for the two soils and five water table depths, respectively.

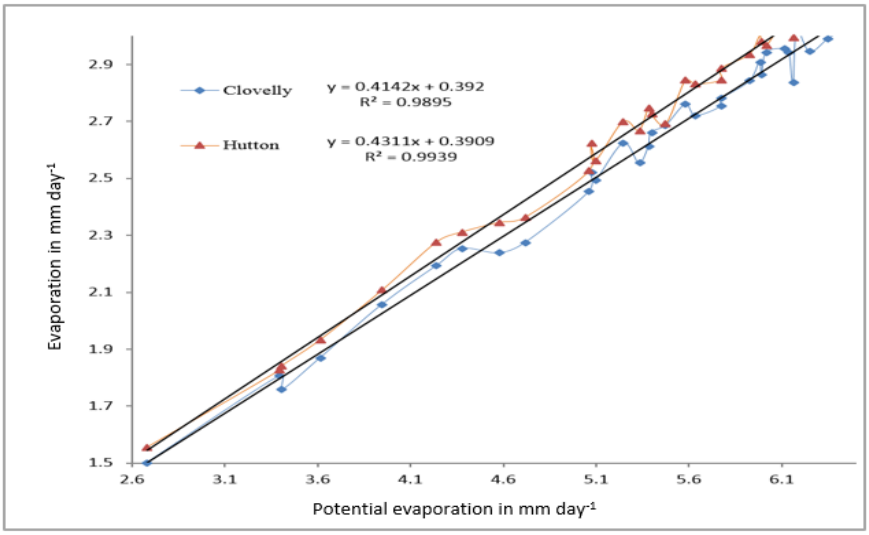

Figure 5.10 Comparison of daily evaporation in the two soil types.

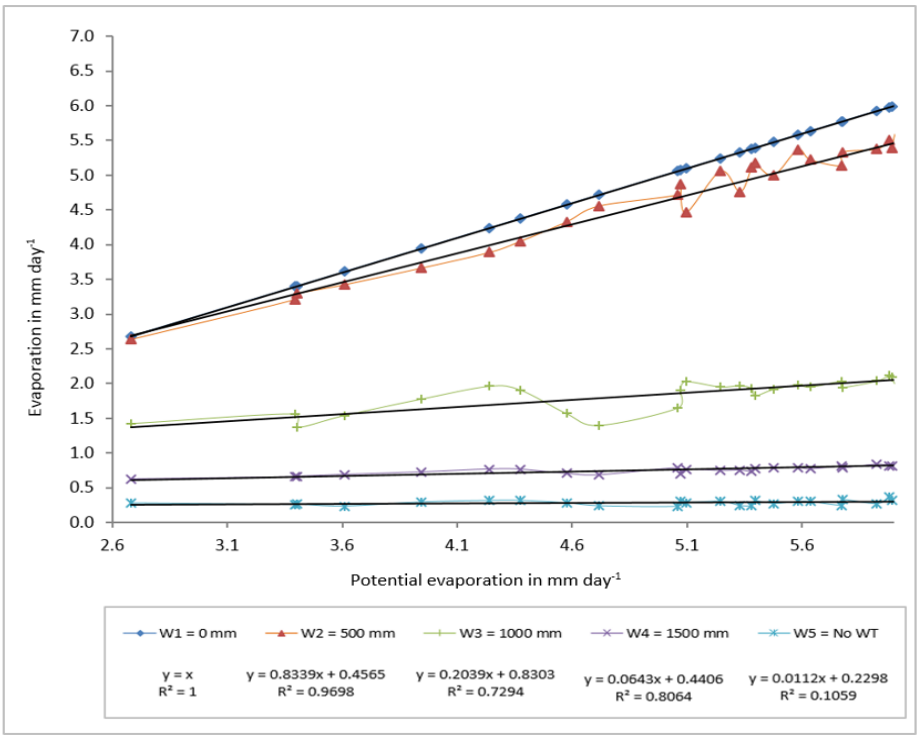

Figure 5.11 Comparison of daily evaporation in the five water table depths.

Lastly, an empirical equation was developed based on the relationships between evaporation and the potential evaporation and the depth of water tables (Equation 5.3). A model validation (Figure 5.12) was done and the statistical analysis (R^2 = 0.84 and RMSE = 1.15) shows this equation can be used to predict the amount of soil water evaporation from shallow water tables by using the potential evaporation and water table depths only.

$$E_s = exp\left[0.45006 + 0.16274PE - 0.00054WT \right], \quad (5.3)$$

where E_s is the soil water evaporation (mm day^{-1}), PE is the potential evaporation (mm day^{-1}) and WT is the depth of the water table (mm) from the soil surface.

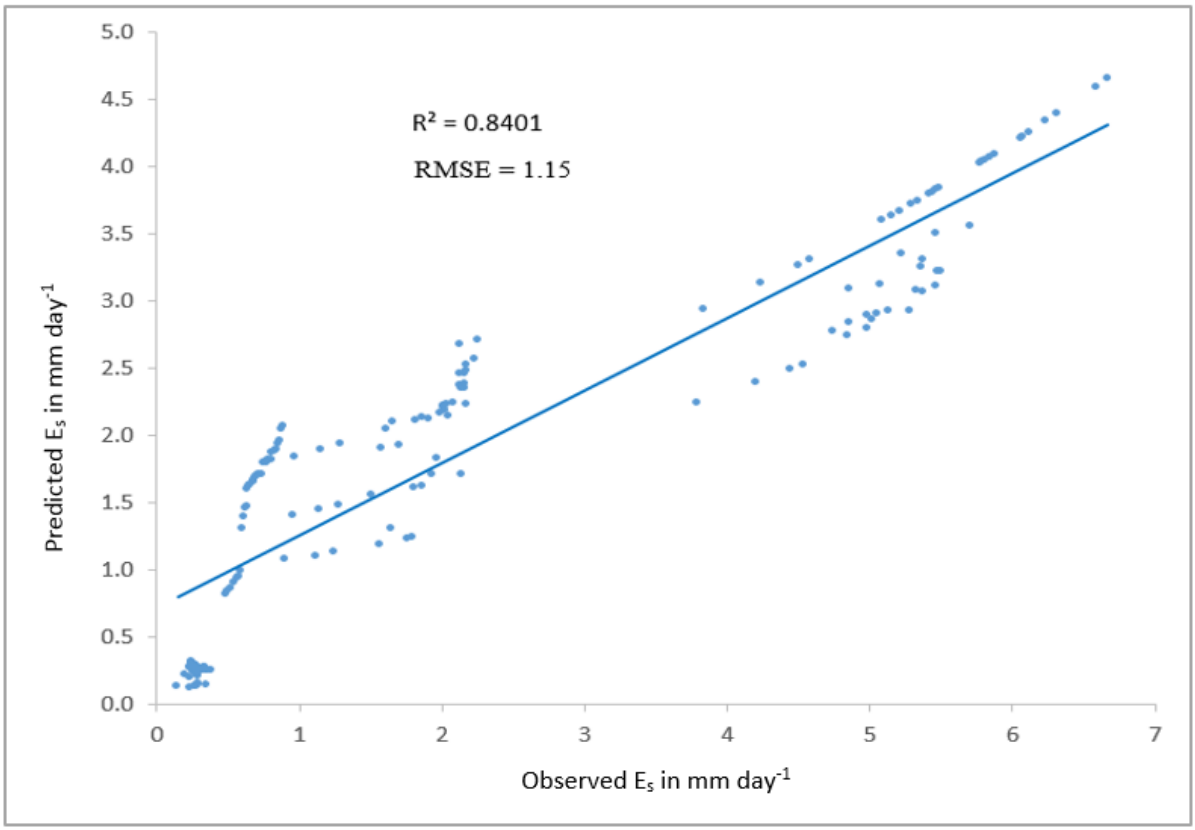

Figure 5.12 Validation of the empirical model to estimate evaporation from the relationships with water table depth and potential evaporation.

5.4.2 The influence of water table depth to temperature distribution

The ANOVA of the effect of soil type and depths of measurement and water table and measurement depths on the amplitude as an indicator for variation of temperature were given in Tables 5.5 and 5.6, respectively. The separation of the means of temperature amplitude due to the interactive effects of water table and depths of measurement are summarized in Table 5.7. These interaction effects are also depicted in Figure 5.9.

The results of the ANOVA revealed that there is no difference in the temperature distribution between the two soils which is consistent with the results discussed in Chapter 4 indicating that there is no significant difference between the thermal properties of the two soils. Therefore, the source of soil temperature variation in this experiment are three types. Firstly, temporal variations which are due to the time of measurement. This consists of a change in soil temperature in hourly, daily, monthly, etc. basis. For example the minimum and maximum soil surface temperature values were recorded in the morning (06:00-09:00) and late afternoon (15:00-18:00), respectively. The variation of the daily temperature in the four water tables and six measurement depths are summarized in Table 5.9. The variation in time at which the

minimum and maximum temperatures were recorded is due to the variation of solar radiation, cloud cover, wind, etc. As a result of this, a change in temporal variation was observed in the soil profile. Similar results reported by Arya (2001), Popiel *et al.* (2001) and Hillel (2004). Secondly, variation due to the depth of measurement. This variation is dependent on the depth at which the measurement was taken. The variation of temperature due to the position of the measurement depth also depends on the depth of the water table. In soil profiles with water tables of 500 mm and shallower, the soil temperature increased down the profile which is indicated by the position of the daily temperature was greater than the water table mean in deeper measurements. The profiles with water tables deeper than 500 mm depth had higher temperatures in the surface and it decreased down the profile. As the water table depth decreases, the ground surface will be wet enough, hence most of the energy will be lost due to latent heat of vaporization. Therefore, lower amount of heat energy will be available to heat up the soil, and as a result, the surface temperature decreases. The reverse is true for deeper water tables as similarly reported by Asaeda and Ca (1993) and Arya (2001). Thirdly, variation due to the water table depth. Profiles with shallower water table depths had lower temperature than deeper and no water table treatments. For example, profiles with water table depths greater than 1000 mm have higher soil temperature on the ground surface than the other depths. But the reverse is true for water tables shallower than 1000 mm. The explanation for this is similar as in the second case above. The decrease in surface temperature for wet soils than dry one is consistent with the reports of Asaeda and Ca (1993), Arya (2001) and Hillel (2004).

Generally, as the depth increases from the ground surface down the profile, the effect of all the three types of variations (due to temporal variations, depth of measurement and water table depth) change and after some measurement depths the soil temperatures converge to one constant value, which is mostly considered to be the annual soil temperature (Popiel *et al.*, 2001; Shahran and Jadhav, 2002; Hillel, 2004; Florides and Kalogirou, 2005).

5.5 Conclusion

The main objective of this chapter was to quantify the daily rate and cumulative evaporation as affected by constant shallow water tables and soil types under lysimeter conditions. It also investigated the influence of different water tables and soil types on soil profile temperature distribution.

The study showed that the daily rate of evaporation (E_s) and the cumulative evaporation ($\sum E_s$) was influenced by daily potential evaporation (also dependent on daily weather conditions) and soils ability to supply water to the evaporation zone. For shallow water table depths of 0-500

mm, E_s was shown to be dependent on the potential evaporation. However, as the water table depth increased beyond 500 mm, the soil hydraulic properties were the determinant factors.

The contribution of water table depths to the atmospheric evaporative demand was significantly different ($P \leq 0.05$). The shallowest water table depth (0 mm) and no water table depth were the respective highest and the lowest contributors irrespective of soil type. Evaporation cycles from the 0 mm water table depth had an average value of 100% while the no water table recorded only 5.55%. The 500 mm, 1000 mm and 1500 mm water table depths contributed 92.1%, 36.6% and 14.9% of the atmospheric evaporative demand, respectively. These results conclusively demonstrated that water table contributions to evaporation decreased with depth.

Soil profile temperature distribution was also found to depend on water table depth. Soil profile temperature increased with depth of the water table and vice versa. Soil type had no effect ($P \leq 0.05$) on soil profile temperature distribution and was consistent with the lack of effect on thermal properties observed in the previous chapter.

CHAPTER 6

PERSPECTIVE

Aeolian soils cover a surface area of about 909 million ha (Thomas *et al.,* 2005) in Africa and 303 million ha (Thomas *et al.*, 2005; Harmse and Hattingh, 2012) in Southern Africa (Figure 6.1), and by far play a critical role in supporting crop production (both dry land and irrigation) and pasture. Given the dry climates under which aeolian soils are developed the water balance components has been the major focus of research. Soil profile water storage potential of soils developed from aeolian soils was studied in South Africa under different tillage management systems by Hensley *et al.* (2000). In this work aeolian soils that overlaid a C horizon with an impermeable material or clay layer were found to be suitable for dry land crop production under conservation tillage practices. Deep aeolian soils overlaying above a permeable fractured rock have high drainage properties and were suitable for irrigation. Aeolian soils overlying on

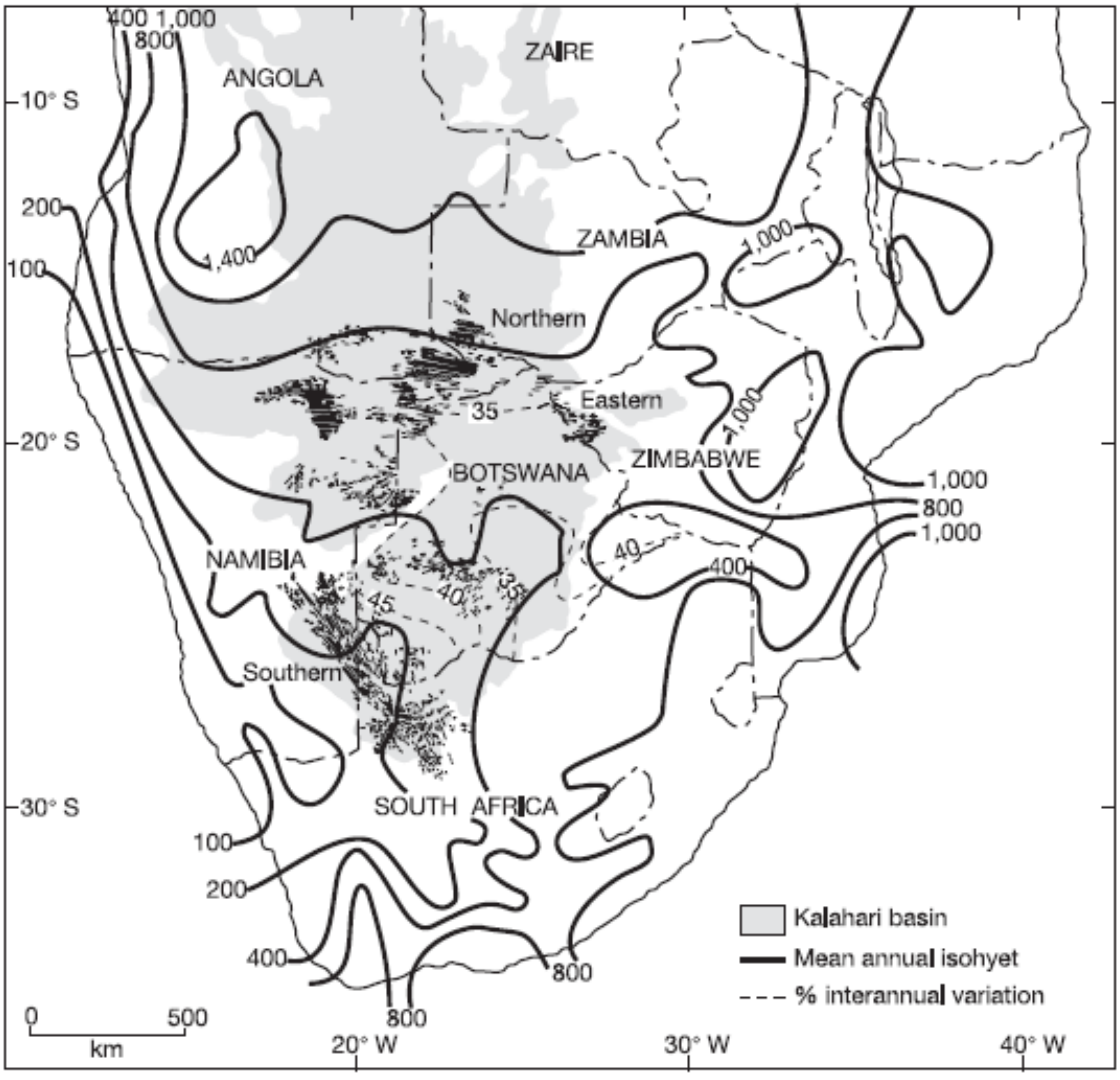

Figure 6.1 The Southern African Kalahari Basin and dune systems (Thomas *et al.,* 2005).

impermeable horizons despite their high rainwater harvesting properties were also found to have appreciable bare evaporation losses (Botha, 2006). Presence of a perched water table above the impermeable horizon and its contribution to evapo-transpiration was investigated by Ehlers *et al.* (2003). Studies that attempted to determine evaporation on aeolian soils were conducted in the absence of shallow water tables (Haka, 2010; Nhlabatsi, 2010). However, under the challenges of global warming and need to increase food production, irrigation is increasingly extended to aeolian soils with lesser drainage properties and more susceptible to perched water tables (Ehlers *et al.*, 2007).

To provide informed soil water management strategies to dry land and irrigation farmers, this study was conducted to determine the contribution of shallow or perched water tables to bare soil evaporation and its effect on soil profile temperature distribution. Aeolian soils were represented by the Clovelly and Hutton soil forms. Bare soil evaporation was described on the basis of soil hydraulic and thermal properties. Relationships between pore size distribution and cumulative pore volume was found to be non-linear. The classification of pores with relation to their function proposed by Lal and Shukla (2004) was modified based on the concepts of field water capacity in this work. Therefore, pore sizes were classified as residual/or bonding (if their radius is less than 0.005 μm), storage (if their radius is between 0.005 to 9.44 μm) and transmission pores (if their radius is above 9.44 μm). In the presence of a shallow water table or during the incidence of restricting horizons in soil profiles, the different pore sizes served as storage pores in the water table or in closer proximity to the water table, a result that indicate influential role played by water tables on the soil water balance and hydrology. The use of this dynamic approach is also preferable than the fixed boundary approach that ignored the overlapping nature of textural pores.

The study also showed that soil water contents and temperature combinations had an interaction effect on soil thermal properties (volumetric heat capacity, thermal conductivity and thermal diffusivity). Three important soil water-temperature combination groups were identified, namely wetting of a dry soil (0.08 mm^3 mm^{-3}) with increasing temperature (0-60^oC), freezing (0^oC) and thawing (10^oC) with increasing water content (0-0.39 mm^3 mm^{-3}) and excessive wetting (0.16-0.39 mm^3 mm^{-3}) of soils with increasing temperature (0-60^oC).

In the wetting of dry soils, all the thermal properties of the aeolian soils were improved significantly. Hence, a 94, 703 and 346% increase in C, K_t and D was observed between dry and slightly wetted soils, respectively. On the other hand, C was decreased by 55%, K_t and D were increased by 137% and 367%, respectively with increasing temperature.

In the freezing and thawing of soils, there was a significant influence in the volumetric heat capacity of the soils unlike K_t and D. There was an average 8% increase in C as the temperature changed from 0 to 10^{o}C. But the effect of water was significant in all the three properties. Hence, a 32% and 11% decrease and a 10% increase of C, K_t and D was recorded due to an increase in water content from 0 to 0.39 mm^3 mm^{-3}, respectively.

In the excessive wetting of soils, volumetric heat capacity and thermal conductivity increased at a decreasing rate with addition of water up to DUL. On the other hand thermal diffusivity increased remarkably with increasing water content up to 0.16 mm^3 mm^{-3}, but no change have been observed thereafter. Regarding the influence of temperature, volumetric heat capacity increased at all water contents and temperature levels. Thermal conductivity and diffusivity also increased with temperature up to DUL and 0.16 mm^3 mm^{-3}, respectively where after it decreased with increasing temperature.

The soil's hydraulic and thermal properties were then integrated into the main experiment where the effect of soil type and water table depth on daily rate and cumulative evaporation was investigated. The effect of shallow water tables on the temperature distribution on the soil profile was also investigated. The different constant water table depths were created artificially on a lysimeter with diameter of 1800 mm and depth of 2000mm. The time series soil water content and temperature variations were measured using calibrated DFM soil water sensors. Daily evaporation was calculated by using the equation of soil water balance. The experimental mean, water table mean and daytime amplitude temperatures were calculated as indicators of variation in soil temperature.

The potential evaporation and the ability of the soils to supply water to the evaporation zone affected daily rates of evaporation (E_s) and the cumulative evaporation ($\sum E_s$). Evaporation rates from shallow water table depths of 0-500 mm were primarily dependent on the potential evaporation. However, as the water table depth increased beyond 500 mm, the soil hydraulic properties determined the daily rate of evaporation. This result suggests that managing of shallow water table below the 500 mm depth would minimize the effect of high atmospheric demand experienced in arid and semi-arid climates.

The contribution of evaporation from shallow water tables to the atmospheric evaporative demand was significantly different ($P \leq 0.05$). The shallowest water table depth (0 mm) had the highest contribution of 100% to the atmospheric evaporative demand while the no water table contributed 5.6%. Water table depths at 500 mm, 1000 mm and 1500 mm contributed 92.1%, 36.6% and 14.9% of the atmospheric evaporative demand, respectively. This result

demonstrated that water table contributions to evaporation decreased with water table depth and farmers especially under irrigation could improve soil profile water storage by keeping water table depth low enough to reduce evaporation and high enough to improve capillary contribution to the root zone. Ehlers (2003) found that water table depth of 1000 mm was appropriate for capillary contribution to field crops. Soil profile temperature was observed to increase with increasing depth of the water table and vice versa. The diurnal variation of surface temperature was observed to increase in relatively deeper water tables, a result showing that soil water stabilizes the profiles temperature in aeolian soils. However, soil type had no significant effect ($P \leq 0.05$) on soil profile temperature distribution in this study.

Another important output of the study was the development of a pedotransfer function that integrated water table depth and potential evaporation as shown in Equation 6.1.

$$E_s = R \times PE \tag{6.1}$$

Where E_s is the actual evaporation (mm day^{-1}), R is the ratio of E_s to PE (unit less), and PE is the potential evaporation (mm day^{-1}).

From the relationship between the daily evaporation and the potential evaporation, the ratio of E_s to PE was calculated. This ratio was regressed with the corresponding water table depth as shown in Figure 6.2. The contribution of shallow water table to evaporation can be calculated by using the depth of water table and the potential evaporation. The water table depth is important to read the ratio of E_s to PE from Figure 6.2. Then E_s can be calculated easily by applying Equation 6.1. This equation would be important in the estimation of the capillary contribution for crop water demands during irrigation scheduling in the incidence of shallow water tables.

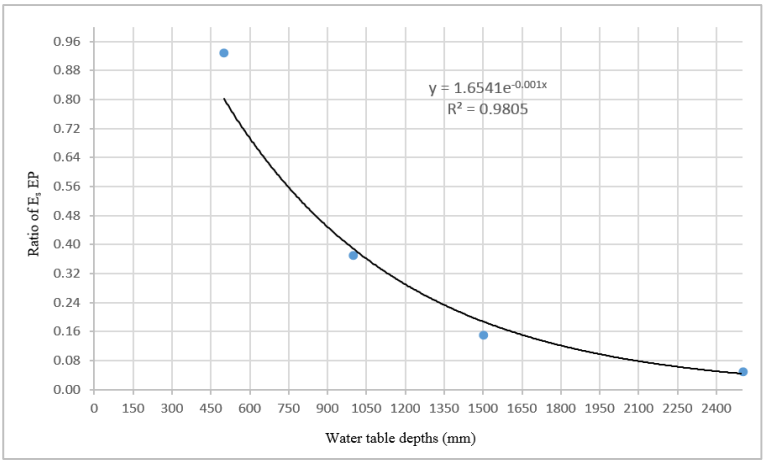

Figure 6.2 The regression analysis of the ratio of E_s to PE to water table depth to develop a simple pedo-transfer function to estimate the contribution of water tables to evaporation.

Although the coverage of aeolian soils is significant in the Southern African region, very little have been known on their short and long term impacts to the environment. This area is also identified as one of the most vulnerable regions in Africa to global warming (Boko *et al.,* 2007; Eriksen *et al.*, 2008). The impacts of aeolian soils (dune-field dynamics) in the local, regional and global climate change should be well understood. Thomas *et al.* (2005) explained that the dune-field dynamics are dependent on surface erodibility (which is also dependent on vegetation cover and soil water content) and the atmospheric erosivity (determined by wind energy). Particularly, the impact of evaporation from shallow water tables to climate change is not well understood while the latent heat fluxes are an integral part of the climate system linking the surface energy balance and the hydrologic cycle (Miller and Yates, 2006; Ban-Weiss *et al.*, 2011; Huber *et al.*, 2014). It is obvious that as the soil water evaporation increases, there will be a cooling process in the area where evaporation occurred. The impact of local evaporative cooling and the effect of water vapor due to evaporation is also not understood yet (Ban-Weiss *et al.*, 2011). Generally it is possible to conclude that the study of soil water evaporation from shallow water tables would have an important contribution on the impact of climate change. Climate change also has a significant impact on soil water resources, soil temperature, land use-land cover and on the soil water and energy balance in the arid and semi-arid regions (Boko *et al.*, 2007; Ban-Weiss *et al.*, 2011; Kumar, 2012). Therefore, the following important issues are recommended for further study. (i) The contributions of shallow water table depths on evaporation under different conservation tillage practices should be studied. (ii) The effect of freezing temperature ($<0^{o}C$) and higher temperatures greater than $60^{o}C$ on soil thermal properties should also be studied as these temperature are also important. (iii) The effect of evaporation from shallow water tables to local, regional and global climate change needs a further study.

REFERENCES

ABRISQUETA, J., PLANA, V., CANALES, A. & RUIZ-SÁNCHEZ, M. (2006). Unsaturated hydraulic conductivity of disturbed and undisturbed loam soil. *Spanish Journal of Agricultural Research,* 4(1), 91-96.

ADHANOM, G., STIRZAKER, R., LORENTZ, S., ANNANDALE, J. & STEYN, J. (2012). Comparison of methods for determining unsaturated hydraulic conductivity in the wet range to evaluate the sensitivity of wetting front detectors. *Water SA,* 38(1), 67-76.

ALKHAIER, F., FLERCHINGER, G. & SU, Z. (2012). Shallow groundwater effect on land surface temperature and surface energy balance under bare soil conditions: modeling and description. *Hydrology and Earth System Sciences,* 16(7), 1817-1831.

AMOOZEGAR, A. & WILSON, G. V. (1999). Methods for measuring hydraulic conductivity and drainable porosity. *Agricultural drainage,* 1149-1205.

ANDERSON, D. & MORGENSTERN, N. (1973). Physics, chemistry and mechanics of frozen ground: a review. *Permafrost: The North American Contribution to the Second International Conference*, pp. 257-288.

ARCHER, E., ENGELBRECHT, F., LANDMAN, W., LE ROUX, A., VAN HUYSSTEEN, E., FATTI, C., NKAMBULE, C., LE MAITRE, D., DIEDERICKS, G. P. J., DAVIS, C., COLVIN, C. & AKOON, I. H. (2010). *South African risk and vulnerability atlas.* Pretoria, South Africa: Department of Science and Technology.

ARYA, P. S. (2001). *Introduction to micrometeorology* (2nd ed.). (R. Dmowska, J. R. Holton, & H. Rossby, Eds.) Raleigh, NC, USA: Academic press.

ASAEDA, T. & CA, V. T. (1993). The subsurface transport of heat and moisture and its effect on the environment: a numerical model. *Boundary-Layer Meteorology,* 65(1 - 2), 159-179.

AŞKIN, T. & ÖZDEMIR, N. (2003). Soil bulk density as related to soil particle size distribution and organic matter content. *Poljoprivreda/Agriculture,* 9, 52-55.

ASSOULINE, S., TYLER, S. W., SELKER, J. S., LUNATI, I., HIGGINS, C. W. & PARLANGE, M. B. (2013). Evaporation from a shallow water table: diurnal dynamics of water and heat at the surface of drying sand . *Water Resources Research ,* 49(7), 4022-4034.

BABKIN, V. I. (2009). Evaporation from the surface of the globe. *Hydrological cycle,* 2, pp. 48.

BACHMANN, J. & VAN DER PLOEG, R. R. (2002). A review in recent developments in soil water retention: interfacial tension and temperature effects. *Journal of Plant Nutrition and Soil Science,* 165, 468 - 478.

BAN-WEISS, G., BALA, G., CAO, L., PONGRATZ, J. & CALDEIRA, K. (2011). Climate forcing and response to idealized changes in surface latent and sensible heat. *Environmental Research Letters,* 6(3). pp. na.

BARGAHI, K. & MOOSAVI, S. A. (2006). Effects of Shallow Water Table and Groundwater Salinity on Contribution of Groundwater to Evapotranspiration of Safflower (Carthamus tinctorius L.) in Greenhouse. *JWSS-Isfahan University of Technology,* 10(3), 59-70.

BARNARD, J. H., VAN RENSBURG, L. D. & BENNIE, A. T. P. (2010). Leaching irrigated saline sandy to sandy loam apedal soils with water of different salinity. *Irigation Science,* 28, 191 - 201.

BENHIN, J. K. (2006). *Climate Change and South African Agriculture: impacts and adaptation options.* Pretoria, South Africa: University of Pretoria: "Centre for Environmental Economics and Policy in Africa".

BENNIE, A. & KRYNAUW, G. (1985). Causes, adverse effects and control of soil compaction. *South African Journal of Plant and Soil,* 2(3), 109-114.

BENNIE, A. T. P. & HENSLEY, M. (2001). Maximizing precipitation utilization in dryland agriculture in South Africa-a review. *Journal of Hydrology,* 241 (1), 124-139.

BENNIE, A. T. P. (1994). Managing the profile available water capacity of soils for the irrigation of annual crops. *15th International Congress of Soil Science* (pp. 17-18). Acapulco, Mexico: International Society of Soil Science, Mexican Society of Soil Science.

BENNIE, A. T. P., HOFFMAN, J. & COETZEE, M. (1995). Sustainable crop production on aeolian sandy semi-arid soils in South Africa. *African Crop Science Journal,* 3(1), 67-72.

BIO INTELLIGENCE SERVICE. (2014). *Soil and water in a changing environment, Final Report.* BIO Intelligence Service. Luxembourg: European Commission (DG ENV).

BLAKE, G. (1965). Bulk density . In C. Black (Ed.), *Methods of soil analysis. part 1. physical and mineralogical properties, including statistics of measurement and sampling* (pp. 374-390). Madison, WI: American Society of Agronomy.

BLIGNAUT, J., UECKERMANN, L. & ARONSON, J. (2009). Agriculture production's sensitivity to changes in climate in South Africa. *South African Journal of Science,* 105(1 & 2), 61-68.

BOKO, M., NIANG, I., NYONG, A., VOGEL, C., GITHEKO, A., MEDANY, M., OSMAN-ELASHA, B., TABO, R. & YANDA, P. (2007). Africa: climate change 2007: impacts, adaptation and vulnerability. In *Climate change 2007: impacts, adaptation and vulnerability, Contribution of Working Group II to the Fourth Assessment Report of the Intergovernmental Panel on Climate Change*. (pp. 433-467). Cambridge, UK: Cambridge University Press.

BØRGESEN, C. & SCHAAP, M. (2005). Point and parameter pedotransfer functions for water retention predictions for Danish soils. *Geoderma,* 127, 154–167.

BOTHA JJ, (2006). Evaluation of maize and sunflower production in semi-arid area using in field rainwater harvesting. Ph.D. thesis in Soil Science, University of the Free State, Bloemfontein, South Africa.

BOUWER, H. (1964). Measuring horizontal and vertical hydraulic conductivity of soil with the double-tube method. *Soil Science Society of America,* 28(1), 19-23.

BRANDON, T. L. & MITCHELL, J. K. (1989). Factors influencing thermal resistivity of sands. *Journal of Geotechnical Engineering,* 115 (12), 1683-1698.

BREWER, R. (1964). *Fabric and Mineral Analysis of Soils.* New York, USA: Wiley.

BRISTOW, K. (1998). Measurement of thermal properties and water content of unsaturated sandy soil using dual-probe heat-pulse probes. *Agricultural and forest meteorology,* 89(2), 75-84.

BRISTOW, K. L. (2002). Thermal Conductivity. In J. H. Dane, & G. C. Topp (Eds.), *Methods of soil analysis: part 4 - physical methods* (pp. 1209 - 1226). Madison, USA: SSSA Book Series 5.

BROOKS, R. H., & COREY, A. T. (1964). *Hydraulic properties of porous media.* Colorado State University. Fort Collins, Colorado, USA: Fort Collins.

BRUTSAERT, H. (1982). *Evaporation into the atmosphere D.* Dordrecht, Holland: D Reidel PUBLISHING COMPANY.

BUDYKO, M. I. (1958). *The heat balance of the earth's surface.* Washington, D. C.: US Department of Commerce.

BUSBY, J. (2015). *Determination of thermal properties for horizontal ground collector loops*. Nottingham, UK: British Geological Survey.

CALLISTER, W. D. (2001). *Fundamentals of materials science and engineering: An interactive e-text* (5th ed.). New York, USA: John, Willey and Sons.

CAMPBELL, G. S. (1974). A simple method for determining unsaturated conductivity from moisture retention data. *Soil Science,* 117(6), 311-314.

CAMPBELL, G., JUNGBAUER JR, J., BIDLAKE, W. & HUNGERFORD, R. (1994). Predicting the effect of temperature on soil thermal conductivity. *Soil Science,* 158(5), 307-313.

CARSLAW, H. S. & JAEGER, J. C. (1959). *Conduction of heat in solids* (2nd ed.). Oxford Science Publications.

CARY, J. W. (1965). Water flux in moist soil: thermal versus suction gradients. *Soil Science,* 100(3), 165 - 175.

CARY, J. W. (1966). Soil moisture transport due to themal gradients: practical aspect. *Soil Science Society of America Journal,* 30(4), 428 - 433.

CHARI, M. M., NEMATI, F., AFRASIAB, P. & DAVARI, A. (2012). Prediction of evaporation from shallow water table using regression and artificial neural networks. *Journal of Agricultural Science,* 5 (1), 168-180.

CHAUDHARI, P., AHIRE, D., AHIRE, V., CHKRAVARTY, M. & MAITY, S. (2013). Soil bulk density as related to soil texture, organic matter content and available total nutrients of Coimbatore soil. *International Journal of Scientific and Research Publications,* 3(2), 1-8.

CHEN, S. (2008). Thermal conductivity of sands. *Heat and Mass Transfer,* 44(10), 1241-1246.

CHEN, X. & HU, Q. (2004). Groundwater influences on soil moisture and surface evaporation. *Journal of Hydrology,* 297(1), 285-300.

CHIMUNGU, J. (2009). *Comparison of field and laboratory measured hydraulic properties of selected diagnostic soil horizons.* MSc Thesis, University of Free State, Bloemfontein, South Africa.

CHOLPANKULOV, E. D., INCHENKOVA, O. P., PAREDES, P. & PEREIRA, L. S. (2008). Cotton irrigation scheduling in Central Asia: model calibration and validation with consideration of groundwater contribution. *Irrigation and drainage,* 57(5), 516-532.

CHUNG, S. & HORTON, R. (1987). Soil heat and water flow with a partial surface mulch. *Water Resources Research,* 23(12), 2175 - 2186.

CORNELIS, W. M., KHLOSI, M., HARTMANN, R., VAN MEIRVENNE, M. & DE VOS, B. (2005). Comparison of unimodal analytical expressions for the soil-water retention curve. *Soil Science Society of America Journal,* 69, 1902–1911.

CÔTÉ, J. & KONRAD, J. (2005). A generalized thermal conductivity model for soils and construction materials. *Canadian Geotechnical Journal,* 42(2), 443-458.

DANE, J. H. AND HOPMANS, J. W. (2002). Water Retention and Storage. In: *Methods of Soil Analysis: Part 4 -Physical Methods.* Madison, USA: Soil Science Scociety of America, Inc., pp. 671 - 692.

DARCY, H. (1856). *Les fontaines publiques de la ville de Dijon.* Dijon, France.

DASHTAKI, S., HOMAEE, M. & KHODAVERDILOO, H. (2010). Derivation and validation of pedotransfer functions for estimating soil water retention curve using a variety of soil data. *Soil use and management*, 26(1), 68-74.

DE VRIES, D. (1952). The thermal conductivity of soil. *Mededelingen van de Land-bouwhogeschool te Wageningen,* 52(1), 1–73.

DE VRIES, D. (1952). The thermal conductivity of soil. *Mededelingen van de Land-bouwhogeschool te Wageningen,* 52(1), p. 1–73.

DE VRIES, D. A. (1958). Simultaneous transfer of heat and moisture in porous media. *Transactions, American Geophysical Union,* 39, 909 - 916.

DE VRIES, D. A. (1963). Thermal Properties of Soils. In W. R. Wijk (Ed.), *Physics of Plant and Environment* (pp. 210 - 235). Amsterdam, The Netherlands: North Holland Publishing Company.

DEC, D., DÖRNER, J., BECKER-FAZEKAS, O. & HORN, R. (2008). Effect of bulk density on hydraulic properties of homogenized and structured soils. *Journal of Soil Scvience and Plant Nutririon,* 8(1), 1-13.

DECAGON DEVICES INC. (2011). *KD2 Pro thermal properties analyzer operator's manual version 4* (4 ed.). Pullman, USA: Decagon Devices.

DIRKSEN, C. (1999). *Direct hydraulic conductivity measurements for evaluating approximate and indirect determinations*. Riverside, USA: University of California.

DOS SANTOS, W. (2003). Effect of moisture and porosity on the thermal properties of a conventional refractory concrete. *Journal of the European Ceramic Society,* 23(5), 745-755.

DRZAL, M., KEITH CASSEL, D. & FONTENO, W. (1997, May). Pore fraction analysis: a new tool for substrate testing. *International Symposium on Growing Media and Hydroponics* 481, pp. 43-54.

DUNBAR, C. O. & RODGERS, J. (1958). *Principles of stratigraphy* (3rd ed.). New York: John Wiley and Sons.

EDOGA, R. (2010). Comparison of saturated hydraulic conductivity measurement methods for Samaru-Nigeria soils. *Libyan Agriculture Research Center Journal International,* 1(14), 269-273.

EHLERS, L., BARNARD, J., DIKGWATLHE, S., VAN RENSBURG, L., CERONIO, G., DU PREEZ, C. & BENNIE, A. (2007). *Effect of irrigation water and water table salinity on the growth and water use of selected crops.* WRC Report No. 1359/1/07, Water Research Commision, Pretoria, South Africa.

EHLERS, L., BENNIE, A. T. & DU PREEZ, C. C. (2003). *The contribution of root accessible water tables towards the irrigation requirements of crops.* WRC Report No. 1089/1/03, Water Research Commission, Pretoria, South Africa.

EIJKELKAMP AGRICULTURAL EQUIPMENT. (2004). *Compact constant head permeameter: User's manual.* Giesbeek, Netherlands.

EL HOWAYEK, A., HUANG, P., BISNETT, R. & SANTAGATA, M. (2011). *Identification and Behavior of Collapsible Soils.* West Lafayette, Indiana: Joint Transportation Research Program, Indiana Department of Transportation and Purdue.

ELANGO. (2011). *Hydraulic conductivity-issues determination and application.* Rijeka, Croatia: Intech Open Access Publisher.

ERIKSEN, S., O'BRIEN, K. & ROSENTRATER, L. (2008). *Climate change in Eastern and Southern Africa: Impacts, vulnerability and adaptation.* Oslo, Norway: University of Oslo.

FAN, Y. & MIGUEZ-MACHO, G. (2010). Potential groundwater contribution to Amazon evapotranspiration. *Hydrology and Earth System Sciences,* 14(10), 2039-2056.

FAROUKI, O. T. (1981). *Thermal properties of soils (No. CRREL -MONO-81-1.).* New Hampshire: Cold Regions Research And Engineering Lab NH.

FAYER, M. J. (2000). *UNSAT-H Version 3.0: Unsaturated Soil Water and Heat Flow Model, Theory, User Manual, and Examples.* Washington, USA: Pacific Northwest National Laboratory.

FEY, M. (2010). *Soils of South Africa: Their distribution, properties, classification, genesis, use and environmental significance.* Cambridge, UK: Cambridge University Press.

FLERCHINGER, G. N. (2000). *The simultaneous heat and water (SHAW) model: technical documentation.* Boise, Idaho: Northwest Watershed Research Center. USDA Agricultural Research Service .

FLORIDES, G. & KALOGIROU, S. (2005). Annual ground temperature measurements at various depths. *In 8th REHVA World Congress.* Clima, Lausanne.

FRICKE, B. (1992). *Soil thermal conductivity: effects of saturation and dry density.* Kansas City, USA: A PhD dissertation, University of Missouri-Kansas City.

GALLAGE, C., KODIKARA, J. & UCHIMURA, T. (2013). Laboratory measurement of hydraulic conductivity functions of two unsaturated sandy soils during drying and wetting processes. *Soils and Foundations,* 53(3), 417–430.

GARDNER, W. R. (1958). Some steady state solutions of the unsturated moisture flow equation with application to evaporation from a water table. *Soil science,* 85(4), 228 - 232.

GONÇALVES, R., GLOAGUEN, T., FOLEGATTI, M., LIBARDI, P., LUCAS, Y. & MONTES, C. (2010). Pore size distribution in soils irrigated with sodic water and wastewater. *Revista Brasileira de Ciência do Solo,* 34(3), 701-707.

GOWING, J., KONUKCU, F. & ROSE, D. (2006). Evaporative flux from a shallow water table: the influence of a vapor–liquid phase transition. *Journal of Hydrology,* 321 , 77 – 89.

GREEN, R. E., AHUJA, L. R. & CHONG, S. K. (1986). Hydraulic conductivity, diffusivity and sorptivity of unsaturated soils: Filed methods. In A. Klute (Ed.), *Methods of Soil Analysis. Part 1. 2nd ed. Agronomy monograph 9* (pp. 771 - 798). Madison, USA: ASA and SSSA.

GREENLAND, D. (1977). Soil damage by intensive arable cultivation: temporary or permanent? *Philosophical Transaction of the Royal Society London B,* 281, 193–208.

GUBER, A. K. & PACHEPSKY, Y. A. (2010). *Multimodeling with Pedotransfer Functions: documentation and user manual for PTF Calculator, Version 2.0.* USA: USDA-ARS.

GUBER, A. K., PACHEPSKY, Y. A., VAN GENUCHTEN, M. TH., RAWLS, W. J., SIMUNEK, J., JACQUES, D., NICHOLSON, T. J. & CADY, R. E. (2006). Field-scale water flow simulations using ensembles of pedotransfer functions for soil water retention. *Vadose Zone Journal,* 5, 234 - 247.

HAKA, I. B. (2010). *Quantifying evaporation and transpiration in field lysimeters using the soil water balance.* PhD Dissertation, University of the Free State, Bloemfontein, South Africa.

HANSON, J. L., EDIL, T. B. & YESILLER, N. (2000). Thermal properties of high water contnt materials. In T. B. Fox (Ed.), *Geotechnics of high water content materials, ASTM special technical publication 1374* (pp. 137–151). West Conshohocken, Pa: ASTM.

HANSON, L. J., NEUHAEUSER, S., YESILLER, N. (2004). Development and calibration of a large-scale thermal conductivity probe. ASTM International, pp. 1-11.

HARMSE, H. J. (1963). *The sedimentary petrology of the aeolian sands in the northwest Orange Free State.* MSc Dissertation, Pochestron University, South Africa.

HARMSE, H. V. & HATTINGH, A. M. (2012). *The sedimentary petrology of aeolian sands in wester Free State and adjacent areas north of the Vaal River (South Africa).* North West University.

HEINEMANN, Z. E. (2005). *Fluid flow in porous media, Text book series: Volume 1.* Leoben, Austria: University of Leoben, Petroleum Engineering Department.

HELLWIG, D. H. (1973). Evaporation of water from sand, 4: The influence of the depth of the water-table and the particle size distribution of the sand. *Journal of Hydrology,* 18(3), 317-327.

HENSLEY, M. (2000). *Optimizing rainfall use efficiency for developing farmers with limited access to irrigation water.* Water Research Commission, Pretoria, South Africa.

HENSLEY, M., BENNIE, A., VAN RENSBURG, L. & BOTHA, J. (2011). Review of'plant available water'aspects of water use efficiency under irrigated and dryland conditions. *Water SA,* 37(5), 771-779.

HERNÁNDEZ-LÓPEZ, M. F., GIRONÁS, J., BRAUD, I., SUÁREZ, F. & MUÑOZ, J. F. (2014). Assessment of evaporation and water fluxes in a column of dry saline soil subject to different water table levels. *Hydrological Processes,* 28(10), 3655-3669.

HILLEL, D. (1977). *Computer Simulation of Soil- Water Dynamics: A Compendium of Recent Work.* Ottawa: International Development Research Centre.

HILLEL, D. (1998). *Environmental soil physics* (2nd ed.). San Diego, CA: Elsevier Academic Press.

HILLEL, D. (2004). *Introduction to environmental soil physics. Academic press.* San Diego, USA: Elsevier Science.

HIRAIWA, Y. & KASUBUCHI, T. (2000). Temperature dependence of thermal conductivity of soil over a wide range of temperature (5–75 C). *European Journal of Soil Science*, *51*(2), 211-218.

HOLMES, T. R., OWE, M., DE JEU, R. A. & KOOI, H. (2008). Estimating the soil temperature profile from a single depth observation: A simple empirical heat flow solution. *Water Resources Research,* 44(2), doi:10.1029/2007WR005994.

HOPMANS, J. W., SIMUNEK, J. & BRISTOW, K. L. (2002). Indirect estimation of soil thermal properties and water flux using heat pulse probe measurements: Geometry and dispersion effects. *Water Resources Research,* 38(1), doi: 10.1029/2000WR000071.

HUBER, D., MECHEM, D. & BRUNSELL, N. (2014). The effects of Great Plains irrigation on the surface energy balance, regional circulation, and precipitation. *Climate,* 2(2), 103-128.

IDSO, S. B., AASE, J. K. & JACKSON, R. D. (1975). Net radiation-soil heat flux relations as influenced by soil water content variations. *Boundary-Layer Meteorology,* 9(1), 113-122.

JALILI, S., SAEED, S., MOAZED, H. & NASERI, A. (2011). Effect of shallow saline-groundwater depth in evaporation rate. *World Rural Observations,* 3(4), 65-70.

JOHANSEN, O. (1977). *Thermal conductivity of soils (No. CRREL-TL-637).* Hanover, USA: Cold Region Research and Engineering Lab Hanover NH.

JOHNSON, W. M., MCCALEB, S., ULRICH, R., HARPER, W. & HUTCHINGS, T. (1960). Classification and description of soil pores. *Soil Science,* 89(6), 319-321.

JOVANOVIC, N., MU, Q., BUGAN, R. D. & ZHAO, M. (2015). Dynamics of MODIS evapotranspiration in South Africa. *Water SA,* 41(1), 79-90.

KADHIM, A. (2011). Models to predict unsaturated hydraulic conductivity with the use of RETC code. *The Iraqi Journal of Agricultural Sciences,* 42, 105-163.

KERSTEN, M. S. (1949). Thermal properties of frozen ground. *Permafrost International Conference*, pp. 301-305.

KHLOSI, M., CORNELIS, W. M., DOUAIK, A. & VAN GENUCHTEN, M. T. (2008). Performance evaluation of models that describe the soil water retention curve between saturation and oven dryness. *Vadose Zone Journal,* 7(1), 87-96.

KLUTE, A. & DIRKSEN, C. (1986). Hydraulic conductivity and diffusivity: Laboratory methods. In A. Klute (Ed.), *Methods of soil analysis. part 1. 2nd ed. Agronomy monograph 9* (pp. 687 - 734). Madison, USA: ASA and SSSA.

KLUTE, A. (1965). Laboratory measurement of hydraulic conductivity of saturated soil. In *Methods of soil analysis: part 1- physical and mineralogical properties, including statistics of measurement and sampling* (pp. 210-221).

KOSUGI, K. (1999). General model for unsaturated hydraulic conductivity for soils with log-normal pore-size distribution. *Soil Science Society of America,* 63, 270–277.

KOSUGI, K., HOPMANS, J. W. & DANE, J. H. (2002). Parametric Models. In J. H. Topp (Ed.), *Methods of soil analysis:part 4 - physical mthods* (pp. 73 -757). Wisconsin, USA: SSSA, Inc.

KRAMER, P. J. & BOYER, J. S. (1995). *Water relations of plants and soils* (2nd ed.). Academic press.

KUMAR, C. (2012). Climate change and its impact on groundwater resources. *International Journal of Engineering Science,* 1(5), 43-60.

KUMAR, C. P. & MITTAL, S. (2007). *Soil moisture retention characteristics and hydraulic conductivity for different areas in India in selected states.* National Institute of Hydrology, Roorkee, India.

KUTÍLEK, M. & JENDELE, L. (2008). The structural porosity in soil hydraulic functions-a review. *Soil and Water Research,* 3(1), S7-S20.

KUTILEK, M., JENDELE, L. & KYRIAKOS, P. (2006). The influence of uniaxial compression upon pore size distribution in bi-modal soils. *Soil Tillage Research,* 86, 27-37.

LAL, R. & SHUKLA, M. K. (2004). *Principles of soil physics.* CRC Press.

LAMOND, J. F. AND PIELERT, J. H. (2006). Significance of tests and properties of concrete and concrete-making materials. ASTM International, West Conshohocken, PA.

LE ROUX, P. A. L., DU PREEZ, C., MG, S., LD, V. R. & ATP., B. (2007). Effect of irrigation on soil salinity profiles along the Lower Vaal River, South Africa. *Water SA,* 33, 473-478.

LE ROUX, P. A. L., DU PLESSIS, M. J., TURNER, D. P., VAN DER WAALS, J. & BOOYENS, H. B. (2013). *South African Soil Surveyers Organization field book for classification of South African soils* (1st ed.). Bloemfontein, South Africa: Reach Publishers.

LEWAN, E. & JANSSON, P. (1996). Implications of spatial variability of soil physical properties for simulation of evaporation at the field scale . *Water resources research,* 32(7), 2067-2074.

LI, X., CHANG, S. & SALIFU, K. (2013). Soil texture and layering effects on water and salt dynamics in the presence of a water table: a review. *Environmental Reviews,* 22(1), 41-50.

LILLAK, H. (1969). *Effect of soil texture on evaporation with implications for plants.* MSc Thesis , Kansas State University, Manhattan, Kansas, USA.

LOLL, P. & MOLDRUP, P. (2000). *Soil characterization and polluted soil assessment.* Aalborg, Denmark: Aalborg University.

LOUKILI, Y., WOODBURY, A. D. & SNELGROVE, K. R. (2008). SABAE-HW: an enhanced water balance prediction in the Canadian Land Surface Scheme compared with existing models. *Vadose Zone Journal,* 7(3), 865-877.

LUO, Y. & SOPHOCLEOUS, M. (2010). Seasonal groundwater contribution to crop-water use assessed with lysimeter observations and model simulations. *Journal of Hydrology,* 389(3), 325-335.

LUXMOORE, R. (1981). Micro-, Meso- and macroporosity of soil . *Soil Science Society of America Journal,* 45, 241-285.

ŁYDŻBA, D., RAJCZAKOWSKA, M., RÓŻAŃSKI, A. & STEFANIUK, D. (2014). Influence of the moisture content and temperature on the thermal properties of soils: laboratory investigation and theoretical analysis. *Procedia Engineering,* 91, 298-303.

MARIA, A. (1997). Introduction to modeling and simulation. *Proceedings of the 29th conference on winter simulation* (pp. 7-13). IEEE Computer Society.

MARSHALL, T. J., HOLMES, J. W., & ROSE, C. W. (1996). *Soil physics* (3rd ed.). Cambridge University Press.

MAXWELL, R.M., CHOW, F.K. AND KOLLET, S.J. (2007). The groundwater–land-surface–atmosphere connection: Soil moisture effects on the atmospheric boundary layer in fully-coupled simulations. *Advances in Water Resources*, *30*(12), pp. 2447-2466.

MCHANEY, R. (2009). *Understanding computer simulation* (1st ed.). Bookboon.

MCKENZIE, N. J. & JACQUIER, D. W. (1958). *Procedures for field sampling and laboratory measurment of saturated and unsaturated hydraulic conductivity on large soil cores*. CSIRO Australia, Division of Soils.

MCKENZIE, R. H. (2010). *Agricultural soil compaction: Causes and management.* Edmonton, Canada: Alberta Agriculture and Forestry.

MERVA, G. (1987). The velocity permeameter technique for rapid determination of hydraulic conductivity in-situ . *Proceedings of the 3rd international workshop on land drainage* (pp. 55-66). Colombus, Ohio: Ohio State University.

MILLER, K. & YATES, D. (2006). *Climate change and water resources: a primer for municipal water providers.* Denver, USA: American Water Works Association.

MISRA, A., BECKER, B. & FRICKE, B. (1995). A theoretical model of the thermal conductivity of idealized soil. *HVAC&R Research,* 1(1), 81-96.

MIYAZAKI, T. (2006). *Water flow in soils* (2nd ed.). Boca Raton, Florida: CRC Press.

MULLER, K. & FETTERMAN, B. (2002). *Regression and ANOVA: an integrated approach using SAS software.* SAS Institute.

NASSAR, I. N. & HORTON, R. (1992). Simultaneous transfer of heat, water, and solute in porous media: 1. theoretical development. *Soil Science Society of America Journal,* 56(5), 1350 - 1356.

NHLABATSI, N. N. (2010). *Soil surface evaporation studies on the Glen/Bonheim ecotope.* A PhD Thesis, University of the Free State, Bloemfontein, South Africa.

NIMMO, J. (2005). Unsaturated Zone Flow Processes. In M. a. Anderson (Ed.). *Encyclopedia of Hydrological Sciences: Part 13--Groundwater*. Chichester, UK.

NIU, G. Y., SUN, S. F. & HONG, Z. X. (1997). Water and heat transport in the desert soil and atmospheric boundary layer in western China. *Boundary-Layer Meteorology,* 85(2), 179-195.

NOBEL, P. S. & GELLER, G. N. (1987). Temperature modelling of wet and dry desert soils. *Journal of Ecology, 75*(1), *247-258.*

OJO, O. I. (2013). *Mapping and modeling of irrigation induced salinity of Vaal-Harts.* A PhD thesis, Tshwane University of Technology, Pretoria, South Africa.

OLADUNJOYE, M. A. & SANUADE, O. A. (2012). Thermal Diffusivity, Thermal Effusivity and Specific Heat of Soils in Olorunsogo Powerplant, Southwestern Nigeria. *International Journal of Research and Reviews in Applied Sciences,* 13(2), 502-521.

OLADUNJOYE, M. A., SANUADE, O. A. & OLAOJO, A. A. (2013). Variability of soil thermal properties of a seasonally cultivated agricultural teaching and research farm, university of Ibadan, south-western Nigeria. *GJSFR-D: Agriculture and Veterinary,* 13(8), 41-64.

OMER, A. & OMER, A. (2014). Soil thermal properties and the effects of groundwater on closed loops. *International Journal of Sustainable Energy and Environmental Research,* 3(1), 34-52.

OMUTO, C. (2009). Biexponential model for water retention characteristics. *Geoderma,* 149(3), 235-242.

OR, D. & TULLER, M. (2005). Capillarity. In H. D. (Ed.), *Encyclopedia of Soils in the Environment* (pp. 155-164). Oxford, UK: Elsevier Sciences.

OR, D., LEHMANN, P. & SHOKRI, N. (2007). Characteristic lengths affecting evaporation from heterogeneous porous media with sharp textural boundaries. *Estudios de la Zona No Saturada del Suelo,* 8, 1-8.

OSBORNE, J. W. (2010). Improving your data transformations: applying the box-cox transformation. *Practical Assessment, Research & Evaluation ,* 15(12), 1-9.

PELTIER, M. R., WILCOX, C. J. & SHARP, D. C. (1998). Technical note: application of the box-cox data transformation to animal science experiments. *Journal of animal science,* 76(3), 847-849.

PERFECT, E. (2005). Modeling the primary drainage curve of prefractal porous media. *Vadose Zone Journal,* 4(4), 959-66.

PERKINS, K. S. (2011). *Measurement and modeling of unsaturated hydraulic conductivity.* United States Geological Survey.

PERROUX, K. & WHITE, I. (1988). Designs for disc permeameters. *Soil Science Society of America Journal,* 52(5), 1205-1215.

PHILIP, J. R. & DE VRIES, D. A. (1957). Moisture movement in porous materials under temperature gradients. *Eos, Transactions American Geophysical Union,* 38(2), 222-232.

PHILIP, J. R. (1957). Evaporation, and moisture and heat fields in the soil. *Journal of Meteorology,* 14(4), 354 - 366.

PIETERSEN, K., HANS E. BEEKMAN, H. E. & HOLLAND, M. (2011). *South african groundwater governance case study.* Pretoria: Water Research Commission.

POPIEL, C. O., WOJTKOWIAK, J. & BIERNACKA, B. (2001). Measurements of temperature distribution in ground. *Experimental Thermal and Fluid Science,* 25(5), 301 - 309.

QIN, Z., BERLINER, P. & KARNIELI, K. (2002). Numerical solution of a complete surface energy balance model for simulation of heat fluxes and surface temperature under bare soil environment. *Applied MAthematics and Computation,* 130, 171 - 200.

RASHEED, H. R., AL-ANAZ, H. & ABID, K. A. (1989). Evaporation from soil surface in presence of shallow water tables. *In New directions for surface water modeling; proceedings of a symposium held in Baltimore.* pp. 353-361. Maryland: IAHS Publication.

RAWLS, W. & BRAKENSIEK, D. (1985). Prediction of soil water properties for hydrologic modeling. *Watershed management in the eighties* , pp. 293-299.

REYNOLDS, W. & ELRICK, D. (1986). A Method for simultaneous *in situ* measurement in the vadose zone of field-saturated hydraulic conductivity, sorptivity and the conductivity-pressure head relationship. *Groundwater Monitoring & Remediation,* 6(1), 84-95.

REYNOLDS, W. D. & TOPP, G. C. (2008). Soil water analyses: principles and parameters. In *Soil sampling and methods of analysis.* USA: CRC press, Tailor and Francis group.

REYNOLDS, W. D. (2002). Chapter 76: Saturated Hydraulic Properties: Well permeameter. In M. C. Gregorich (Ed.), *Soil sampling and methods of analysis* (2nd ed.). Boca Raton, Florida: CRC press, Tailor and Francis group.

RICHARDS, L. A. (1931). Capillary conduction of liquids through porous mediums. *Journal of Applied Physics,* 1(5), 318-333.

RIPPLE, C. D., RUBIN, J. & VAN HYLCKAMA, T. E. A. (1972). *Estimating steady-state evaporation rates from bare soils under conditions of high water table.* US Government Printing Office.

ROBINSON, G. W. (1922). A new method for the mechanical analysis of soils and other dispersions. *The Journal of Agricultural Science,* 12(3), 306-321.

ROSE, D., KONUKCU, F. & GOWING, J. (2005). Effect of watertable depth on evaporation and salt accumulation from saline groundwater. *Soil Research,* 43(5), 565-573.

ROSSI, C. & NIMMO, J. R. (1994). Modeling of soil water retention from saturation to oven dryness. *Water Resource Research,* 30(3), 701-708.

ROWELL, D. (2014). *Soil science: methods & applications.* New York, USA: Routledge.

RUAN, H. & ILLANGASEKARE, T. H. (1999). *A model of the relative hydraulic conductivity of unsaturated sandy soils.* Riverside, USA: University of California.

RUBIO, C. M. (2013). A laboratory procedure to determine the thermal properties of silt loam soils based on ASTM D 5334. *Applied Ecology and Environmental Sciences,* 1(4), 45-48.

SAITO, H., SIMUNEK, J. & MOHANTY, B. (2006). Numerical analysis of coupled water, vapor, and heat transport in the vadose zone. *Vadose Zone Journal,* 5, 784–800.

SANTAMARINA, J. C. (2012). *Thermal properties of soils.* Atlanta, Georgia: ALERT Doctoral School.

SAS INSTITUTE. (2013). *Base SAS 9.3 procedures guide: Statistical procedures*. SAS Institute.

SAWADA, S. (1977). *Temperature dependence of thermal conductivity of frozen soils*. Kirami Technical College, research report-volume 9(1), 111-122.

SAXENA, G. S. (1969). *Effect of environmental factors and water table depths on evaporation rates from soils in the presence of water table.* PhD disseration, Ohio State University, Columbus, Ohio.

SAXTON, K. & RAWLS, W. (2006). Soil water characteristic estimates by texture and organic matter for hydrologic solutions. *Soil Science Society of America Journal,* 70(5), 1569-78.

SCHAAP, M. G. & VAN GENUCHTEN, M. T. (2006). A modified Mualem–van Genuchten formulation for improved description of the hydraulic conductivity near saturation. *Vadose Zone Journal,* 5, 27 - 34.

SCHAAP, M. G., SHOUSE, P. J. & MEYER, P. D. (2003). *Laboratory measurements of the unsaturated hydraulic properties at the vadose zone transport field study site.* Richland, USA: Pacific Northwest National Laboratory.

SCHEINOST, A., SINOWSKI, W. & AUERSWALD, K. (1997). Regionalization on of soil water retention curves in a highly variable soilscape: 1. Developing pedotransfer function. *Geoderma,* 78, 129-143.

SCHLEGEL, G., HARMSE, H., J. V. & BRUKE, O. (1989). The Kalahari sands of Southern Africa. *Journal of Geology,* 29, 207-222.

SCHROEDER, P. R. & GIBSON, A. C. (1982). *Supporting documentation for the hydrologic simulation model for estimating percolation at solid waste disposal sites (HSSWDS).* US Environmental Protection Agency, Cincinnati, OH.

SCHROEDER, P. R., DOZIER, T. S., ZAPPI, P. A., MCENROE, B. M., SJOSTROM, J. W. AND PEYTON, R. L. (1994). *The Hydrologic Evaluation of Landfill Performance (HELP) Model: Engineering Documentation for Version 3 ,* Cincinnati, Ohio: U.S. Environmental Protection Agency, Risk Reduction Engineering Laboratory.

SCHWARTZ, K. (1985). Collapsible soils: problem soils in South Africa-state of the art. *Civil Engineer in South Africa ,* 27(7), 379-381.

SEN, Z. (2015). *Practical and applied hydrogeology* (1st ed.). Elsevier Academic Press.

SEPASKHAH, A. R. & BOERSMA, L. (1979). Thermal conductivity of soils as a function of temperature and water content. *Soil Science Society of America Journal,* 43(3), 439-444.

SHAHRAN, G. & JADHAV, R. (2002). *Soil Temperatures Regime at Ahmedabad Indian Institute of Management.* Ahmedabad, India: Indian Institute of Management.

SHOKRI, N. & SALVUCCI, G. (2011). Evaporation from porous media in the presence of a water table. *Vadose Zone Journal*, 10(4), 1309-1318.

SIMUNEK, J., HUANG, K., SEJNA, M. & VAN GENUCHTEN, M. T. (1998). *The HYDRUS-1D software package for simulating the one-dimensional movement of water, heat, and multiple solutes in variably-saturated media-Version 2.0.* Golden, Colorado: IGWMC-TPS-70, International Ground Water Modeling Center, Colorado School of Mines.

ŠIMŮNEK, J., VAN GENUCHTEN, M. T. AND ŠEJNA, M., (2012). HYDRUS: model use, calibration, and validation. 55(4), pp. 1261 - 1274.

SINGER, M., HOWARD, R. & FRANTZ, G. (1981). Effects of soil properties, water content and compactive effort on the compaction of selected California forest and range soils. *Soil Science Society of America Journal* , 45(2), 231-236.

SMETTEM, K. R., BROADBRIDGE, P. & WOOLHISER, D. A. (2002). *Infiltration theory for hydrologic applications.* (R. E. Smith, Ed.) American Geophysical Union.

SMITS, K. M., SAKAKI, T., L. A. & ILLANGASEKARE, T. H. (2009). *Determination of the thermal conductivity of sands under varying moisture, drainage/wetting, and porosity conditions-applications in near-surface soil moisture distribution analysis*. (pp. 57 - 65). Goldon, USA: AGU Hydrology Days.

SOIL CLASSIFICATION WORKING GROUP. (1991). *Soil Classification: a taxonomic system for South Africa.* A report on a research project conducted under the auspices of the Soil and Irrigation Research Institute, Department of Agricultural Development, Pretoria, South Africa.

SOKOLOWSKI, J. & BANKS, C. (2010). *Modeling and simulation fundamentals: theoretical underpinnings and practical domains.* John Wiley & Sons.

SOKOLOWSKI, J. A. & BANKS., C. M. (EDS.). (2011). *Principles of modeling and simulation: a multidisciplinary approach.* John Wiley & Sons.

TARNAWSKI, V. R. & LEONG, W. H. (2000). Thermal conductivity of soils at very low moisture content and moderate temperatures. *Transport in Porous Media,* 41(2), 137-147.

TESFUHUNEY, W. A. (2012). *Optimizing runoff to basin ratios for maize production with in-field rainwater harvesting.* A PhD Thesis in the University of the Free State, Bloemfontein, South Africa.

Thomas, D. S. G. and Shaw, P. A. (1990). The deposition and developments of the Kalahari Group sediments. Centeral Southern Africa. *Journal of African Earth Science*, 10. 180-197.

THOMAS, D., KNIGHT, M. & WIGGS, G. (2005). Remobilization of Southern African desert dune systems by twenty-first century global warming. *Nature,* 435(7046), 1218-1221.

TOMBUL, M., AKYÜREK, Z. & SORMAN, A. Ü. (2004). Research note: determination of soil hydraulic properties using pedotransfer functions in a semi-arid basin, Turkey. *Hydrology and Earth System Sciences, 8*(6), 1200-1209.

TOO, V. K., OMUTO, C. T., BIAMAH, E. K. & OBIERO, J. P. (2014). Review of soil water retention characteristic (SWRC) models between saturation and oven dryness. *Open Journal of Modern Hydrology,* 40(04), 173-182.

TOWNEND, J., REEVE, M. & CARTER, A. (2001). Water release characteristic. In K. A. Mullins (Ed.), *Soil and environmental analysis: physical methods* (pp. 95-140). New York, USA: Marcel Dekker, Inc.

TRITT, T.M. (2005). *Thermal conductivity: theory, properties, and applications*. Springer Science & Business Media.

TULLER, M. & OR, D. (2004). Retention of water in soil and the soil water characteristic curve. In *Encyclopedia of soils in the environment* (4 ed., pp. 278-289). USA.

UMALI, D. L. (1993). *Irrigation-induced salinity.* World Bank technical paper 215, World Bank, Washington DC, USA.

USOWICZ, B., KOSSOWSKI, J. & BARANOWSKI, P. (1996). Spatial variability of soil thermal properties in cultivated fields. *Soil & Tillage Research,* 39 , 85 - 100.

USOWICZ, B., MARCZEWSKI, W., LIPIEC, J., USOWICZ, J. B., SOKOŁOWSKA, Z., DĄBKOWSKA-NASKRĘT, H., HAJNOS, M. & UKOWSKI, M. I. (2010). *Spatial variability of texture and wetness: effects on the thermal conductivity of soil.* Dublin, Poland: Institute of Agrophysics.

VAN BAVEL, C. H. & HILLEL, D. I. (1976). Calculating potential and actual evaporation from a bare soil surface by simulation of concurrent flow of water and heat. *Agricultural Meteorology,* 17, 453 - 476.

VAN GENUCHTEN, M. T. & PACHEPSKY, Y. (2011). Hydraulic properties of unsaturated soils. In *Encyclopedia of agrophysics* (pp. 368-376). Springer Netherlands.

VAN GENUCHTEN, M. T. (1980). A closed form equation for predicting the hydraulic conductivity of unsaturated soils. *Soil Science Society of America,* 44, 892 - 898.

VAN GENUCHTEN, M. T., LEIJ, F. J. & YATES, S. R. (1991). *The RETC code for quantifying the hydraulic functions of unsaturated soils.* U.S. Environmental Protection Agency, Riverside, CA.

VAN GENUCHTEN, M., LEIJI, F. AND LUND, L. (1992). *Indirect methods for estimating the hydraulic properties of unsaturated soils.* University of California, Riverside, California, p. 718.

VAN RENSBURG, L. D. (1988). *Die voorspelling van grondgeinduseerde plantwaterstremming vir geselekteerde grond-plant-atmosfeersisteme.* MSc Dissertation, University of the Orange Free State, Bloemfontein, South Africa.

VAN RENSBURG, L. D. (2010). Advances in soil physics: Application in irrigation and dryland crop production. *South African Journal of Plant and Soil,* 27(1), 9-18.

VAN RENSBURG, L., DE CLERCQ, W., BARNARD, J., & DU PREEZ, C. (2011). Case studies from Water Research Commission projects along the Lower Vaal, Riet, Berg and Breede Rivers. *Water SA*, 37(5), 739-749.

VEREECKEN, H., WEYNANTS, M., JAVAUX, M., PACHEPSKY, Y., SCHAAP, M. G. & VAN GENUCHTEN, M. T. (2010). Using pedotransfer functions to estimate the van Genuchten-Mualem soil hydraulic properties: a review. *Vadose Zone Journal,* 9, 795-820.

VERMA, O. (1974). *Evaporation Studies in the Presence of Water table.* A PhD Thesis in the Graduate College of the University of Illinois, Urbana-Champaign, USA.

VERSEGHY, D. L. (1991). CLASS-a Canadian land surface scheme for GCMs. I. soil model. *International Journal of Climatology,* 11(2), 111-133.

VERSEGHY, D. L., MCFARLANE, N. A. & LAZARE, M. (1993). CLASS—a Canadian land surface scheme for GCMs, II. vegetation model and coupled runs. *International Journal of Climatology,* 13(4), 347-370.

VERWEY, P.M.J. AND VERMEULEN, P.D. (2011). Influence of irrigation on the level, salinity and flow of groundwater at Vaal harts Irrigation scheme. *Water SA*, *37*(2), pp.155-164.

VOGEL, T. & CISLEROVA, M. (1988). On the reliability of unsaturated hydraulic conductivity calculated from the moisture retention curve. *Transport in porous media,* 3(1), 1-15.

VOGEL, T., VAN GENUCHTEN, M. & CISLEROVA, M. (2000). Effect of the shape of the soil hydraulic functions near saturation on variably-saturated flow predictions. *Advances in Water Resources,* 24(2), 133-144.

VOGEL, T., VAN GENUCHTEN, M. T. AND CISLEROVA, M., (2000). Effect of the shape of the soil hydraulic functions near saturation on variably-saturated flow predictions. *Advances in Water Resources,* Volume 24, pp. 133 - 144.

WELLER, U., IPPISCH, O., KÖHNE, M. & VOGEL, H. J. (2011). Direct measurement of unsaturated conductivity including hydraulic nonequilibrium and hysteresis. *Vadose Zone Journal,* 10(2), 654 - 661.

WESTERMANN, S. (2010). *Sensitivity of Permafrost.* Heidelberg, Germany: A PhD dissertation in Combined Faculties of Natural Sciences and Mathematics, University of Heidelberg.

WILLIS, W. O. & RANEY, W. A. (1971). Effects of compaction on content and transmission of heat in soils. In K. K. Barnes (Ed.), *Compaction of agricultural soils* (1st ed., pp. 165-177). American Society of Agricultural Engineers.

WILLMOTT, C. (1982). Some comments on the evaluation of model performance. *American meteorological Society,* 63, 1309-1313.

WÖSTEN, J. H., LILLY, A., NEMES, A. & LE BAS, C. (1999). Development and use of a database of hydraulic properties of European soils. *Geoderma,* 90(3), 169-185.

WYTHERS, K., LAUENROTH, W. & PARUELO, J. (1999). Bare soil evaporation under semi-arid field conditions. *Soil Science Society of America Journal,* 63(5), 1341-1349.

YOUNG, C., WALLENDER, W., SCHOUPS, G., FOGG, G., HANSON, B., HARTER, T., HOPMANS, J, HOWITT, R., HSIAO, T., PANDAY, S., TANJI, K., USTIN, S. & WARD, K. (2007). Modeling shallow water table evaporation in irrigated regions. *Irrigation and Drainage Systems,* 21(2), 119-132.

YU, D., SHRESTHA, B. & BAIK, O. (2015). Thermal conductivity, specific heat, thermal diffusivity, and emissivity of stored canola seeds with their temperature and moisture content. *Journal of Food Engineering,* 165, 156-165.

ZERE, T. B. (2005). *The hydropedology of selected soils in the Weatherley Catchment in the Eastern Cape Province of South Africa* . Doctoral dissertation, University of the Free State, Bloemfontein, South Africa.

ZERIZGHY, M. G. (2012). *Integrating rainfall runoff and evaporation models for estimating soil water storage during fallow under in-field rainwater harvesting.* Doctoral dissertation, University of the Free State, Bloemfontein, South Africa.

ZHANG, F. (2010). *Soil water retention and relative permeability for full range of saturation.* Washington DC, USA: Pacific Northwest National Laboratory.

ZHANG, Z. F. (2011). Soil water retention and relative permeability for conditions from oven-dry to full saturation. *Vadose Zone Journal,* 10, 1299 - 1308.

Appendix 3: Soil hydraulic properties

Appendix 3.1 Measured data of the SWRC of the four horizons

Soil horizons							
Clovelly-Ap		Clovelly-B		Hutton-Ap		Hutton-B	
θ	ψ	θ	ψ	θ	ψ	θ	ψ
0.070	1250.35	0.051	1250.35	0.091	1500.00	0.095	1500.00
0.074	899.96	0.055	899.96	0.096	1000.00	0.106	1000.00
0.078	500.04	0.059	500.04	0.106	500.00	0.124	500.00
0.080	299.99	0.068	299.99	0.122	300.00	0.141	300.00
0.100	100.03	0.084	100.03	0.159	100.00	0.186	100.00
0.118	50.00	0.104	50.00	0.186	50.00	0.205	50.00
0.182	10.00	0.141	10.00	0.217	10.00	0.239	10.00
0.250	8.14	0.235	8.14	0.272	5.00	0.301	5.00
0.288	5.88	0.300	5.88	0.317	3.00	0.327	3.00
0.376	2.55	0.363	2.55	0.329	2.00	0.340	2.00
0.384	0.39	0.399	0.39	0.354	1.00	0.349	1.00
0.391	0.00	0.401	0.00	0.364	0.38	0.362	0.38
-	-	-	-	0.374	0.00	0.366	0.00

Appendix 3.2 Fitted data of the SWRC with Van Genuchten model using the RETC program

Clovelly-Ap		Clovelly-B		Hutton-Ap		Hutton-B	
θ	**ψ**	**θ**	**ψ**	**θ**	**ψ**	**θ**	**ψ**
0.0523	3.15E+06	0.0537	7.34E+04	0.0917	1.39E+08	0.0957	1.40E+09
0.0531	1.12E+06	0.0546	4.14E+04	0.0924	2.99E+07	0.0964	2.39E+08
0.0549	3.98E+05	0.0564	2.33E+04	0.0939	6.42E+06	0.0978	4.06E+07
0.0583	1.41E+05	0.0599	1.32E+04	0.0968	1.38E+06	0.1005	6.92E+06
0.0618	7.73E+04	0.0635	9.40E+03	0.0997	5.61E+05	0.1033	2.46E+06
0.0653	5.03E+04	0.067	7.41E+03	0.1026	2.97E+05	0.1061	1.18E+06
0.0687	3.61E+04	0.0706	6.15E+03	0.1054	1.81E+05	0.1088	6.67E+05
0.0722	2.75E+04	0.0741	5.29E+03	0.1083	1.21E+05	0.1116	4.19E+05
0.0757	2.18E+04	0.0777	4.65E+03	0.1112	8.57E+04	0.1144	2.82E+05
0.0791	1.79E+04	0.0812	4.16E+03	0.1141	6.37E+04	0.1171	2.01E+05
0.0826	1.50E+04	0.0848	3.77E+03	0.117	4.91E+04	0.1199	1.49E+05
0.0861	1.28E+04	0.0883	3.45E+03	0.1199	3.88E+04	0.1227	1.14E+05
0.0895	1.11E+04	0.0919	3.19E+03	0.1228	3.14E+04	0.1254	8.90E+04
0.093	9.74E+03	0.0954	2.96E+03	0.1257	2.59E+04	0.1282	7.13E+04
0.0964	8.64E+03	0.099	2.77E+03	0.1285	2.17E+04	0.1309	5.81E+04
0.0999	7.73E+03	0.1025	2.60E+03	0.1314	1.84E+04	0.1337	4.81E+04
0.1034	6.96E+03	0.1061	2.45E+03	0.1343	1.58E+04	0.1365	4.03E+04
0.1068	6.32E+03	0.1096	2.32E+03	0.1372	1.37E+04	0.1392	3.42E+04

Clovelly-Ap		Clovelly-B		Hutton-Ap		Hutton-B	
θ	ψ	θ	ψ	θ	ψ	θ	ψ
0.1103	5.77E+03	0.1132	2.20E+03	0.1401	1.19E+04	0.142	2.93E+04
0.1138	5.29E+03	0.1168	2.09E+03	0.143	1.05E+04	0.1448	2.53E+04
0.1172	4.87E+03	0.1203	2.00E+03	0.1459	9.32E+03	0.1475	2.20E+04
0.1207	4.51E+03	0.1239	1.91E+03	0.1488	8.32E+03	0.1503	1.93E+04
0.1242	4.19E+03	0.1274	1.83E+03	0.1516	7.46E+03	0.1531	1.70E+04
0.1276	3.90E+03	0.131	1.76E+03	0.1545	6.72E+03	0.1558	1.51E+04
0.1311	3.64E+03	0.1345	1.69E+03	0.1574	6.08E+03	0.1586	1.35E+04
0.1346	3.41E+03	0.1381	1.63E+03	0.1603	5.53E+03	0.1614	1.21E+04
0.138	3.20E+03	0.1416	1.57E+03	0.1632	5.05E+03	0.1641	1.09E+04
0.1415	3.02E+03	0.1452	1.51E+03	0.1661	4.62E+03	0.1669	9.84E+03
0.145	2.84E+03	0.1487	1.46E+03	0.169	4.24E+03	0.1697	8.92E+03
0.1484	2.69E+03	0.1523	1.41E+03	0.1719	3.91E+03	0.1724	8.12E+03
0.1519	2.54E+03	0.1558	1.37E+03	0.1747	3.61E+03	0.1752	7.42E+03
0.1554	2.41E+03	0.1594	1.33E+03	0.1776	3.35E+03	0.178	6.80E+03
0.1588	2.29E+03	0.1629	1.29E+03	0.1805	3.11E+03	0.1807	6.24E+03
0.1623	2.18E+03	0.1665	1.25E+03	0.1834	2.89E+03	0.1835	5.75E+03
0.1658	2.07E+03	0.1701	1.21E+03	0.1863	2.69E+03	0.1863	5.30E+03
0.1692	1.98E+03	0.1736	1.18E+03	0.1892	2.51E+03	0.189	4.91E+03
0.1727	1.89E+03	0.1772	1.14E+03	0.1921	2.35E+03	0.1918	4.55E+03
0.1762	1.80E+03	0.1807	1.11E+03	0.195	2.20E+03	0.1946	4.22E+03
0.1796	1.72E+03	0.1843	1.08E+03	0.1978	2.07E+03	0.1973	3.93E+03
0.1831	1.65E+03	0.1878	1.06E+03	0.2007	1.95E+03	0.2001	3.66E+03
0.1865	1.58E+03	0.1914	1.03E+03	0.2036	1.83E+03	0.2028	3.42E+03
0.19	1.52E+03	0.1949	1.00E+03	0.2065	1.73E+03	0.2056	3.20E+03
0.1935	1.45E+03	0.1985	9.76E+02	0.2094	1.63E+03	0.2084	2.99E+03
0.1969	1.40E+03	0.202	9.52E+02	0.2123	1.54E+03	0.2111	2.81E+03
0.2004	1.34E+03	0.2056	9.28E+02	0.2152	1.45E+03	0.2139	2.63E+03
0.2039	1.29E+03	0.2091	9.06E+02	0.2181	1.38E+03	0.2167	2.48E+03
0.2073	1.24E+03	0.2127	8.84E+02	0.2209	1.30E+03	0.2194	2.33E+03
0.2108	1.19E+03	0.2162	8.63E+02	0.2238	1.24E+03	0.2222	2.19E+03
0.2143	1.15E+03	0.2198	8.43E+02	0.2267	1.17E+03	0.225	2.07E+03
0.2177	1.11E+03	0.2233	8.23E+02	0.2296	1.11E+03	0.2277	1.95E+03
0.2212	1.07E+03	0.2269	8.04E+02	0.2325	1.06E+03	0.2305	1.84E+03
0.2247	1.03E+03	0.2305	7.85E+02	0.2354	1.01E+03	0.2333	1.74E+03
0.2281	9.90E+02	0.234	7.67E+02	0.2383	9.57E+02	0.236	1.65E+03
0.2316	9.55E+02	0.2376	7.49E+02	0.2412	9.11E+02	0.2388	1.56E+03
0.2351	9.21E+02	0.2411	7.32E+02	0.2441	8.68E+02	0.2416	1.47E+03
0.2385	8.89E+02	0.2447	7.15E+02	0.2469	8.27E+02	0.2443	1.40E+03
0.242	8.58E+02	0.2482	6.99E+02	0.2498	7.88E+02	0.2471	1.32E+03
0.2455	8.28E+02	0.2518	6.83E+02	0.2527	7.51E+02	0.2499	1.26E+03
0.2489	7.99E+02	0.2553	6.68E+02	0.2556	7.17E+02	0.2526	1.19E+03
0.2524	7.71E+02	0.2589	6.52E+02	0.2585	6.84E+02	0.2554	1.13E+03
0.2559	7.44E+02	0.2624	6.37E+02	0.2614	6.52E+02	0.2582	1.07E+03

Clovelly-Ap		Clovelly-B		Hutton-Ap		Hutton-B	
θ	ψ	θ	ψ	θ	ψ	θ	ψ
0.2593	7.19E+02	0.266	6.23E+02	0.2643	6.23E+02	0.2609	1.02E+03
0.2628	6.94E+02	0.2695	6.08E+02	0.2672	5.94E+02	0.2637	9.68E+02
0.2662	6.70E+02	0.2731	5.94E+02	0.27	5.67E+02	0.2664	9.20E+02
0.2697	6.46E+02	0.2766	5.80E+02	0.2729	5.42E+02	0.2692	8.74E+02
0.2732	6.24E+02	0.2802	5.67E+02	0.2758	5.17E+02	0.272	8.30E+02
0.2766	6.02E+02	0.2837	5.53E+02	0.2787	4.94E+02	0.2747	7.89E+02
0.2801	5.81E+02	0.2873	5.40E+02	0.2816	4.71E+02	0.2775	7.49E+02
0.2836	5.60E+02	0.2909	5.27E+02	0.2845	4.50E+02	0.2803	7.12E+02
0.287	5.40E+02	0.2944	5.14E+02	0.2874	4.29E+02	0.283	6.76E+02
0.2905	5.20E+02	0.298	5.01E+02	0.2903	4.09E+02	0.2858	6.42E+02
0.294	5.01E+02	0.3015	4.89E+02	0.2931	3.90E+02	0.2886	6.09E+02
0.2974	4.83E+02	0.3051	4.76E+02	0.296	3.72E+02	0.2913	5.78E+02
0.3009	4.65E+02	0.3086	4.64E+02	0.2989	3.54E+02	0.2941	5.48E+02
0.3044	4.47E+02	0.3122	4.51E+02	0.3018	3.37E+02	0.2969	5.20E+02
0.3078	4.29E+02	0.3157	4.39E+02	0.3047	3.21E+02	0.2996	4.92E+02
0.3113	4.12E+02	0.3193	4.27E+02	0.3076	3.05E+02	0.3024	4.66E+02
0.3148	3.96E+02	0.3228	4.15E+02	0.3105	2.89E+02	0.3052	4.41E+02
0.3182	3.79E+02	0.3264	4.03E+02	0.3134	2.75E+02	0.3079	4.16E+02
0.3217	3.63E+02	0.3299	3.91E+02	0.3162	2.60E+02	0.3107	3.93E+02
0.3252	3.47E+02	0.3335	3.78E+02	0.3191	2.46E+02	0.3135	3.70E+02
0.3286	3.32E+02	0.337	3.66E+02	0.322	2.32E+02	0.3162	3.48E+02
0.3321	3.16E+02	0.3406	3.54E+02	0.3249	2.19E+02	0.319	3.27E+02
0.3356	3.01E+02	0.3442	3.42E+02	0.3278	2.06E+02	0.3218	3.06E+02
0.339	2.86E+02	0.3477	3.29E+02	0.3307	1.94E+02	0.3245	2.86E+02
0.3425	2.71E+02	0.3513	3.17E+02	0.3336	1.81E+02	0.3273	2.67E+02
0.346	2.55E+02	0.3548	3.04E+02	0.3365	1.69E+02	0.3301	2.48E+02
0.3494	2.40E+02	0.3584	2.91E+02	0.3393	1.57E+02	0.3328	2.29E+02
0.3529	2.25E+02	0.3619	2.77E+02	0.3422	1.46E+02	0.3356	2.11E+02
0.3563	2.10E+02	0.3655	2.64E+02	0.3451	1.34E+02	0.3383	1.93E+02
0.3598	1.95E+02	0.369	2.50E+02	0.348	1.22E+02	0.3411	1.76E+02
0.3633	1.80E+02	0.3726	2.35E+02	0.3509	1.11E+02	0.3439	1.58E+02
0.3667	1.64E+02	0.3761	2.20E+02	0.3538	9.96E+01	0.3466	1.41E+02
0.3702	1.48E+02	0.3797	2.03E+02	0.3567	8.81E+01	0.3494	1.24E+02
0.3737	1.31E+02	0.3832	1.86E+02	0.3596	7.64E+01	0.3522	1.07E+02
0.3771	1.13E+02	0.3868	1.67E+02	0.3624	6.45E+01	0.3549	8.94E+01
0.3806	9.43E+01	0.3903	1.46E+02	0.3653	5.21E+01	0.3577	7.15E+01
0.3841	7.32E+01	0.3939	1.20E+02	0.3682	3.88E+01	0.3605	5.25E+01
0.3875	4.78E+01	0.3974	8.73E+01	0.3711	2.37E+01	0.3632	3.14E+01
0.3893	3.14E+01	0.3992	6.36E+01	0.3726	1.46E+01	0.3646	1.89E+01
0.3901	2.07E+01	0.4001	4.64E+01	0.3733	9.01E+00	0.3653	1.14E+01
0.3907	1.19E+01	0.4006	3.06E+01	0.3737	4.78E+00	0.3657	5.90E+00
0.391	3.00E+00	0.401	1.08E+01	0.374	9.77E-01	0.366	1.13E+00
0.391	7.56E-01	0.401	3.80E+00	0.374	2.00E-01	0.366	2.15E-01

Clovelly-Ap		Clovelly-B		Hutton-Ap		Hutton-B	
θ	**ψ**	**θ**	**ψ**	**θ**	**ψ**	**θ**	**ψ**
0.391	0.00E+00	0.401	0.00E+00	0.374	0.00E+00	0.366	0.00E+00

Appendix 3.3 Estimated data of the $K_L(\theta)$ relationship for the four horizons

Clovelly-Ap		Clovelly-B		Hutton-Ap		Hutton-B	
θ	**K_L**	**θ**	**K_L**	**θ**	**K_L**	**θ**	**K_L**
0.0523	6.12E-14	0.0537	4.04E-10	0.0917	5.96E-18	0.0957	3.85E-20
0.0531	2.74E-12	0.0546	7.20E-09	0.0924	7.30E-16	0.0964	7.51E-18
0.0549	1.22E-10	0.0564	1.28E-07	0.0939	8.94E-14	0.0978	1.46E-15
0.0583	5.48E-09	0.0599	2.28E-06	0.0968	1.10E-11	0.1005	2.86E-13
0.0618	5.06E-08	0.0635	1.23E-05	0.0997	1.82E-10	0.1033	6.24E-12
0.0653	2.45E-07	0.067	4.07E-05	0.1026	1.34E-09	0.1061	5.57E-11
0.0687	8.33E-07	0.0706	1.03E-04	0.1054	6.31E-09	0.1088	3.04E-10
0.0722	2.26E-06	0.0741	2.20E-04	0.1083	2.23E-08	0.1116	1.22E-09
0.0757	5.27E-06	0.0777	4.17E-04	0.1112	6.51E-08	0.1144	3.93E-09
0.0791	1.10E-05	0.0812	7.27E-04	0.1141	1.64E-07	0.1171	1.09E-08
0.0826	2.09E-05	0.0848	1.19E-03	0.117	3.72E-07	0.1199	2.66E-08
0.0861	3.73E-05	0.0883	1.84E-03	0.1199	7.72E-07	0.1227	5.93E-08
0.0895	6.30E-05	0.0919	2.74E-03	0.1228	1.50E-06	0.1254	1.23E-07
0.093	1.02E-04	0.0954	3.94E-03	0.1257	2.74E-06	0.1282	2.37E-07
0.0964	1.58E-04	0.099	5.50E-03	0.1285	4.77E-06	0.1309	4.37E-07
0.0999	2.37E-04	0.1025	7.49E-03	0.1314	7.98E-06	0.1337	7.67E-07
0.1034	3.46E-04	0.1061	1.00E-02	0.1343	1.29E-05	0.1365	1.30E-06
0.1068	4.93E-04	0.1096	1.31E-02	0.1372	2.02E-05	0.1392	2.12E-06
0.1103	6.89E-04	0.1132	1.69E-02	0.1401	3.07E-05	0.142	3.36E-06
0.1138	9.43E-04	0.1168	2.15E-02	0.143	4.57E-05	0.1448	5.20E-06
0.1172	1.27E-03	0.1203	2.69E-02	0.1459	6.65E-05	0.1475	7.84E-06
0.1207	1.69E-03	0.1239	3.34E-02	0.1488	9.49E-05	0.1503	1.16E-05
0.1242	2.21E-03	0.1274	4.10E-02	0.1516	1.33E-04	0.1531	1.68E-05
0.1276	2.85E-03	0.131	4.98E-02	0.1545	1.84E-04	0.1558	2.40E-05
0.1311	3.65E-03	0.1345	6.01E-02	0.1574	2.51E-04	0.1586	3.36E-05
0.1346	4.61E-03	0.1381	7.19E-02	0.1603	3.37E-04	0.1614	4.65E-05
0.138	5.78E-03	0.1416	8.55E-02	0.1632	4.48E-04	0.1641	6.35E-05
0.1415	7.18E-03	0.1452	1.01E-01	0.1661	5.89E-04	0.1669	8.56E-05
0.145	8.85E-03	0.1487	1.18E-01	0.169	7.66E-04	0.1697	1.14E-04
0.1484	1.08E-02	0.1523	1.38E-01	0.1719	9.88E-04	0.1724	1.51E-04
0.1519	1.32E-02	0.1558	1.60E-01	0.1747	1.26E-03	0.1752	1.97E-04
0.1554	1.59E-02	0.1594	1.85E-01	0.1776	1.60E-03	0.178	2.56E-04
0.1588	1.91E-02	0.1629	2.13E-01	0.1805	2.01E-03	0.1807	3.28E-04
0.1623	2.28E-02	0.1665	2.44E-01	0.1834	2.51E-03	0.1835	4.19E-04
0.1658	2.70E-02	0.1701	2.78E-01	0.1863	3.11E-03	0.1863	5.30E-04
0.1692	3.20E-02	0.1736	3.16E-01	0.1892	3.84E-03	0.189	6.66E-04
0.1727	3.76E-02	0.1772	3.58E-01	0.1921	4.70E-03	0.1918	8.32E-04

Clovelly-Ap		Clovelly-B		Hutton-Ap		Hutton-B	
θ	K_L	θ	K_L	θ	K_L	θ	K_L
0.1762	4.40E-02	0.1807	4.04E-01	0.195	5.73E-03	0.1946	1.03E-03
0.1796	5.14E-02	0.1843	4.55E-01	0.1978	6.95E-03	0.1973	1.28E-03
0.1831	5.97E-02	0.1878	5.10E-01	0.2007	8.39E-03	0.2001	1.57E-03
0.1865	6.91E-02	0.1914	5.71E-01	0.2036	1.01E-02	0.2028	1.91E-03
0.19	7.97E-02	0.1949	6.37E-01	0.2065	1.20E-02	0.2056	2.32E-03
0.1935	9.17E-02	0.1985	7.09E-01	0.2094	1.43E-02	0.2084	2.81E-03
0.1969	1.05E-01	0.202	7.88E-01	0.2123	1.70E-02	0.2111	3.39E-03
0.2004	1.20E-01	0.2056	8.73E-01	0.2152	2.01E-02	0.2139	4.07E-03
0.2039	1.37E-01	0.2091	9.66E-01	0.2181	2.37E-02	0.2167	4.86E-03
0.2073	1.56E-01	0.2127	1.07E+00	0.2209	2.78E-02	0.2194	5.79E-03
0.2108	1.77E-01	0.2162	1.17E+00	0.2238	3.25E-02	0.2222	6.87E-03
0.2143	2.00E-01	0.2198	1.29E+00	0.2267	3.79E-02	0.225	8.12E-03
0.2177	2.26E-01	0.2233	1.42E+00	0.2296	4.41E-02	0.2277	9.57E-03
0.2212	2.54E-01	0.2269	1.55E+00	0.2325	5.11E-02	0.2305	1.13E-02
0.2247	2.86E-01	0.2305	1.70E+00	0.2354	5.91E-02	0.2333	1.32E-02
0.2281	3.21E-01	0.234	1.86E+00	0.2383	6.82E-02	0.236	1.54E-02
0.2316	3.59E-01	0.2376	2.03E+00	0.2412	7.85E-02	0.2388	1.80E-02
0.2351	4.02E-01	0.2411	2.21E+00	0.2441	9.02E-02	0.2416	2.09E-02
0.2385	4.49E-01	0.2447	2.40E+00	0.2469	1.03E-01	0.2443	2.42E-02
0.242	5.00E-01	0.2482	2.61E+00	0.2498	1.18E-01	0.2471	2.80E-02
0.2455	5.56E-01	0.2518	2.84E+00	0.2527	1.35E-01	0.2499	3.24E-02
0.2489	6.18E-01	0.2553	3.07E+00	0.2556	1.54E-01	0.2526	3.73E-02
0.2524	6.86E-01	0.2589	3.33E+00	0.2585	1.75E-01	0.2554	4.29E-02
0.2559	7.60E-01	0.2624	3.60E+00	0.2614	1.99E-01	0.2582	4.92E-02
0.2593	8.41E-01	0.266	3.90E+00	0.2643	2.25E-01	0.2609	5.64E-02
0.2628	9.30E-01	0.2695	4.21E+00	0.2672	2.55E-01	0.2637	6.46E-02
0.2662	1.03E+00	0.2731	4.54E+00	0.27	2.88E-01	0.2664	7.37E-02
0.2697	1.13E+00	0.2766	4.90E+00	0.2729	3.25E-01	0.2692	8.41E-02
0.2732	1.25E+00	0.2802	5.27E+00	0.2758	3.67E-01	0.272	9.58E-02
0.2766	1.38E+00	0.2837	5.68E+00	0.2787	4.13E-01	0.2747	1.09E-01
0.2801	1.51E+00	0.2873	6.11E+00	0.2816	4.65E-01	0.2775	1.24E-01
0.2836	1.66E+00	0.2909	6.57E+00	0.2845	5.22E-01	0.2803	1.41E-01
0.287	1.83E+00	0.2944	7.06E+00	0.2874	5.86E-01	0.283	1.59E-01
0.2905	2.01E+00	0.298	7.58E+00	0.2903	6.58E-01	0.2858	1.81E-01
0.294	2.20E+00	0.3015	8.13E+00	0.2931	7.37E-01	0.2886	2.04E-01
0.2974	2.41E+00	0.3051	8.73E+00	0.296	8.26E-01	0.2913	2.31E-01
0.3009	2.65E+00	0.3086	9.36E+00	0.2989	9.25E-01	0.2941	2.61E-01
0.3044	2.90E+00	0.3122	1.00E+01	0.3018	1.04E+00	0.2969	2.95E-01
0.3078	3.17E+00	0.3157	1.08E+01	0.3047	1.16E+00	0.2996	3.33E-01
0.3113	3.48E+00	0.3193	1.15E+01	0.3076	1.29E+00	0.3024	3.75E-01
0.3148	3.81E+00	0.3228	1.23E+01	0.3105	1.45E+00	0.3052	4.24E-01
0.3182	4.17E+00	0.3264	1.32E+01	0.3134	1.62E+00	0.3079	4.78E-01
0.3217	4.56E+00	0.3299	1.41E+01	0.3162	1.81E+00	0.3107	5.39E-01

Clovelly-Ap		Clovelly-B		Hutton-Ap		Hutton-B	
θ	K_L	θ	K_L	θ	K_L	θ	K_L
0.3252	4.99E+00	0.3335	1.51E+01	0.3191	2.02E+00	0.3135	6.08E-01
0.3286	5.47E+00	0.337	1.62E+01	0.322	2.26E+00	0.3162	6.86E-01
0.3321	5.99E+00	0.3406	1.73E+01	0.3249	2.53E+00	0.319	7.74E-01
0.3356	6.56E+00	0.3442	1.86E+01	0.3278	2.83E+00	0.3218	8.75E-01
0.339	7.19E+00	0.3477	1.99E+01	0.3307	3.17E+00	0.3245	9.89E-01
0.3425	7.89E+00	0.3513	2.13E+01	0.3336	3.56E+00	0.3273	1.12E+00
0.346	8.67E+00	0.3548	2.29E+01	0.3365	4.00E+00	0.3301	1.27E+00
0.3494	9.53E+00	0.3584	2.45E+01	0.3393	4.49E+00	0.3328	1.44E+00
0.3529	1.05E+01	0.3619	2.63E+01	0.3422	5.07E+00	0.3356	1.64E+00
0.3563	1.16E+01	0.3655	2.83E+01	0.3451	5.73E+00	0.3383	1.87E+00
0.3598	1.28E+01	0.369	3.04E+01	0.348	6.49E+00	0.3411	2.15E+00
0.3633	1.42E+01	0.3726	3.28E+01	0.3509	7.39E+00	0.3439	2.47E+00
0.3667	1.58E+01	0.3761	3.54E+01	0.3538	8.45E+00	0.3466	2.85E+00
0.3702	1.77E+01	0.3797	3.83E+01	0.3567	9.73E+00	0.3494	3.32E+00
0.3737	1.99E+01	0.3832	4.16E+01	0.3596	1.13E+01	0.3522	3.91E+00
0.3771	2.26E+01	0.3868	4.53E+01	0.3624	1.33E+01	0.3549	4.66E+00
0.3806	2.60E+01	0.3903	4.98E+01	0.3653	1.59E+01	0.3577	5.66E+00
0.3841	3.05E+01	0.3939	5.53E+01	0.3682	1.96E+01	0.3605	7.11E+00
0.3875	3.73E+01	0.3974	6.26E+01	0.3711	2.56E+01	0.3632	9.57E+00
0.3893	4.30E+01	0.3992	6.79E+01	0.3726	3.12E+01	0.3646	1.19E+01
0.3901	4.75E+01	0.4001	7.17E+01	0.3733	3.60E+01	0.3653	1.40E+01
0.3907	5.20E+01	0.4006	7.49E+01	0.3737	4.14E+01	0.3657	1.64E+01
0.391	5.85E+01	0.401	7.86E+01	0.374	5.05E+01	0.366	2.07E+01
0.391	6.12E+01	0.401	7.96E+01	0.374	5.53E+01	0.366	2.32E+01

Appendix 3.4 Estimated values of the $D_f(\theta)$ relationships

Clovelly-Ap		Clovelly-B		Hutton-Ap		Hutton-B	
θ	K_L	θ	K_L	θ	K_L	θ	K_L
0.0523	3.31E-04	0.0537	2.77E-02	0.0917	2.55E-06	0.0957	1.99E-07
0.0531	2.64E-03	0.0546	1.39E-01	0.0924	3.35E-05	0.0964	3.31E-06
0.0549	2.10E-02	0.0564	6.96E-01	0.0939	4.41E-04	0.0978	5.50E-05
0.0583	1.67E-01	0.0599	3.50E+00	0.0968	5.80E-03	0.1005	9.13E-04
0.0618	5.61E-01	0.0635	8.99E+00	0.0997	2.62E-02	0.1033	4.72E-03
0.0653	1.33E+00	0.067	1.76E+01	0.1026	7.64E-02	0.1061	1.52E-02
0.0687	2.59E+00	0.0706	2.96E+01	0.1054	1.75E-01	0.1088	3.75E-02
0.0722	4.46E+00	0.0741	4.53E+01	0.1083	3.45E-01	0.1116	7.84E-02
0.0757	7.08E+00	0.0777	6.50E+01	0.1112	6.12E-01	0.1144	1.47E-01
0.0791	1.06E+01	0.0812	8.89E+01	0.1141	1.01E+00	0.1171	2.52E-01
0.0826	1.50E+01	0.0848	1.17E+02	0.117	1.56E+00	0.1199	4.06E-01
0.0861	2.06E+01	0.0883	1.50E+02	0.1199	2.31E+00	0.1227	6.22E-01
0.0895	2.75E+01	0.0919	1.88E+02	0.1228	3.29E+00	0.1254	9.16E-01
0.093	3.57E+01	0.0954	2.31E+02	0.1257	4.54E+00	0.1282	1.30E+00

Clovelly-Ap		Clovelly-B		Hutton-Ap		Hutton-B	
θ	K_L	θ	K_L	θ	K_L	θ	K_L
0.0964	4.54E+01	0.099	2.79E+02	0.1285	6.12E+00	0.1309	1.80E+00
0.0999	5.67E+01	0.1025	3.33E+02	0.1314	8.07E+00	0.1337	2.44E+00
0.1034	6.98E+01	0.1061	3.93E+02	0.1343	1.04E+01	0.1365	3.22E+00
0.1068	8.48E+01	0.1096	4.58E+02	0.1372	1.33E+01	0.1392	4.19E+00
0.1103	1.02E+02	0.1132	5.30E+02	0.1401	1.66E+01	0.142	5.36E+00
0.1138	1.21E+02	0.1168	6.08E+02	0.143	2.06E+01	0.1448	6.76E+00
0.1172	1.43E+02	0.1203	6.93E+02	0.1459	2.52E+01	0.1475	8.42E+00
0.1207	1.67E+02	0.1239	7.85E+02	0.1488	3.05E+01	0.1503	1.04E+01
0.1242	1.93E+02	0.1274	8.84E+02	0.1516	3.66E+01	0.1531	1.26E+01
0.1276	2.23E+02	0.131	9.91E+02	0.1545	4.36E+01	0.1558	1.53E+01
0.1311	2.55E+02	0.1345	1.11E+03	0.1574	5.15E+01	0.1586	1.83E+01
0.1346	2.91E+02	0.1381	1.23E+03	0.1603	6.04E+01	0.1614	2.18E+01
0.138	3.30E+02	0.1416	1.36E+03	0.1632	7.04E+01	0.1641	2.57E+01
0.1415	3.72E+02	0.1452	1.50E+03	0.1661	8.16E+01	0.1669	3.02E+01
0.145	4.18E+02	0.1487	1.65E+03	0.169	9.40E+01	0.1697	3.52E+01
0.1484	4.68E+02	0.1523	1.81E+03	0.1719	1.08E+02	0.1724	4.09E+01
0.1519	5.22E+02	0.1558	1.97E+03	0.1747	1.23E+02	0.1752	4.72E+01
0.1554	5.80E+02	0.1594	2.15E+03	0.1776	1.40E+02	0.178	5.43E+01
0.1588	6.43E+02	0.1629	2.34E+03	0.1805	1.59E+02	0.1807	6.21E+01
0.1623	7.11E+02	0.1665	2.54E+03	0.1834	1.79E+02	0.1835	7.08E+01
0.1658	7.83E+02	0.1701	2.75E+03	0.1863	2.01E+02	0.1863	8.03E+01
0.1692	8.61E+02	0.1736	2.98E+03	0.1892	2.26E+02	0.189	9.09E+01
0.1727	9.45E+02	0.1772	3.21E+03	0.1921	2.52E+02	0.1918	1.03E+02
0.1762	1.03E+03	0.1807	3.46E+03	0.195	2.81E+02	0.1946	1.15E+02
0.1796	1.13E+03	0.1843	3.73E+03	0.1978	3.12E+02	0.1973	1.29E+02
0.1831	1.23E+03	0.1878	4.01E+03	0.2007	3.46E+02	0.2001	1.44E+02
0.1865	1.34E+03	0.1914	4.30E+03	0.2036	3.83E+02	0.2028	1.61E+02
0.19	1.46E+03	0.1949	4.61E+03	0.2065	4.23E+02	0.2056	1.79E+02
0.1935	1.58E+03	0.1985	4.94E+03	0.2094	4.65E+02	0.2084	1.99E+02
0.1969	1.71E+03	0.202	5.28E+03	0.2123	5.12E+02	0.2111	2.20E+02
0.2004	1.85E+03	0.2056	5.64E+03	0.2152	5.62E+02	0.2139	2.43E+02
0.2039	2.00E+03	0.2091	6.02E+03	0.2181	6.15E+02	0.2167	2.68E+02
0.2073	2.16E+03	0.2127	6.43E+03	0.2209	6.73E+02	0.2194	2.95E+02
0.2108	2.33E+03	0.2162	6.85E+03	0.2238	7.35E+02	0.2222	3.24E+02
0.2143	2.50E+03	0.2198	7.29E+03	0.2267	8.02E+02	0.225	3.56E+02
0.2177	2.69E+03	0.2233	7.76E+03	0.2296	8.73E+02	0.2277	3.90E+02
0.2212	2.90E+03	0.2269	8.26E+03	0.2325	9.50E+02	0.2305	4.27E+02
0.2247	3.11E+03	0.2305	8.78E+03	0.2354	1.03E+03	0.2333	4.66E+02
0.2281	3.34E+03	0.234	9.33E+03	0.2383	1.12E+03	0.236	5.09E+02
0.2316	3.58E+03	0.2376	9.91E+03	0.2412	1.22E+03	0.2388	5.55E+02
0.2351	3.84E+03	0.2411	1.05E+04	0.2441	1.32E+03	0.2416	6.04E+02
0.2385	4.11E+03	0.2447	1.12E+04	0.2469	1.43E+03	0.2443	6.57E+02
0.242	4.40E+03	0.2482	1.19E+04	0.2498	1.54E+03	0.2471	7.15E+02

Clovelly-Ap		Clovelly-B		Hutton-Ap		Hutton-B	
θ	K_L	θ	K_L	θ	K_L	θ	K_L
0.2455	4.71E+03	0.2518	1.26E+04	0.2527	1.67E+03	0.2499	7.76E+02
0.2489	5.03E+03	0.2553	1.33E+04	0.2556	1.80E+03	0.2526	8.42E+02
0.2524	5.38E+03	0.2589	1.41E+04	0.2585	1.94E+03	0.2554	9.14E+02
0.2559	5.75E+03	0.2624	1.50E+04	0.2614	2.10E+03	0.2582	9.90E+02
0.2593	6.15E+03	0.266	1.59E+04	0.2643	2.26E+03	0.2609	1.07E+03
0.2628	6.57E+03	0.2695	1.69E+04	0.2672	2.44E+03	0.2637	1.16E+03
0.2662	7.02E+03	0.2731	1.79E+04	0.27	2.63E+03	0.2664	1.26E+03
0.2697	7.50E+03	0.2766	1.90E+04	0.2729	2.83E+03	0.2692	1.36E+03
0.2732	8.01E+03	0.2802	2.01E+04	0.2758	3.05E+03	0.272	1.47E+03
0.2766	8.56E+03	0.2837	2.13E+04	0.2787	3.29E+03	0.2747	1.59E+03
0.2801	9.15E+03	0.2873	2.26E+04	0.2816	3.54E+03	0.2775	1.72E+03
0.2836	9.77E+03	0.2909	2.40E+04	0.2845	3.81E+03	0.2803	1.86E+03
0.287	1.05E+04	0.2944	2.55E+04	0.2874	4.11E+03	0.283	2.01E+03
0.2905	1.12E+04	0.298	2.71E+04	0.2903	4.43E+03	0.2858	2.18E+03
0.294	1.20E+04	0.3015	2.88E+04	0.2931	4.77E+03	0.2886	2.35E+03
0.2974	1.28E+04	0.3051	3.06E+04	0.296	5.14E+03	0.2913	2.55E+03
0.3009	1.37E+04	0.3086	3.26E+04	0.2989	5.55E+03	0.2941	2.76E+03
0.3044	1.47E+04	0.3122	3.47E+04	0.3018	5.99E+03	0.2969	2.99E+03
0.3078	1.58E+04	0.3157	3.70E+04	0.3047	6.47E+03	0.2996	3.24E+03
0.3113	1.69E+04	0.3193	3.95E+04	0.3076	7.00E+03	0.3024	3.51E+03
0.3148	1.82E+04	0.3228	4.22E+04	0.3105	7.57E+03	0.3052	3.81E+03
0.3182	1.96E+04	0.3264	4.51E+04	0.3134	8.20E+03	0.3079	4.14E+03
0.3217	2.11E+04	0.3299	4.83E+04	0.3162	8.90E+03	0.3107	4.51E+03
0.3252	2.27E+04	0.3335	5.18E+04	0.3191	9.66E+03	0.3135	4.91E+03
0.3286	2.46E+04	0.337	5.57E+04	0.322	1.05E+04	0.3162	5.36E+03
0.3321	2.66E+04	0.3406	6.00E+04	0.3249	1.15E+04	0.319	5.86E+03
0.3356	2.89E+04	0.3442	6.48E+04	0.3278	1.25E+04	0.3218	6.42E+03
0.339	3.14E+04	0.3477	7.01E+04	0.3307	1.37E+04	0.3245	7.06E+03
0.3425	3.43E+04	0.3513	7.62E+04	0.3336	1.51E+04	0.3273	7.78E+03
0.346	3.76E+04	0.3548	8.30E+04	0.3365	1.66E+04	0.3301	8.60E+03
0.3494	4.13E+04	0.3584	9.08E+04	0.3393	1.84E+04	0.3328	9.54E+03
0.3529	4.56E+04	0.3619	9.99E+04	0.3422	2.04E+04	0.3356	1.06E+04
0.3563	5.07E+04	0.3655	1.10E+05	0.3451	2.29E+04	0.3383	1.19E+04
0.3598	5.67E+04	0.369	1.23E+05	0.348	2.57E+04	0.3411	1.35E+04
0.3633	6.39E+04	0.3726	1.38E+05	0.3509	2.92E+04	0.3439	1.54E+04
0.3667	7.28E+04	0.3761	1.57E+05	0.3538	3.35E+04	0.3466	1.77E+04
0.3702	8.40E+04	0.3797	1.81E+05	0.3567	3.89E+04	0.3494	2.06E+04
0.3737	9.87E+04	0.3832	2.12E+05	0.3596	4.60E+04	0.3522	2.44E+04
0.3771	1.19E+05	0.3868	2.56E+05	0.3624	5.58E+04	0.3549	2.97E+04
0.3806	1.49E+05	0.3903	3.22E+05	0.3653	7.02E+04	0.3577	3.76E+04
0.3841	2.00E+05	0.3939	4.36E+05	0.3682	9.46E+04	0.3605	5.08E+04
0.3875	3.14E+05	0.3974	7.07E+05	0.3711	1.48E+05	0.3632	7.98E+04
0.3893	4.70E+05	0.3992	1.11E+06	0.3726	2.19E+05	0.3646	1.18E+05

Clovelly-Ap		Clovelly-B		Hutton-Ap		Hutton-B	
θ	**K_L**	**θ**	**K_L**	**θ**	**K_L**	**θ**	**K_L**
0.3901	6.81E+05	0.4001	1.70E+06	0.3733	3.12E+05	0.3653	1.67E+05
0.3907	1.07E+06	0.4006	2.93E+06	0.3737	4.74E+05	0.3657	2.52E+05
0.391	3.04E+06	0.401	1.08E+07	0.374	1.18E+06	0.366	6.06E+05
0.391	8.00E+06	0.401	3.86E+07	0.374	2.63E+06	0.366	1.30E+06

Appendix 4: Thermal properties

Appendix 4.1 Mean comparison summary-volumetric heat capacity

Water*Temp	Clovelly-Ap	Clovelly-B	Hutton-Ap	Hutton-B
1 1	1.0095 ^{l}	1.0008 ^{o}	0.9128 ^{n}	0.9528 ^{l}
1 2	0.9628 ^{l}	1.0778 ^{o}	1.0818 ^{m}	0.9300 ^{l}
1 3	1.2088 ^{k}	1.1070 ^{no}	1.1070 ^{m}	1.1505 ^{k}
1 4	1.6608 ^{hij}	1.7693 ^{klm}	1.2338 ^{lm}	1.6540 ^{j}
1 5	1.9833 ^{efg}	2.2168 ^{fghi}	1.5628 ^{ijk}	2.0340 ^{ghi}
2 1	1.5435 ^{ij}	1.3280 ^{n}	1.5938 ^{ijk}	2.2938 ^{efg}
2 2	1.5063 ^{j}	1.7068 ^{lm}	1.3593 ^{kl}	1.6790 ^{j}
2 3	1.7940 ^{ghi}	1.5373 ^{mn}	1.5933 ^{ij}	1.6955 ^{j}
2 4	1.9013 ^{fgh}	1.8428 ^{jkl}	1.4570 ^{jk}	2.2353 ^{efg}
2 5	1.9000 ^{fgh}	2.0965 ^{ghij}	1.7623 ^{hi}	2.1685 ^{fghi}
3 1	1.9485 ^{fgh}	1.9498 ^{ijkl}	1.9655 ^{gh}	2.3710 ^{defg}
3 2	1.8568 ^{gh}	2.0178 ^{hijkl}	2.1063 ^{fg}	1.8570 ^{hij}
3 3	1.9420 ^{fgh}	2.1355 ^{fghij}	2.1425 ^{efg}	1.8340 ^{ij}
3 4	2.1945 ^{cdef}	2.0660 ^{ghijk}	2.5160 ^{bcde}	2.5290 ^{cdef}
3 5	2.0998 ^{defg}	2.3060 ^{efg}	2.3393 ^{cdef}	2.6905 ^{abcd}
4 1	2.5723 ^{abc}	2.3505 ^{defg}	2.7150 ^{bcd}	2.6380 ^{bcde}
4 2	2.3465 ^{bcde}	2.9040 ^{bc}	2.3610 ^{cdef}	2.2143 ^{efgh}
4 3	2.0603 ^{efg}	2.5978 ^{cde}	2.7345 ^{abc}	2.2255 ^{efgh}
4 4	2.3943 ^{bcd}	2.7233 ^{bcd}	2.7525 ^{ab}	2.8350 ^{abc}
4 5	2.6188 ^{ab}	3.1105 ^{b}	2.4315 ^{bcdef}	2.7770 ^{abcd}
5 1	2.4943 ^{abcd}	4.0645 a	3.1853 ^{a}	3.2605 ^{a}

Water*Temp	Clovelly-Ap	Clovelly-B	Hutton-Ap	Hutton-B
5 2	2.4643 bcd	2.2803 efgh	2.3235 def	2.4228 cdefg
5 3	2.7490 ab	2.4625 def	2.5315 bcd	2.4610 cdef
5 4	2.5438 abc	2.8958 bc	2.6668 bcd	2.7950 abcd
5 5	2.9680 a	3.1033 b	2.7513 ab	3.0815 ab

Appendix 4.2 Mean comparison summary-thermal conductivity

Water*Temp	Clovelly-Ap	Clovelly-B	Hutton-Ap	Hutton-B
1 1	0.1905 k	0.1985 m	0.2150 j	0.1740 l
1 2	0.1888 k	0.2210 m	0.2398 j	0.1775 kl
1 3	0.2313 j	0.2138 m	0.2118 j	0.2315 k
1 4	0.2985 i	0.3128 l	0.2858 i	0.2800 j
1 5	0.3903 h	0.5325 k	0.3980 h	0.4620 i
2 1	1.6423 g	1.2380 j	1.3238 g	1.4113 gh
2 2	1.6338 g	1.3038 ij	1.2543 g	1.3050 h
2 3	1.7630 g	1.3848 ij	1.3563 g	1.4143 gh
2 4	1.7048 g	1.4635 i	1.7828 f	1.3023 g
2 5	2.0350 f	1.9728 fg	2.2303 cde	1.7503 ef
3 1	2.2050 cdef	1.8695 gh	2.1138 de	1.9898 def
3 2	2.0275 f	1.6948 h	2.1390 de	1.7828 f
3 3	2.0788 ef	1.7850 gh	2.1393 de	1.9623 def
3 4	2.0178 f	1.7353 h	2.0673 e	1.8425 f
3 5	2.1705 def	2.1223 ef	2.2948 bcde	2.1033 cde
4 1	2.3433 abcd	2.8963 b	2.5955 b	2.4855 b
4 2	2.4470 abc	2.4435 cd	2.3393 bcd	2.2605 bcd
4 3	2.1703 def	2.5228 c	2.4873 bc	2.2145 bc
4 4	2.2360 cdef	2.2455 de	2.3678 bcd	2.1660 bcd
4 5	2.3498 abcd	2.3995 cd	2.3433 bcd	2.2070 bcd
5 1	2.6055 a	3.6855 a	3.1328 a	2.6875 a
5 2	2.5760 ab	2.4180 cd	2.3780 bcd	2.2965 bc

Water*Temp	Clovelly-Ap	Clovelly-B	Hutton-Ap	Hutton-B
5 3	2.3195 bcde	2.3875 cd	2.3513 bcd	2.2948 bc
5 4	2.3200 bcde	2.3650 cde	2.3100 bcde	2.2423 bcd
5 5	2.3193 bcde	2.3605 cde	2.3338 bcde	2.2518 bcd

Appendix 4.3 Mean comparison summary-thermal diffusivity

Water*Temp	Clovelly-Ap	Clovelly-B	Hutton-Ap	Hutton-B
1 1	0.1880 g	0.2000 ij	0.2353 f	0.1823 j
1 2	0.1955 g	0.2050 i	0.2218 fg	0.1923 ij
1 3	0.1910 g	0.1930 ij	0.1913 g	0.2013 ij
1 4	0.1800 g	0.1765 j	0.2318 f	0.1690 j
1 5	0.1970 g	0.2403 h	0.2540 f	0.2273 i
2 1	1.0685 abc	0.9373 bcde	0.8948 de	0.6373 gh
2 2	1.1118 ab	0.7660 g	0.9338 cde	0.7770 f
2 3	0.9955 abcde	0.9008 cdef	0.8513 de	0.8363 cdef
2 4	0.8960 def	0.7955 fg	1.2280 a	0.5848 h
2 5	1.0725 abc	0.9485 bcde	1.2750 a	0.8190 cdef
3 1	1.1363 a	0.9650 bcd	1.1033 ab	0.8513 bcdef
3 2	1.1035 ab	0.8783 cdefg	1.0403 bc	0.9583 abc
3 3	1.0713 abc	0.8388 defg	1.0060 bcd	1.0698 a
3 4	0.9208 cdef	0.8458 cdefg	0.8223 e	0.7328 fg
3 5	1.0350 abcd	0.9220 cde	0.9823 bcd	0.7868 ef
4 1	0.9313 cdef	1.2513 a	0.9645 bcde	0.9643 abc
4 2	1.0515 abcd	0.8468 cdefg	1.0068 bcd	1.0330 a
4 3	1.0998 abc	0.9745 bc	0.9130 cde	1.0060 ab
4 4	0.9363 bcde	0.8268 efg	0.8603 de	0.7728 f
4 5	0.8973 def	0.7738 g	0.9640 bcde	0.7998 def
5 1	1.0543 abcd	0.9018 cdef	0.9738 bcde	0.8870 bcdef
5 2	1.0500 abcd	1.0715 b	1.0243 bc	0.9523 abcd
5 3	0.8720 ef	0.9738 bc	0.9338 bcde	0.9358 abcde
5 4	0.9173 cdef	0.8233 efg	0.8678 cde	0.8025 cdef
5 5	0.7930 f	0.7628 g	0.8500 de	0.7350 fg

Appendix 4.4 t-statistics for the comparison of thermal conductivity between the two soil types

Thermal property	t-Test: Paired Two Sample for Means		
	Statistics	*Clovelly*	*Hutton*
Volumetric heat capacity	Mean	0.6935	0.6947
	Variance	0.0984	0.108
	Observations	25	25
	Pear. Correlation	0.9515	
	df	24	
	t Stat	-0.0605	
	P(T<=t) one-tail	0.4761	
	t Critical one-tail	1.7109	
	P(T<=t) two-tail	0.9522	
	t Critical two-tail	2.0639	
Thermal conductivity	Mean	0.3166	0.3104
	Variance	0.7718	0.7776
	Observations	25	25
	Pear. Correlation	0.9971	
	df	24	
	t Stat	0.4598	
	P(T<=t) one-tail	0.3249	
	t Critical one-tail	1.7109	
	P(T<=t) two-tail	0.6498	
	t Critical two-tail	2.0639	
Thermal diffusivity	Mean	-0.377	-0.4028
	Variance	0.4162	0.3624
	Observations	25	25
	Pearson Correlation	0.9912	
	df	24	
	t Stat	1.3827	
	P(T<=t) one-tail	0.0897	
	t Critical one-tail	1.7109	
	P(T<=t) two-tail	0.1795	
	t Critical two-tail	2.0639	

Appendix 5 Characterizing bare soil evaporation

Appendix 5.1 Some regression plots during the calibration of DFM water sensors

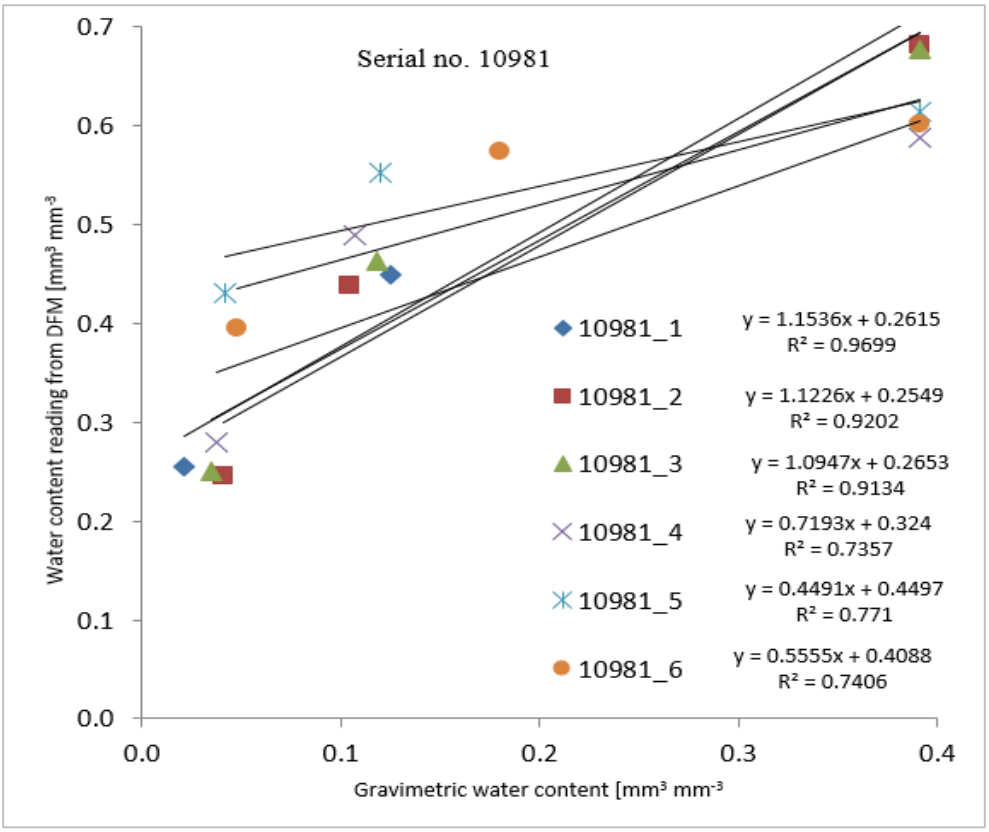

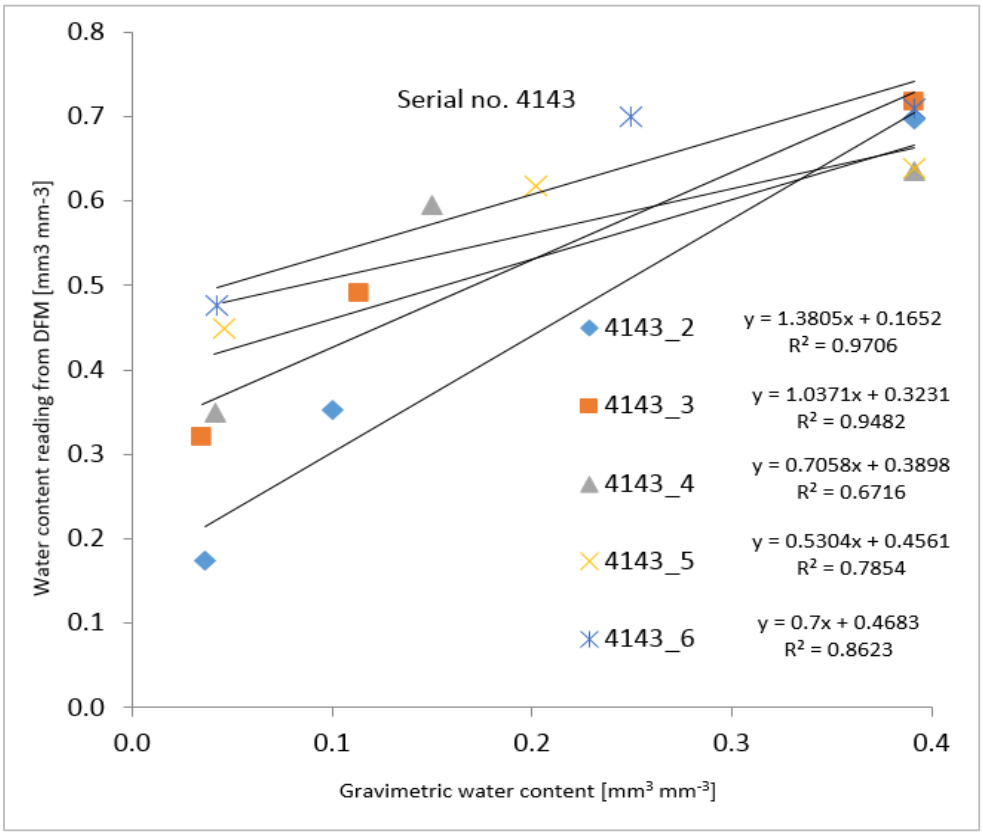

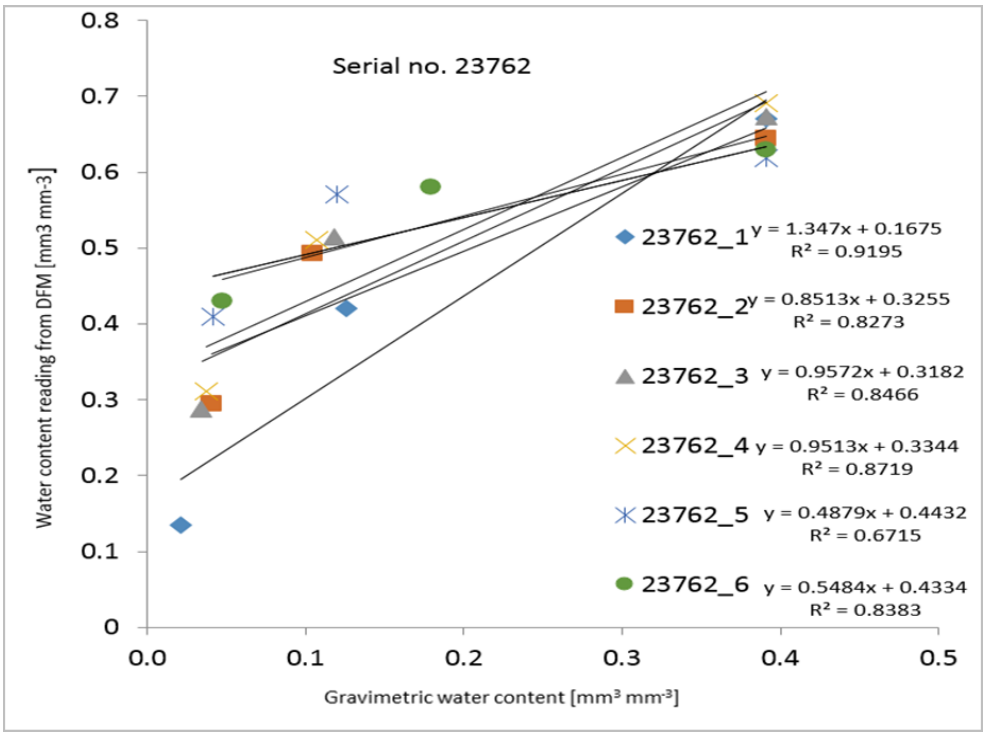
Serial no. 23762
Water content reading from DFM [mm3 mm-3]
Gravimetric water content [mm³ mm-³]
0.8
0.7
0.6
0.5
0.4
0.3
0.2
0.1
0
0.0
0.1
0.2
0.3
0.4
0.5
23762_1 y = 1.347x + 0.1675 R² = 0.9195
23762_2 y = 0.8513x + 0.3255 R² = 0.8273
23762_3 y = 0.9572x + 0.3182 R² = 0.8466
23762_4 y = 0.9513x + 0.3344 R² = 0.8719
23762_5 y = 0.4879x + 0.4432 R² = 0.6715
23762_6 y = 0.5484x + 0.4334 R² = 0.8383

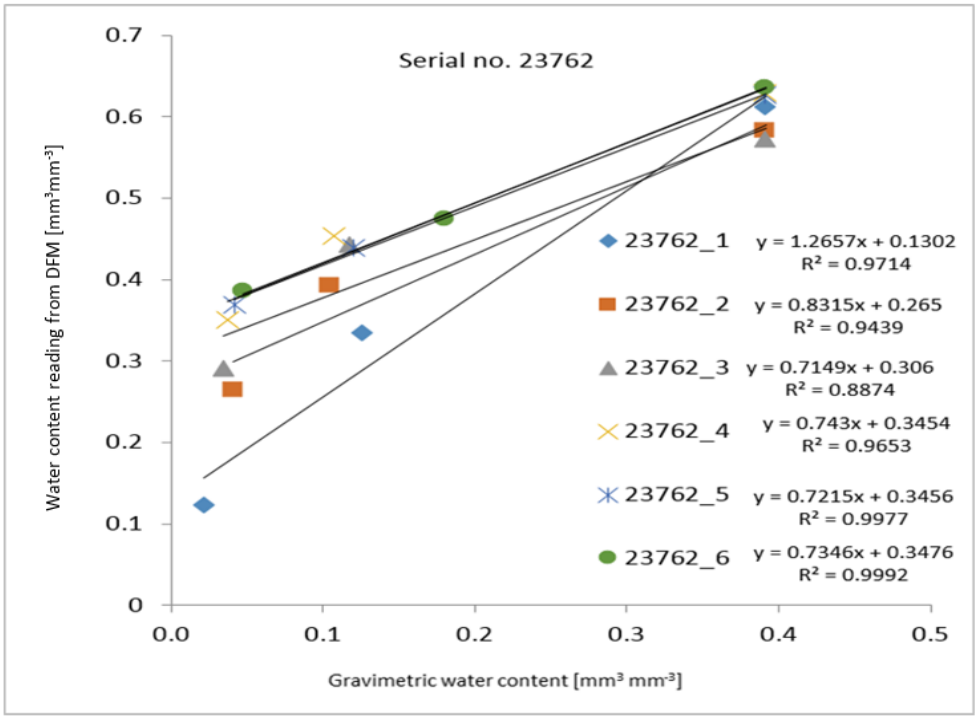
Serial no. 23762
Water content reading from DFM [mm³mm-³]
Gravimetric water content [mm³ mm-³]
0.7
0.6
0.5
0.4
0.3
0.2
0.1
0
0.0
0.1
0.2
0.3
0.4
0.5
23762_1 y = 1.2657x + 0.1302 R² = 0.9714
23762_2 y = 0.8315x + 0.265 R² = 0.9439
23762_3 y = 0.7149x + 0.306 R² = 0.8874
23762_4 y = 0.743x + 0.3454 R² = 0.9653
23762_5 y = 0.7215x + 0.3456 R² = 0.9977
23762_6 y = 0.7346x + 0.3476 R² = 0.9992

Appendix 5.2 A regression plot during the calibration of DFM temperature sensors